Interim Report

October 1970

B-1

FEASIBILITY STUDY OF SLANTING FOR COMBINED NUCLEAR WEAPONS EFFECTS (Revised)

Volume 2: Appendices

For:

OFFICE OF CIVIL DEFENSE
OFFICE OF THE SECRETARY OF THE ARMY
WASHINGTON, D.C. 20310

CONTRACT DAHC 20-67-C-0136
OCD Work Unit 1154E

SRI Project MU-6300-501

STANFORD RESEARCH INSTITUTE
Menlo Park, California 94025 · U.S.A.

STANFORD RESEARCH INSTITUTE
Menlo Park, California 94025 · U.S.A.

Interim Report

October 1970

FEASIBILITY STUDY OF SLANTING FOR COMBINED NUCLEAR WEAPONS EFFECTS (Revised)

Volume 2: Appendices

By: H. L. MURPHY

For:

OFFICE OF CIVIL DEFENSE
OFFICE OF THE SECRETARY OF THE ARMY
WASHINGTON, D.C. 20310

CONTRACT DAHC 20-67-C-0136
OCD Work Unit 1154E

SRI Project MU-6300-501

Appendix A

NUCLEAR WEAPONS EFFECTS

By J. H. Iverson

Appendix A

NUCLEAR WEAPONS EFFECTS

By J. H. Iverson

The purpose of this appendix is to describe the derivation of Figs. 2-1 through 2-8. In all but one case, these figures were based on Reference 1,* hereinafter referred to as ENW.

Figures 3.67a and 3.67b of ENW were used in the preparation of Table A-1. Heights-of-burst (HOB) were optimized to obtain the maximum range for each overpressure shown in the air burst portion of the table. HOB equal to zero was used to obtain the contact surface burst ranges.

Table A-1

DATA FOR A 1 kt WEAPON YIELD

Peak Overpressure (psi)	Air Burst		Contact Surface Burst
	Range (ft)	HOB (ft)	Range (ft)
6	2000	917	1367
8	1707	830	1133
10	1456	727	1021
15	1194	650	818
20	945	614	709
30	672	565	584
40	565	500	510
50	525	466	459

* References are listed at the end of this appendix.

Figure 2-1

The air burst curves were derived as follows:

1. The data in Table A-1 were used in ENW Figure 3.69 to obtain positive phase duration on the ground versus overpressure and versus dynamic pressure at eight pressures each.

2. The best least squares curve fit of six curve types was chosen and the positive phase duration was cube root scaled to 1 Mt.

3. Curves for overpressure and dynamic pressure were plotted, each versus positive phase duration. The equation of each curve is:

   a. For overpressure: $t = 1/(0.282831 + 0.009655p)$
   b. For dynamic pressure: $t = 3.71018 - 0.013855p$

   where t and p are positive phase duration and pressure, respectively.

The surface burst curves were derived as follows:

1. Ground distances were recorded from ENW Figure 3.69 at the point where each positive phase duration curve intersected HOB = 0.

2. These ground distances versus the positive phase duration values for overpressure and dynamic pressure were each subjected to a least squares curve fit of six different curves; the best fit in each case was:

   a. For overpressure: $t = d/(3110.49 + 1.07867d)$
   b. For dynamic pressure: $t = 0.419881 - (57.8975/d)$

   where d is the distance from ground zero for 1 kt.

3. The data shown in Table A-1 were then substituted into these equations, which resulted in eight relationships between overpressure and positive phase duration and eight relationships between dynamic pressure and positive phase duration.

4. The best least squares curve fit of six curve types was then obtained for both overpressure and dynamic pressure versus positive phase duration. The equations (scaled to 1 Mt) for the curves plotted are:

   a. For overpressure: $t = 6.03979p^{-0.398083}$
   b. For dynamic pressure: $t = 1/(0.258683 + 0.0016909p)$

   where t and p are positive phase duration and pressure, respectively.

Data obtained from Brode,[2]* Figs. 24 and 25, were also plotted on Fig. 2-1. Data points for positive phase duration versus peak overpressure were extracted from Brode for overpressure and dynamic pressure. Each set of data was subjected to a least squares curve fit of six different curves; the best fit in each case was:

a. For overpressure: $t = 5.03615\ p^{-0.430266}$

b. For dynamic pressure: $t = 1/(0.262811 + 0.0121185p)$

where t and p are positive phase duration and peak overpressure, respectively. The curves of these two equations were plotted on both parts of Fig. 2-1 since Brode indicates that positive phase duration for a given peak overpressure is independent of HOB.

Figures 2-2 Through 2-8

Figures 2-2 through 2-8 required that air burst slant range be calculated from the data in Table A-1 (for a contact surface burst, the slant range equals the range). Cube-root scaling provided the scaled, slant ranges shown in Table A-2 needed for the derivation of these figures.

Table A-2

SLANT RANGES FOR 200 kt AND 1 Mt

Overpressure	Air Burst				Contact Surface Burst			
	200 kt		1 Mt		200 kt		1 Mt	
(psi)	Yards	Miles	Yards	Miles	Yards	Miles	Yards	Miles
6	4290	2.44			2666	1.51	4560	2.59
8	3701	2.10			2211	1.26	3780	2.15
10	3173	1.80	5424	3.08	1989	1.13	3400	1.93
15	2651	1.51	4531	2.57	1597	0.91	2730	1.55
20	2197	1.25	3756	2.13	1381	0.78	2360	1.34
30	1712	0.97	2926	1.66	1141	0.65	1950	1.11
40	1471	0.84	2515	1.43	994	0.56	1700	0.96
50	1368	0.78	2340	1.33	895	0.51	1530	0.87

* Superscript numerals are related to the reference list at the end of this appendix.

Figure 2-2 depicts thermal energy as a function of peak overpressure. To prepare the air burst curves, the Table A-2 values were used in ENW Fig. 7.105 to obtain values of radiant exposure (thermal energy). These data were then scaled to 200 kt and 1 Mt by multiplying by 200 and 1000, respectively (ENW page 364). To prepare the surface burst curves, an existing computer program[3] was used to obtain data for plotting.

Figures 2-4 and 2-7, the free-field gamma radiation intensity curves, were derived by applying the data in Table A-2 to ENW Figs. 8.27a and 8.27b. The units of roentgens were changed to rads in accordance with note 9, ENW, page 579.

Figures 2-5 and 2-8 values were obtained as follows:

1. The integrated neutron flux, obtained by entering ENW Fig. 8.61 with the data in Table A-2, was multiplied by 1.8×10^{-9} rad to obtain dose in rads (ENW paragraph 11.90).

2. These data were scaled to 200 kt and 1 Mt by multiplying by 200 and 1000, respectively, as described in ENW paragraph 8.61.

Figure 2-3 is merely a summation of the data found in Figs. 2-4 and 2-5, and Fig. 2-6 is a similar summation of the data found in Figs. 2-7 and 2-8.

REFERENCES

1. Glasstone, S., editor, The Effects of Nuclear Weapons, U.S. Dept. of Defense and Atomic Energy Commission, February 1964 reprint (with changes) of 1962 edition (Supt. of Documents, Washington, D.C.).

2. Brode, H. L., A Review of Nuclear Explosion Phenomena Pertinent to Protective Construction, RAND Corp. rpt. R-425-PR, prepared for USAF Project RAND, May 1964 (AD-601 139). Brode has published a later version, "Review of Nuclear Weapons Effects," Annual Review of Nuclear Science, Vol. 18, 1968 (Annual Reviews, Inc., Palo Alto, Calif., 94306).

3. Martin, S., and S. Holton, Preliminary Computer Program for Estimating Ignition Ranges for Nuclear Weapons, USNRDL-TR-866, U.S. Naval Radiological Defense Laboratory, San Francisco, California, June 1965.

Appendix B

FIRE HAZARD REDUCTION

By R. G. Carroll

Appendix B

FIRE HAZARD REDUCTION

By R. G. Carroll

Section 1 - Siting for Fire Hazard Reduction

Introduction

The incendiary characteristics of a nuclear explosion are associated with both thermal and blast effects of a weapon.

Air burst megaton weapons, under conditions of 6 to 12 miles visibility, are capable of causing thermal ignitions of newsprint and similar tinder materials at a ground radius out to where the blast overpressure is approximately 2 psi.[1-3] The types of fuel susceptible to ignition by thermal radiation are thin combustible materials such as newspapers, dry grass and leaves, and window-exposed fuels such as curtains and drapes. In general, the variables affecting the critical ignition energy, or the amount of thermal energy necessary to cause ignition, of tinder fuels are thickness, composition, color, and moisture content. Ignition of tinder fuels does not necessarily mean that a fire will develop. Other, heavier combustible materials must be in proximity to sustain combustion, and this condition is prevalent in residential and commercial buildings.[4] Therefore, it is probable that ignition of window fuels, i.e., drapes, shades, and curtains, would determine the range of sustained ignitions and multiple fires.

Variables that tend to mitigate the effects of the thermal pulse are atmospheric obscuration and visibility,[3] number or density of ignition points, degree of fuel shielding from thermal radiation, window glass, and window screens. Ordinary, clean, single-pane window glass, for example, has a thermal transmittance in the range of 0.75.[5] Since thermal radiation is emitted within a few seconds (80% of total thermal energy within 8 seconds for a 1 MT air burst[1]), window glass and screens would survive long enough before the arrival of the blast wave to be effective in attenuating the thermal radiation.

When all of these factors and variables are considered, the net effect is a decreased probable range of sustained ignition. As an example, for a condition of 6 to 12 miles visibility and a 1 MT air burst, the ignition ground radius for beige cotton curtains shielded by window glass and screens is 2 to 3 miles[6] (8-12 psi range). As another approach, under the same conditions, Crowley et al.[7] estimate that for a completely exposed dwelling room, the probability of sustained room ignition is 50%. Therefore, it can be expected that sustained ignitions sufficient to cause rapid build-up of extensive fires would occur within the limits of the 5 psi radius in areas where buildings and structures are not otherwise destroyed or suffering extremely severe damage.

In the regions beyond the 5 psi perimeter, the density of ignitions would diminish with distance. Although large fires, even mass fires or conflagrations, may occur in scattered locations, the rate of build-up and fire-spread would be slow enough that sufficient time would be available for occupants of threatened shelters to take remedial action and, if necessary, to evacuate, hopefully to other shelters.

At all overpressure levels out to the 2 psi range, the fire raising potential of the thermal pulse would be augmented by blast-induced, secondary fires. According to Moll,[8] secondary ignitions are estimated to have a frequency of 0.006 per 1,000 sf of total floor area that has sustained damage by overpressures of 2 psi or more. This corresponds to about one ignition per 100 houses.

The worst fire conditions for a shelter would be within the 5 psi perimeter. Even so, survival in this region is considered probable. Of some 280,000 people in the Hamburg firestorm of July 27-28, 1943, 85% survived and the majority of casualties were suffered by those in relatively primitive, basement-type shelters.[9] Of those people who occupied specially designed bunkers and splinter-proof shelters, 100% survived the firestorm. This is not meant to suggest that firestorms are probable in the United States as a result of a nuclear attack. Rodden et al.[10] state that the optimum combination of the many conditions necessary to initiate a firestorm would be encountered infrequently.

No matter how fires are started, subsequent development and spread would be determined by the amount and distribution of combustible materials in the vicinity. Since measures would be taken to protect the slanted shelter building from thermal effects and blast induced fires, the primary concern is to minimize the probability of ignitions stemming from burning buildings adjacent to the shelter building. Studies have shown that the probability of fire-spread depends on building density, or "built-upness," of an area and therefore the distance between buildings.[11]

Given that most buildings would not be equipped with protective window screens or other reflective devices and the interior fire load of combustible furnishings and materials in all buildings would be sufficient to sustain combustion after ignition,[4] there is a possibility that structures and buildings adjacent to a shelter building would be on fire an hour or two after an attack. However, even though a shelter building may be equipped with thermal protection devices over all window openings, these would be blown away by the blast wave immediately subsequent to the thermal pulse. The shelter building would therefore be exposed to ignition by thermal radiation and convection from adjacent building fires.

Objective

The objective of this section is to provide a method for determining separation distances to minimize the chances of fire-spread from adjacent buildings to the shelter building. The method is basically that developed by Margaret Law.[12] The Law method provides separation distances only for thermal radiation emanating from the vertical wall openings of adjacent burning buildings; therefore, additional methods have been introduced to give consideration to the effects of flame and to bending of flames by wind. Exposure to the effects of convection currents has not been considered. At the end of this appendix, there are (1) a reference list, including all references used in the preparation of this appendix; (2) a bibliography, listing the most pertinent other literature reviewed; and (3) Annex A, describing alternative methods for developing building separation distances.

Background

Two major factors enter into consideration when planning building separation distances:

- The level of radiation received from a fire in an adjacent building.
- The level of radiation that will ignite materials both on the outside of buildings and within rooms exposed by window openings.

The basis for determining these factors is oven-dry, unpainted wood whose behavior has been shown by tests to be representative of most combustible materials. Spontaneous ignition of such wood occurs only at intensities of radiation above 0.8 cal/cm^2-sec. In the open, spontaneous ignition takes place rather quickly after exposure to radiation and either

occurs within about 2 minutes or not at all.[12] Pilot ignition occurs when a secondary source of ignition is brought sufficiently near to ignite the gases emitted by a heated surface, but for pilot ignition to occur in the open, heating times of about 10 minutes are needed. Above an intensity of 0.3 cal/cm^2-sec, pilot ignition of wood from sparks or flying brands can take place.[12] Accordingly, 0.3 cal/cm^2-sec is taken as the upper limit of radiation exposure for determining separation distances.

Significant attenuation of incident radiation heat flux through window glass has been noted and measured. However, for purposes of this guide, no credit for such attenuation can be taken for radiation heat flux emanating from adjacent burning buildings since all windows must be assumed to have been destroyed by the blast wave.

Intensity of Thermal Radiation

The intensity of thermal radiation, I, emitted by a radiator can be found from:

$$I = e\sigma T^4$$

where

e = emissivity = 1.0 for this guide

σ = Stefan-Boltzman constant

= 1.36×10^{-12} cal/cm^2-sec^1-deg.C^{-4}

T = absolute temp. = ($^\circ$C + 273°)

The temperature of a fire depends on the rate of burning, and fires may be divided into two types:

- Those in which ventilation is restricted and the rate of burning depends on window size.
- Those in which the window area is approximately the same as the floor area, where the rate of burning depends on the fire load; these are considered to be fully ventilated fires.

Fires with restricted ventilation are not relevant to this guide, and therefore only fully ventilated conditions are considered further.

Peak intensities for test fires are shown in Fig. B-1. From this figure, it is seen that the intensity peaks at about 4 cal/cm^2-sec for all fire loads greater than 12 psf in cubical rooms. In practice, rooms are seldom cubical; therefore, Law recommends using 4 cal/cm^2-sec for all fire levels in excess of 5 psf of floor area and 2 cal/cm^2-sec where fire loads are less than 5 psf.

Configuration Factor

The intensity of radiation, I, on a receiving surface can be related to the intensity, I_o, emitted at the surface of a radiator by the expression.

$$I = \phi I_o$$

where ϕ is the configuration factor. This factor takes into account the geometry of the radiator as "seen" by the receiving surface and the separation distance between the radiator and the receiving surface. In the usual case, many openings in a burning building will be radiating; therefore, the above expression for n openings becomes

$$I = (\phi_1 + \phi_2 + \ldots\ldots \phi_n) I_o$$

Using 0.3 cal/cm^2-sec as the maximum tolerable I on a receiving surface, we have

$$\sum \phi_n = \frac{0.3}{I_o}$$

Thus the separation required becomes the distance where the maximum value of $\sum \phi_n$ is less than the ratio $\frac{0.3}{I_o}$. Since ϕ is proportional to S/C , where S = area of radiating surface and C = the separation distance to the receiving surface, it is possible, given the dimensions and configurations of windows and other openings, to compute the separation distance corresponding to the required value of $\sum \phi_n$. Except for simple radiator geometries, calculation of the magnitude of configuration factors is complicated. Nevertheless, circumstances may arise where the criteria for employing the simplified Law method to determine separation distance cannot be met, or perhaps greater precision in computing distances may be required. In this event, the only recourse is to determine separation distance as a function of ϕ of the radiation surface. Annex A presents two ways in which this may be accomplished: (1) a computational method and (2) an optical analog method.

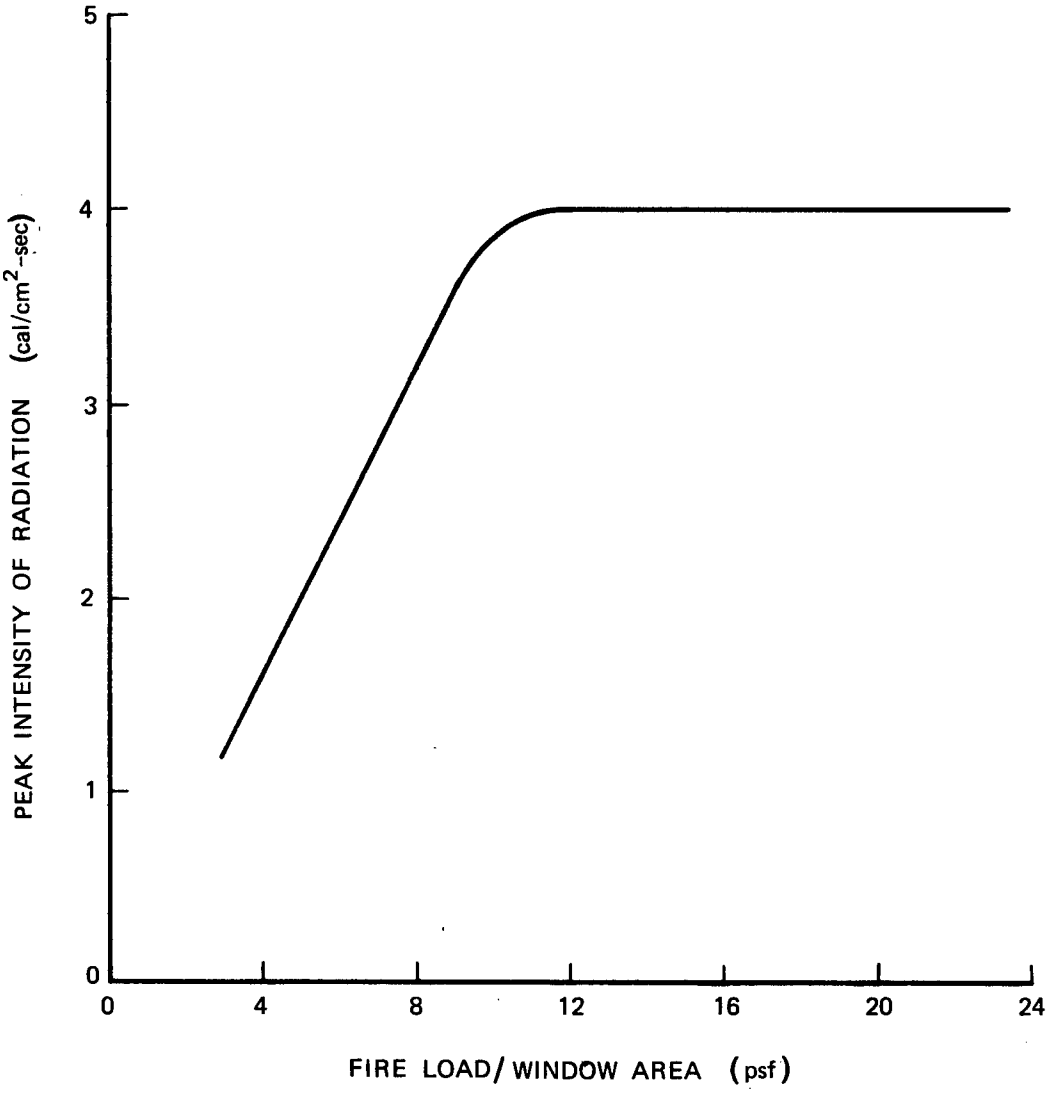

FIG. B-1 TEST FIRE RADIATION INTENSITIES FOR CUBICAL ROOMS[12]
(Floor and window areas approximately equal)

Law's Method

On the premise that most cases will be accommodated if it is assumed that the radiator and receiving surface are parallel to each other, Law has developed a simplified method for determining separation distance.

This method embodies the concept of an "equivalent radiator," which is merely the area on the facade of a building that encloses all facade openings. As used herein, facade or wall openings refer to the area of openings, such as windows and combustible siding, that are capable of transmitting or emitting radiation from the wall of a burning building. Separation distances have been calculated for various percentages of wall openings and the dimension ratio of the equivalent radiator. These are shown in Figs. B-2 and B-3 for fire loads less than, and equal to or greater than, 5 psf. The dimension ratio, N, is a function of the length and height of the equivalent radiator. If the smaller of the two dimensions is designated "A," then N is the ratio of the larger dimension to A. Figure B-4 illustrates the derivation of A and N.

Entering Fig. B-2 or B-3 with the appropriate N and the percentage of wall openings in the equivalent radiator (as shown in Fig. B-4) a value of C/A can be read directly, and, C, the separation distance, is then easily calculated.

As an example using data from Fig. B-4 and assuming a fire load greater than 5 psf:

- N = 2.0
- Percentage of openings = 56%
- Enter Fig. B-2 with N
- Read up to the 56% curve (interpolate)
- Then C/A = 1.95
- C = (1.95)A = (1.95)32 = 62.4 ft.

Building Facade Openings

The separation distance, C, is very sensitive to the percentage of openings in the adjacent burning buildings. Obviously, the most conservative approach would be to assume that a given building has upwards of 100% openings, and this condition will probably prevail at those ground ranges within the 8 psi overpressure region. However there are several reasons

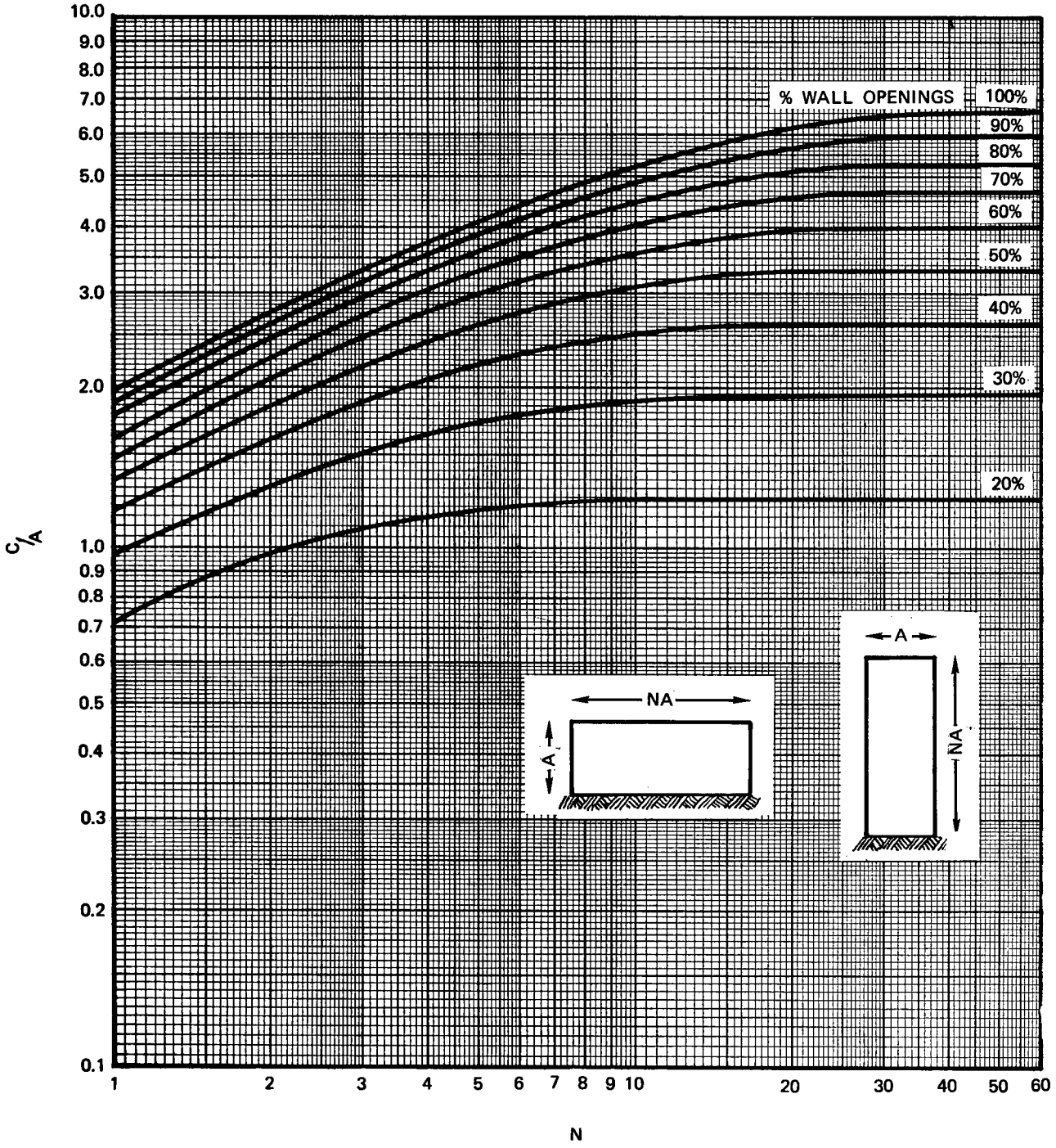

FIG. B-2 SEPARATION DISTANCE "C" FOR FIRE LOAD OF 5 PSF OR MORE[12]

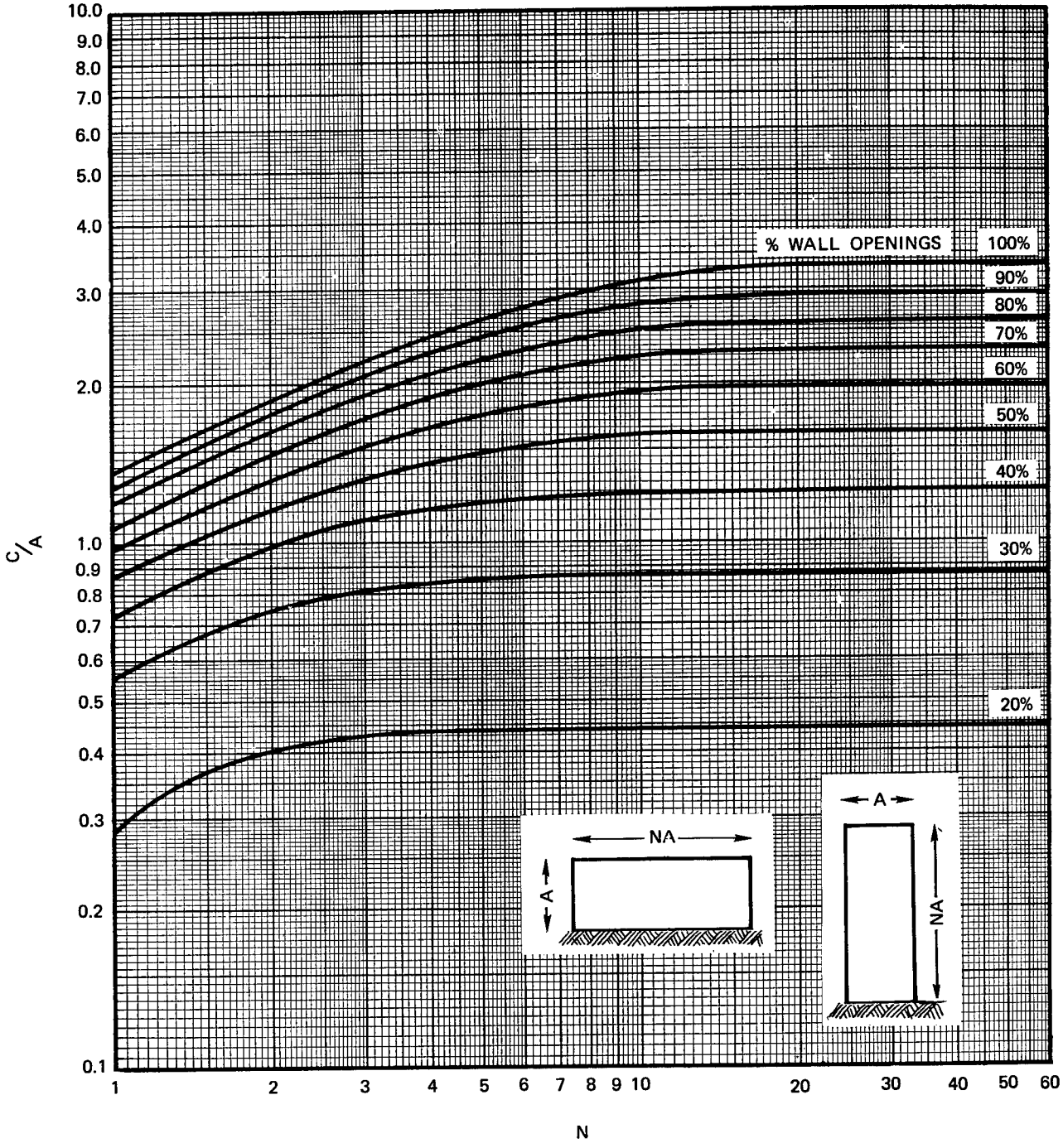

FIG. B-3 SEPARATION DISTANCE "C" FOR FIRE LOAD LESS THAN 5 PSF[12]

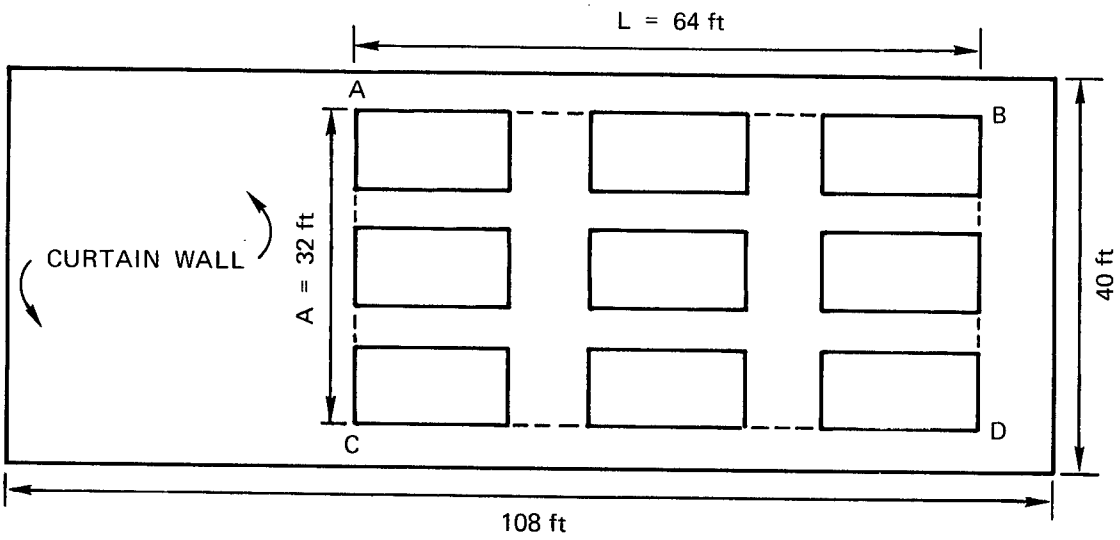

ELEVATION (Scale: 1" ≈ 20 ft)

- H < L, therefore A = H = 32 ft
- L = 64 ft
- N = 64/32 = 2
- Area ABCD = 2048 sf
- Area ABCD encloses all openings and is termed the "equivalent radiator."
- Area of openings (16 x 18) x 9 = 1152 sf
- $\frac{\text{Area of openings}}{\text{Area of ABCD}} = \frac{1152}{2048} = 56\%$

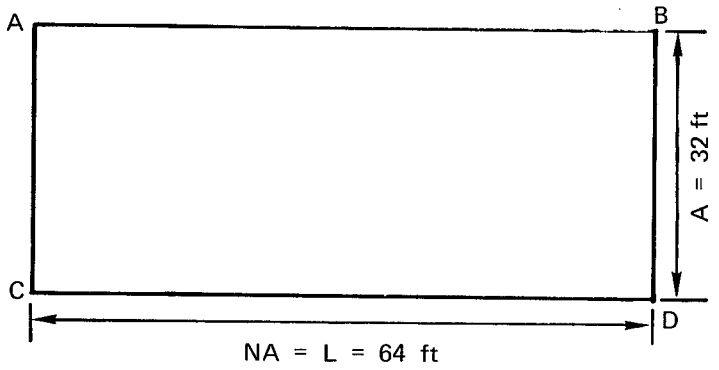

ELEVATION OF EQUIVALENT RADIATOR

FIG. B-4 DERIVATION OF DIMENSIONS FOR EQUIVALENT RADIATOR

for not taking this approach, which would lead to impractically large separation distances.

In this region, blast overpressures would be accompanied by a peak wind velocity exceeding 200 mph. Moll[8] cites studies indicating that many incipient fires would be extinguished in fine fuels by blast winds with a peak velocity greater than 120 feet per second (associated with about 2.2 psi overpressure) and in thicker fuels at 150 feet per second velocities (3.0 psi overpressures). In addition, if curtain walls and windows are demolished in the region inside the 8 psi perimeter, the extremely high blast wind would carry away and scatter the lighter ignition fuels. Admittedly, this is intuitive and a generalization, since in some cases building fuels may be concentrated within a building by blast and thereby aggravate the fire hazard.

These circumstances suggest that, within the 8 psi region, the error caused by selection of building openings as solely the percentage of window and door openings in a facade, ignoring openings caused by curtainwall damage, would be offset in most cases by blast effects on potential ignition points.

Outside the 8 psi region, out to about 2 psi overpressure, there would be regions where framed buildings would also be stripped of curtainwalls and completely exposed by blast--i.e., have 100% openings--without any mitigating effects of blast on ignition points and building fuels. Here again, it is suggested that blast effects on adjacent buildings that offer a fire threat to the shelter building can be ignored. The reasons lie in the following assumptions made by Law:

1. For fuel loads of 5 psi or greater, the thermal radiation is 4 cal/cm^2-sec. This corresponds to a limiting fire temperature of about 1100°C (2000°F).

2. The emissivity of the radiating building is constant at unity.

3. Heat is being radiated simultaneously at the peak intensity from all openings in a building facade.

These assumptions are perfectly suited to the conservative measures advocated for peacetime fires. However, for purposes of fire protection in a nuclear attack environment, they are more restrictive than necessary. For example, thermal radiation is directly proportional to the fourth power of the absolute temperature of the radiating fire. Variations from the limiting fire temperature can cause significant differences in radiation intensity. Also, the emissivity of a building fire would generally be somewhat less than unity, and it would infrequently be the case when all wall

openings are radiating heat of the same intensity in a multistory building. This is so because the combustible contents of buildings and the rate of burning will vary from room to room.

If a mass fire occurred, it is possible that buildings adjacent to the shelter building could ignite and present burning facades that are one expanse of flame. The Law Method, as cited herein, does not accommodate this eventuality. Radiation from such an exposure would exceed the 4 cal/cm^2-sec used by Law as a maximum. However, these conditions would evolve and advance relatively slowly and permit evacuation of an exposed shelter building as an ultimate alternative.

Accordingly, it is recommended that, in the application of the Law Method, determination of openings in exposing, adjacent building facades be limited to the ratio of the area of windows and combustible siding to the area of the facade (this would represent a more hazardous fire situation than the higher overpressure regions where walls have been destroyed but also where fuel loads have been blown away or reduced to debris or rubble).

Recessed Elevations

If a portion of the radiating building facade is set back, as in Fig. B-5, an adjustment in separation distance may be possible.

Generally two types of recesses will be found: (1) a recess with openings on all three sides and (2) a recess with openings only on the rear wall.

With openings on all three sides, the recess will appear as a radiating enclosure. In this case, the area of openings in the recess should be totaled and expressed as a percentage of the area of the aperture. If the total area of openings in the recess is equal to or greater than the area of the aperture, the aperture should be considered as a radiator with 100% openings. In either instance, the aperture is then treated simply as another element of the equivalent radiator representing the facade as a whole, and the corresponding separation distances is found as before. Figure B-5 includes an example problem.

When openings occur only on the rear wall of the recess, a reduction in separation distance is possible. First a value of the separation distance C_1 is found, assuming, as before, that all of the openings within

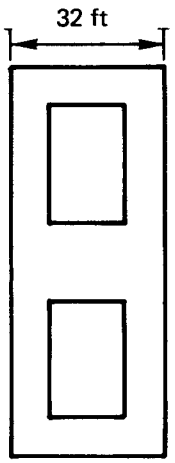

SECTION A-A

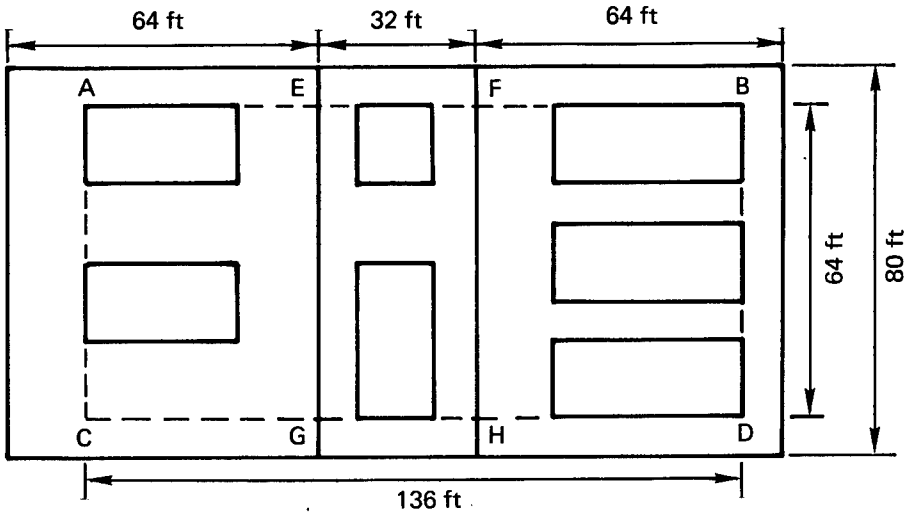

ELEVATION (Scale: 1″≈ 40 ft)

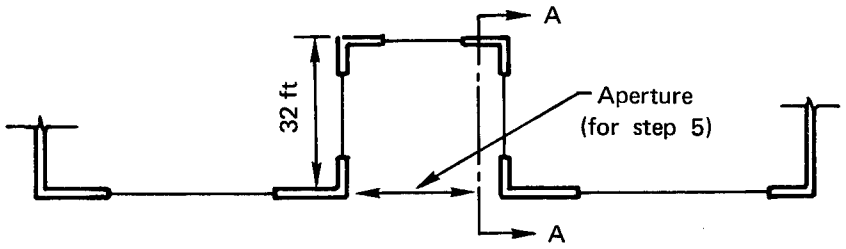

PARTIAL PLAN

1. Area ABCD = 136 x 64 = 8704 sf
2. Area of openings in AECG = 1024 sf
3. Area of openings in FBHD = 1920 sf
4. Area of openings in recess = 2304 sf
5. Area of EFGH = 2048 sf which is less than 2304 sf of recess openings
6. Therefore EFGH = 100% openings
7. Total area of openings = items 2 + 3 + 5 = 4992 sf
8. Percentage openings = $\frac{\text{item 7}}{\text{item 1}} = \frac{4992}{8704} = 57\%$
9. A = 64 ft
10. N = $\frac{136}{64} = 2.13$
11. From Fig. B-2, C/A = 2.1
12. C = A x 2.1 = 64 x 2.1 = 134 ft

FIG. B-5 SEPARATION DISTANCE FOR RECESSED ELEVATION WITH OPENINGS ON ALL RECESS SIDES[12]

the recess are radiating from the aperture. Then the area of openings in the recess are reduced by the factor,

$$\left(\frac{C_1}{C_1 + r}\right)^2$$

where r is the depth of recess. The reduction in the area of openings is possible because of the apparent reduction when viewed from a point at the separation distance. Figure B-6 illustrates the rationale. With the reduction in the area of openings for the recess, a second distance, C_2, is found. An example problem is also given in Fig. B-6.

Elevation with Setback

When a part of a building is set back as shown in Fig. B-7, there can be a corresponding adjustment in separation distance. First the separation distance is found assuming the elevation is in one plane. Then by constructing an equivalent radiator in the manner shown in Fig. B-7, a second separation line is drawn. The final line of separation is then traced as illustrated.

The computation for Fig. B-7 is:

- 21% openings
- A = 30
- More than 5 psf fuel load
- N for ABCD = 110/30 = 3.67
- From Fig. B-2, C/A = 1.18 and C = 35.4 ft
- N for equivalent radiator A'B' = 115/30 = 3.83
- From Fig. B-2, C/A = 1.20 and C' = 36 ft

The space saved is hatched in Fig. B-7.

Elevation with Widely Spaced Openings

If openings, or a group of openings, in a radiating facade are spaced widely apart, a point opposite one may receive a negligible contribution of radiation from the other. When this is true, the openings may be considered separately.

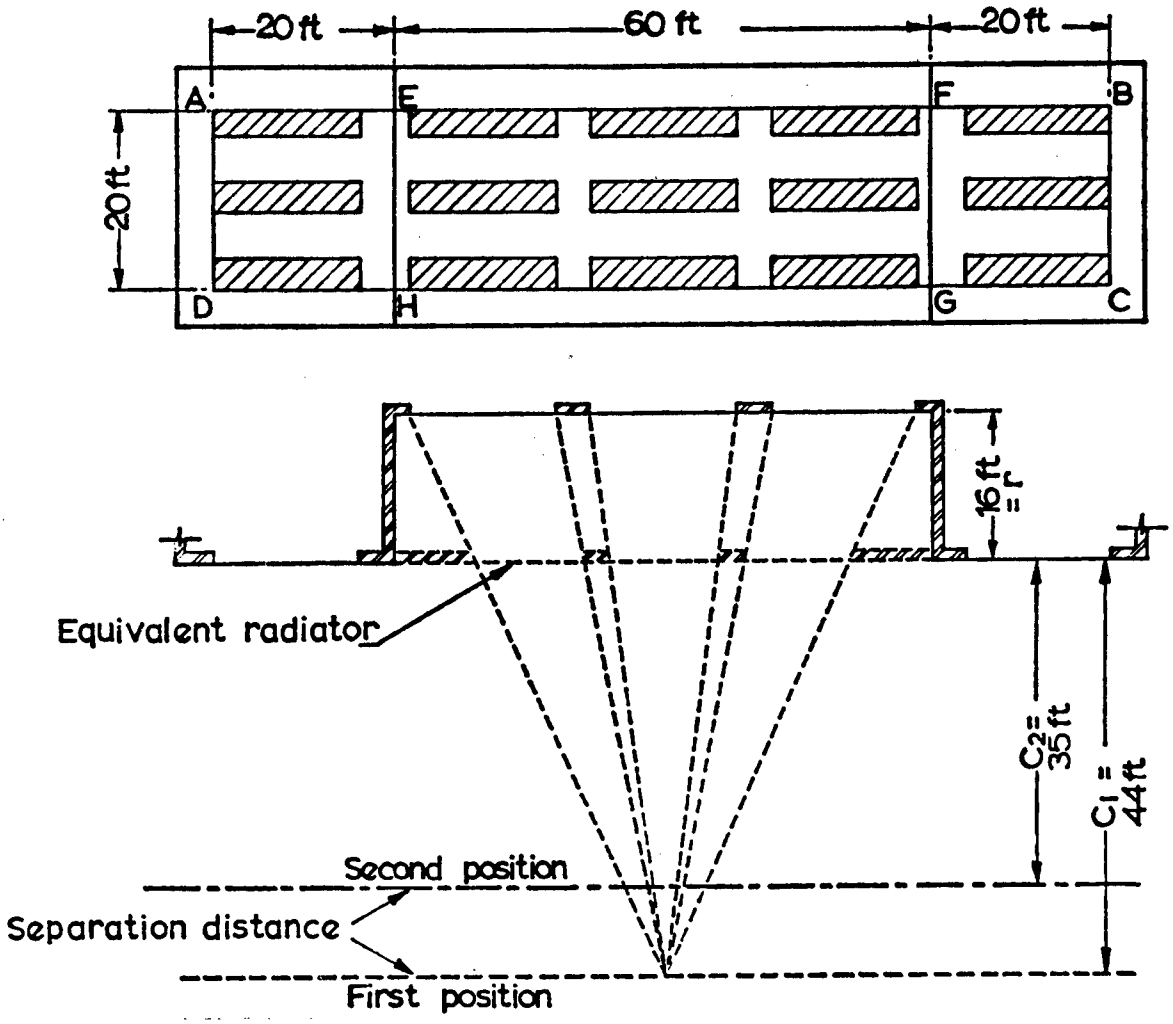

- Given a percentage of openings = 40% for areas AEDH, EFHG, and FBGC
- For the equivalent radiator ABCD, N = 5, A = 20
- From Fig. B-2, a 40% opening gives C_1 = 44 ft.
- Reduction factor = $\left[\frac{C_1}{C_1 + r}\right]^2 = \left[\frac{44}{60}\right]^2 = 0.54$
- Therefore EFGH has 0.54 x 40% = 22% opening
- Then for ABCD overall openings = 29%
- For N = 5, A = 20, from Fig. B-2, $C_2 \approx 35$ ft

FIG. B-6 SEPARATION DISTANCE FOR RECESSED ELEVATION WITH OPENINGS IN REAR WALL ONLY[12]

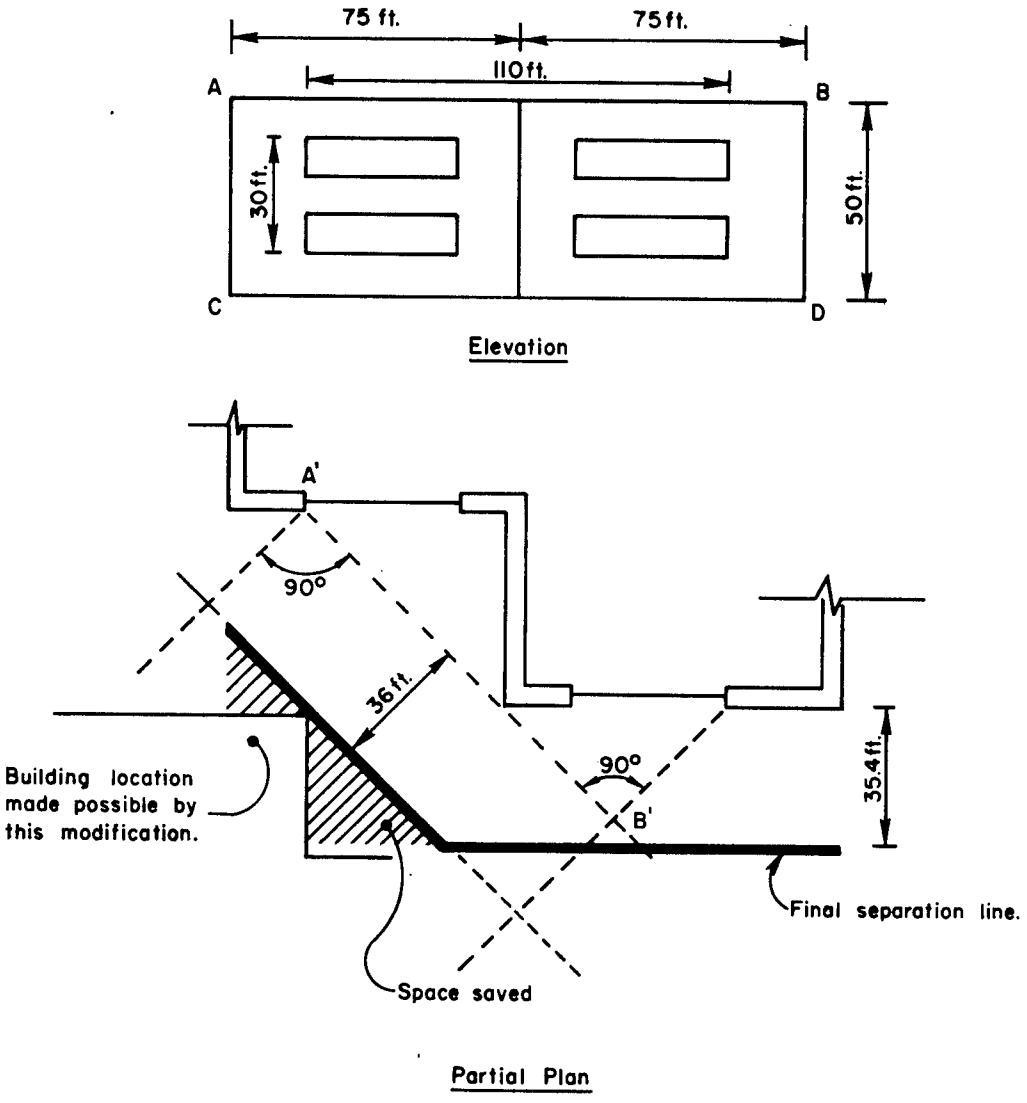

FIG. B-7 SEPARATION DISTANCE WITH SETBACK[12]

The separation distance is calculated first for an equivalent radiator enclosing all openings in the facade. Then, if the horizontal distance between two groups of openings is greater than twice the calculated separation distance, they should be treated as separate radiators. An example is shown in Fig. B-8.

Factors Modifying Separation Distances

Separation distances may be reduced for those facades of shelter buildings that have no openings and are constructed of noncombustible materials. In the extreme, the separation can be zero if a 3-hour fire wall exists between the two buildings.[13] The amount of reduction for other than fire walls is a matter of judgment. Phung[14] states that an examination of German cities suffering fire bombings indicates that a 10-foot separation between two brick buildings "had about a 50% chance of preventing fire spread." Presumably the exposed wall had no openings and, also, the heights of both buildings were comparable.

If exposing, adjacent buildings are one story or more taller than the shelter building, there would be a danger of exposing the shelter building roof to a dangerous level of heat radiation when the calculated separation distance is reduced. Obviously, judgment is required in this eventuality. If the exposed roof is Class A or B, as defined by the National Fire Code,[15] this hazard is nominal. However, for Class C, D, E, or F, danger of ignition is present.

Corrections

The remainder of this section deals with corrections caused by the effects of flames that can be applied to separation distances calculated in accordance with the foregoing Law Method. Application of these corrections will serve to increase separation distances to the extent that an otherwise eligible building may have to be withdrawn as a slanting candidate. Therefore, it is recommended that, as a general rule, flame corrections should be applied only to the extent that candidacy (at least for more detailed consideration) is not obviated. The rationale for this recommendation lies in the fact that 100% protection from firespread, on the basis of building separation distances, is neither practical nor possible in urban areas (e.g., by flying embers). Also, as previously stated, the objective of this appendix is to minimize the chance of firespread on the premise that shelter evacuation is reserved as the ultimate alternative in those instances where the shelter building is dangerously threatened by fire.

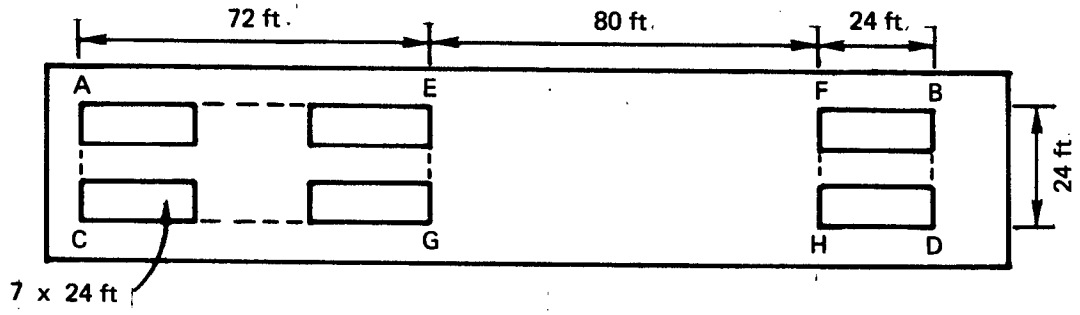

ELEVATION (Scale: 1" ≈ 40 ft.)

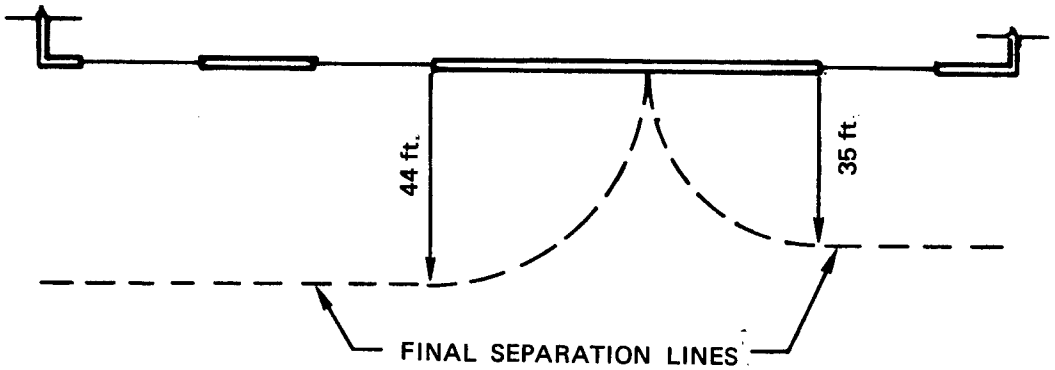

PARTIAL PLAN

- For equivalent radiator ABCD, Area = 176 x 24 = 4224 sf
- A = 24, N = $\frac{176}{24}$ = 7.3
- Area of each opening = 7 x 24 = 168 sf
- Area of all openings in ABCD = 1008 sf
- Percentage openings = $\frac{1008}{4224}$ = 24%
- From Fig. B-2 C/A = 1.45, C = 35 ft
- Since 80 ft is greater than twice 35 ft consider each area, AECG and FBHD, separately
- Area AECG has 39% openings, N = 3, A = 24. Then C from Fig. B-2 = 44 ft
- Area FBHD has 58% openings, N = 1, A = 24. Then C from Fig. B-2 = 35 ft

FIG. B-8 SEPARATION DISTANCE FOR BUILDING WITH WIDELY SPACED OPENINGS[12]

Adjustment for Window Flames

The Law Method does not consider the contribution to the total thermal radiation from a burning building made by flames emitted from windows and other openings. In those instances where an exposing building may have a high interior fuel load and a large percentage of wall openings, a fully involved fire in the building may present a single expanse of flames over 100% of the exposing facade. One way in which to account for this circumstance is an appropriate increase in the percentage of wall openings in the exposing facade.

Adjustment for Roof Flames

Adjustment for roof flames must be approached on a case-by-case basis. The type of roof construction, its age and condition, the number and type of roof openings, and the presence or absence of combustible roof structures--such as cooling towers--are all factors that must be considered.

It is suggested that recommendations of experienced fire department personnel be obtained where the combustibility of roofs may be an issue. Their suggestions as to potential flame height may be accounted for by increasing the area of a burning facade by an amount equal to average flame height multiplied by the horizontal dimension of the facade. The flame area would of course be incorporated into the equivalent radiator.

Cohn[11] recommends roof flame heights as follows:

- flat or slightly peaked wood roofs 30 ft
- medium peaked and bow-string roofs 45 ft
- high peaked roofs 60 ft

Bending of Flames Due to Wind

A rational method to account for the increased separation distance due to bending of flames has not been developed. However, it has been suggested[11] that exposure separation distances should be increased as follows:

- For "light" winds - no increase
- For "average" winds - add 25 feet to the separation distance for light winds

- For "higher" winds - add 40 feet to the separation distance for light winds

Section 2 - Interior Fires and Associated Biological Hazards

Background

Fire hazards and behavior in a shelter building, following an enemy attack, must be regarded differently than peacetime fires. During peacetime, the rate of fire spread and smoke production assumes primary importance in terms of establishing a safe exit time for evacuation of building occupants. Furthermore, building component fire ratings imply that evacuation of the building is possible, organized fire-fighting forces are available, and an adequate water supply exists.[16,17]

On the other hand, evacuation of a shelter building would be hazardous following nuclear attack because of fallout. Since a shelter building fire may compel evacuation if left to grow unchecked, shelter occupants would have to be prepared to suppress incipient fires throughout the shelter building.

Fire Hazard Factors

The most pertinent biological fire hazard factors affecting shelter occupants are:

- Heat
- O_2 depletion; CO_2 and CO build-up
- Smoke

In considering these factors, the shelter area is assumed to be located in the basement of a multistory building for purposes of this guide.

Heat

In circumstances where a shelter wall or ceiling is exposed to a building fire, the hazard to shelter occupants from heat would depend on the fire intensity and duration and the diffusivity and thickness of the exposed shelter component. The most hazardous condition would occur when the shelter ceiling, functioning as the floor slab of the first story, is exposed to a rubble fire.

Fuel, or fire, loads in commercial, industrial, and public buildings commonly exceed 10 psf in a significant proportion of spaces.[4,17]

Leutz[18] states that with a building fire load of approximately 7 psf German investigations determined that it is possible for the debris from a building fire to maintain a temperature of 300-400°C (572-752°F) on a floor slab for periods of up to 5 to 6 hours. Under the assumption that temperatures in the debris will obtain at the exposed surface of the floor slab, Leutz states that modeling techniques indicate a temperature of 50°C (122°F) is reached on the underside of an 8-inch, reinforced concrete floor slab within 2 to 3 hours after a temperature of 300-400°C (572-752°) is reached and sustained on the upper surface of the slab.

It is not known if the effect of ventilation on the underside of the exposed slab was considered by Leutz. Further, his assumption that temperatures inside a burning debris pile, located on a concrete slab, are also developed at the exposed surface of the slab may be overly conservative and needs to be tested by appropriate experiments. However, under these conditions survival of shelter occupants may depend heavily on adequate ventilation or other countermeasures such as removing or cooling off the burning debris on the exposed side of the slab.

Tests have been conducted by the National Bureau of Standards[17] in fire resistive buildings using various fire loads to simulate occupancy types. The time-temperature curves of these tests are plotted against the NBS Standard Time-Temperature Curve and are shown in Fig. B-9. Even for the lightest fire load tested, 8.5 psf, the "cooling out" rate after the peak of the fire gives a residual room temperature of 700°F after 1-1/2 hours, and a conservative extrapolation would still show a residual temperature in excess of 500°F after 2 hours.* However, if the burnout of a building were not accompanied by collapse of structural components, it is unlikely that sufficient heat would be developed in the floor slab to jeopardize shelter occupants. On the other hand, if burnout were accompanied by collapse of structural components, and an accumulation of hot rubble blanketed the floor slab, countermeasures might have to be taken. Rubble fires may smolder for days at a time. A full scale building fire test conducted by the National Bureau of Standards[15] measured temperatures in the rubble pile that persisted "in the vicinity of 1000°F for a period of 2 to 3 days."†

---

* These temperatures were not measured at the surface of floor slabs but rather were taken at some intermediate level within the rooms involved in fire.

† Tests conducted by the U.S. Forest Service, Dept. of Agriculture, on a municipal building registered 1900°F in the rubble pile nearly 24 hours after the building was set on fire.[20] Slab surface temperatures were not reported.

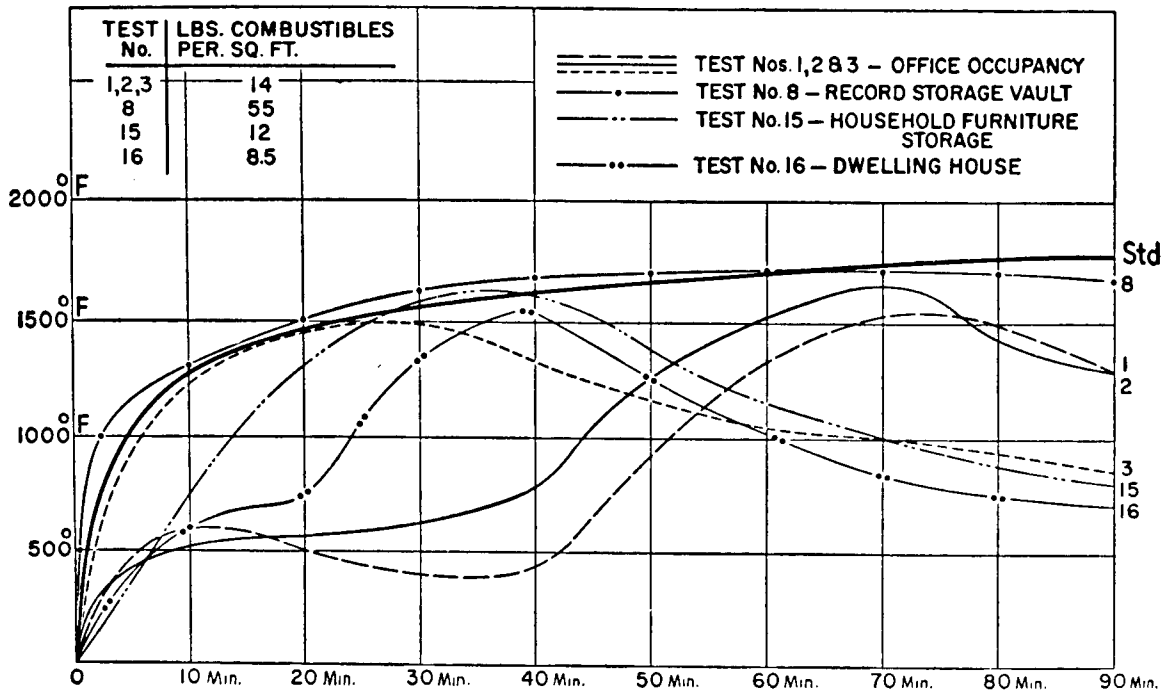

Actual time-temperature curves recorded in tests as compared with the Standard Time-Temperature Curve. This indicates the relative fire severity depending upon different fire loading. The Standard Time-Temperature Curve, while used as a convenient measure for general fire testing, actually represents a condition of high fire severity met in the early stages of actual fires only where combustible materials are of such a character as to favor rapid development of high temperatures.

FIG. B-9 TIME-TEMPERATURE TEST CURVES

Table B-1 lists equivalent fire severities covering a wide range of fire loadings for "offices and light commercial occupancies."

Table B-1

ESTIMATED FIRE SEVERITY FOR OFFICES AND LIGHT COMMERCIAL OCCUPANCIES[17]
(Data for Fire Resistive Buildings with Combustible Furniture and Shelving)

Combustible Content Total, Including Finish of Floor and Trim (psf)	Heat Potential, Assumed* (Btu/sf)	Equivalent Fire Severity, Approximately Equivalent to that of Test Under Standard Curve for the Following Periods:
5	40,000	30 min
10	80,000	1 hr
15	120,000	1-1/2 hrs
20	160,000	2 hrs
30	240,000	3 hrs
40	320,000	4-1/2 hrs
50	380,000	7 hrs
60	432,000	8 hrs
70	500,000	9 hrs

* Heat of combustion of contents taken at 800 Btu/lb up to 40 psf, 7600 Btu/lb for 50 psf, and 7200 Btu/lb for 60 psf and more to allow for relatively greater proportion of paper. The weights contemplated by the tables are those of ordinary combustible materials, such as wood, paper, or textiles.

Safe exposure periods for humans at various combinations of temperature and relative humidity are given in Fig. B-10. If a critical temperature of 50°C (122°F) is assumed, it is readily seen that even under

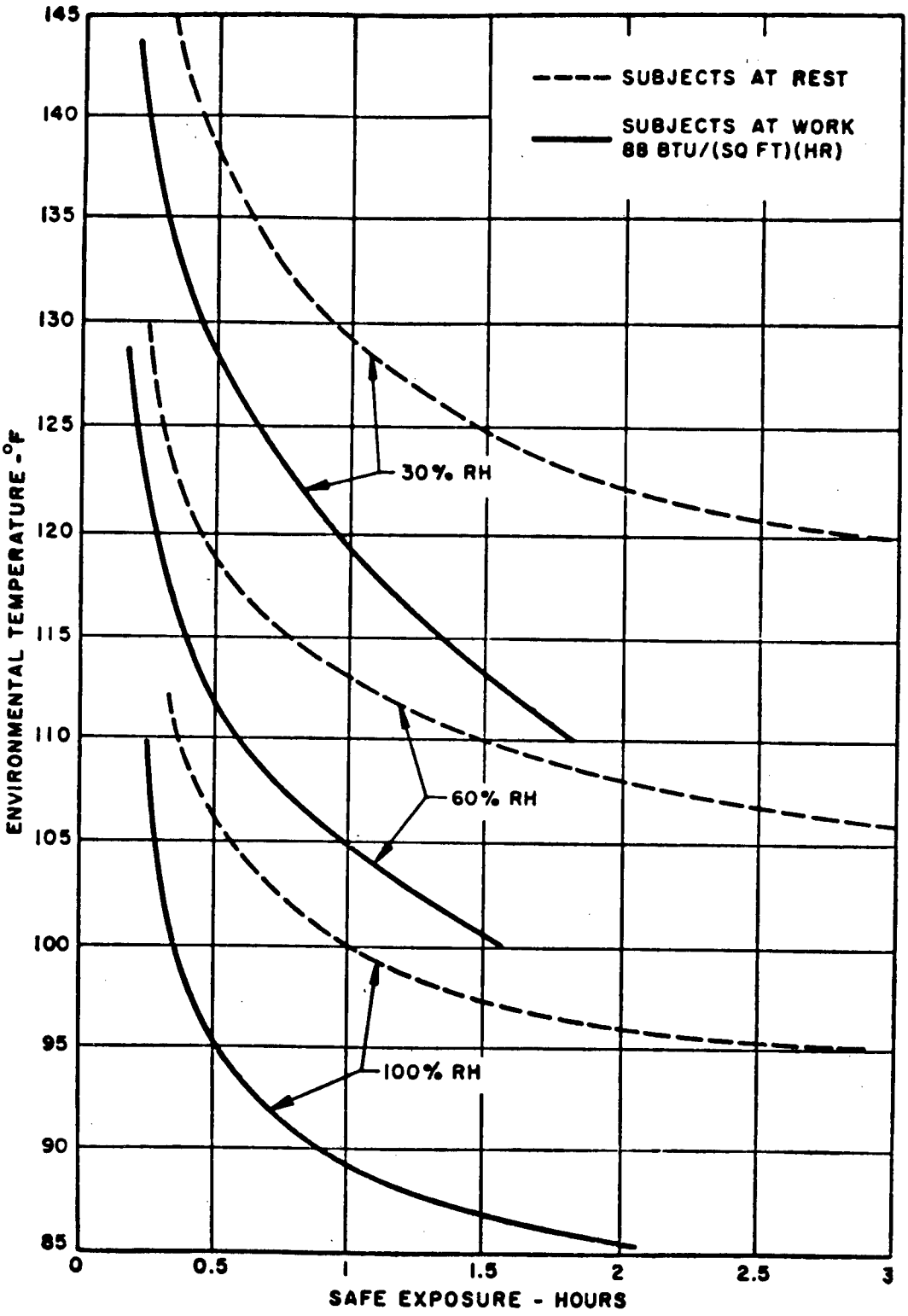

Reprinted by permission from ASHRAE Handbook of Fundamentals (1967)

FIG. B-10 SAFE PERIODS OF EXPOSURE FOR EXTREME ENVIRONMENTAL TEMPERATURES

moderate conditions of 30% relative humidity, those exposed could not survive much beyond 3 hours. Of course, higher humidities can be expected in shelters, and, consequently, safe exposure periods would be considerably less than 3 hours unless special provisions for cooling were undertaken.

As safe exposure periods are exceeded, the physiological effects are disastrous.[19] Body temperatures rapidly rise, metabolism increases, and heat stroke quickly follows.[19]

O_2 Depletion; CO_2 and CO Build-up

Dangerous depletion of oxygen and CO_2 build-up in a shelter in an external fire environment would be unlikely. On the other hand, there could be a danger from CO poisoning. During the Hamburg fire storm of World War II, occupants of bunker type shelters were compelled to shut down ventilation plants until the fire storm had subsided to avoid drawing in heat, smoke, and CO. Yet, in spite of gross overcrowding in the bunkers and extremely uncomfortable conditions, survival was nearly 100%. The bunkers were massive concrete structures and were gasproof, since they were fitted with air locks and gasketed doors. Occupants of the relatively primitive, neighborhood basement shelters were not so fortunate, and deaths from heat, smoke, and CO were common although even here more than 80% of shelter occupants survived.[19,21] Earp[23] concludes that:

> When the ventilating systems (including filtration) of public shelters were worked during incendiary raids and especially during fire storms, there was a danger of carbon monoxide being drawn in because it is not absorbed by the filters; nor does the gas mask protect against it. Hence in the Hamburg raids it was very fortunate for the shelter occupants that so many of the ventilating systems were closed down after a short time. Even when the ventilating plant was stopped, carbon monoxide might get in when doors were opened to admit people during a raid.
>
> It can be concluded that there is a real danger of carbon monoxide poisoning both in shelters and in the streets. The calm appearance of the features and the natural position of many of the corpses found in the Hamburg shelters was a strong indication that death was due to carbon monoxide poisoning or to heat exhaustion.

Nevertheless, it is believed that such conditions would be less severe in the United States, primarily because building densities in this country are substantially less than those in Hamburg during World War II.

Fires within a shelter building, however, would present a danger from O_2 depletion and CO_2 and CO build-up with the maximum hazard occurring when the fire was in the shelter. It is for this reason that shelter occupant countermeasures are so important.

Table B-2 summarizes the biological effects on man of various levels of concentration of O_2, CO_2, and CO. It should be noted that the effects of a varying proportion of each gas assumes an environment with normal concentrations of the other two gases. It is known that O_2 depletion when accompanied by increased levels of CO_2 and CO has a synergistic effect; however, quantification of these aggravated effects is lacking.[23]

Sufficient experimentation to provide an adequate basis for analysis of the behavior of fire-generated gases within structures has not been performed. However, full scale experimental building burns conducted by Waterman[16] do give some specifics in this regard. Some of his conclusions are:

1. Oxygen depletion in an active fire zone of a burning building will be reproduced throughout interconnecting spaces on the same or higher stories of a relatively "tight" structure or structural portion (unless very large volumes are being considered). Oxygen levels as low as 5% were measured (normal air has 20.9% O_2).

2. In a burning building shelters remote from the fire zone within that building--i.e., not exposed to a direct threat from thermal effects--and located on the same or higher floor level as the fire would be exposed to CO concentrations equal to 75% of those recorded in the fire zone. Since CO concentration in the fire zone attained a maximum of 3.3%, the shelters were exposed to levels up to 2.5% CO, well above the lethal limit of 1.28%.

3. In fire resistive construction, downward movement of CO, emanating from fires on floors above a shelter, will probably not occur.

4. However, wind pressures can drive fire gases into shelter spaces even if fire generated pressures are not sufficient to do so. Smoldering fires may produce significant infiltration of toxic gases by this means.

5. Fire gases infiltrating a shelter having otherwise cool floor, walls, and ceiling do not significantly heat the shelter air space and would represent a hazard only because of toxicity or the ignition of combustibles within the shelter.

Table B-2

PHYSIOLOGICAL EFFECTS OF OXYGEN,
CARBON DIOXIDE, AND CARBON MONOXIDE[24]

Effects of Oxygen Deficiency

Oxygen Content of Inhaled Air (percent)	Effects
20.9%	No effects; normal air.
15	No immediate effect.
10	Dizziness; shortness of breath; deeper and more rapid respiration; quickened pulse, especially on exertion.
7	Stupor sets in.
5	Minimal concentration compatible with life.
2-3	Death within one minute.

Effects of Carbon Dioxide

Carbon Dioxide Content of Inhaled Air (percent)	Effects
.04%	No effects; normal air.
2.0	Breathing deeper; tidal volume increased 30%.
4.0	Breathing much deeper; rate slightly quickened; considerable discomfort.
4.5-5	Breathing extremely labored, almost unbearable for many individuals. Nausea may occur.
7-9	Limit of tolerance.
10-11	Inability to coordinate; unconsciousness in about 10 minutes. Symptoms increase, but probably not fatal in 1 hour.
25-30	Diminished respiration; fall of blood pressure; coma; loss of reflexes; anesthesia. Death after some hours.

Table B-2 (concluded)

Effects of Carbon Monoxide

Carbon Monoxide Content of Inhaled Air (percent)	Effects
0.02%	Possible mild frontal headache after 2 to 3 hours.
0.04	Frontal headache and nausea after 1 to 2 hours. Occipital (rear of head) headache after 2-1/2 to 3-1/2 hours.
0.08	Headache, dizziness and nausea in 3/4 hour. Collapse and possible unconsciousness in 2 hours.
0.16	Headache, dizziness, and nausea in 20 minutes. Collapse, unconsciousness, and possible death in 2 hours.
0.32	Headache and dizziness in 5 to 10 minutes, unconsciousness and danger of death in 30 minutes.
0.64	Headache and dizziness in 1 to 2 minutes, unconsciousness and danger of death in 10 to 15 minutes.
1.28	Immediate effect. Unconsciousness and danger of death in 1 to 3 minutes.

6. Although much more data are needed on real fire environments and movement of fire gases through complex structures, the above conclusions lead to a further statement that fires within a "tight" envelope, such as a basement containing a shelter, cannot be tolerated and must be extinguished unless the barrier between the fire and the shelter is perfectly gas tight.

7. A ventilating system equipped to maintain a slight overpressure (1/4 to 1/2 inch of water) in the shelter would normally ensure against infiltration of smoke and toxic gases from fires external to the shelter. (However, if outside fires were present, the ventilating system might have to shut down for a period anyway - a situation that did occur in the Hamburg fire storm. As an alternative to maintaining an in-shelter overpressure, toxic gas infiltration must be avoided by taking appropriate measures to seal all openings in the shelter.)

Smoke

Smoke is the most significant of the lesser known hazard factors in a fire environment. Although each year many hundreds of casualties from smoke inhalation are reported, Lee[23] states that little is known about the actual biological mechanisms involved. This is primarily because smoke is such an ill-defined term. The generic term, "aerosol," defines smoke, fog, hazes, and fumes as a suspension of particles, liquid or solid, in a gaseous phase. However, the chemical constituents of these gaseous suspensions are difficult to evaluate. For example, smoke from the same sample of fuel will vary in the composition of the products or compounds in suspension depending on the rate at which it is heated and burned.

Although opinions vary, some observers state that true cases of fatalities from smoke inhalation are rare and that most casualties ascribed to smoke really are because of asphyxiation or CO poisoning.[23] Nevertheless, a quantitative evaluation of the threat posed by smoke is not possible, in contrast with O_2 depletion and CO_2 and CO build-up, under the emergency conditions that would prevail in a shelter. Therefore, because of the high probability that smoke and fumes would be toxic, it must be assumed that all smoke and fumes are potentially lethal in the immediate environment of a shelter.[25]

Causes of Fire

The principal cause of initial building fires during nuclear attack would be ignition of interior fuels by radiation from the thermal pulse. Following the attack, shelter buildings could be exposed to ignitions stemming from the radiation effects of adjacent burning buildings, flying brands, and secondary ignitions caused by blast damage.

Therefore, by limiting the radiant heat energy that could penetrate a building, a significant reduction in ignitions may be obtained.

Flying brands and embers would pose a continual threat during the entire time in shelter. The thermal radiation from a weapon threatens only for a few seconds and that from adjacent burning buildings no longer than the total burnout time of the buildings, a matter of a few hours to a half day under the worst conditions. However, flying brands emanating from fires elsewhere in the city could be carried great distances. They would become particularly prevalent and dangerous in conjunction with mass fires and conflagrations, which invariably develop large quantities of brands and embers. Usually the most serious threat is to roofs, but in a mass fire environment, wind and convection currents frequently develop a horizontal component sufficiently strong to carry brands into window openings. Fortunately, the threat from flying brands is amenable to control by fire watch teams, as discussed in Section 3 of this appendix.

Building codes commonly require Class A or B roof coverings within the fire limits of a city or wherever fire-resistive building construction is involved.[17] Class C roof coverings are often specified in some cities as a minimum standard. All three classes "possess no flying brand hazard."[17] Nevertheless, the latent protection offered by these classes of roof coverings could be severely taxed in the vicinity of a mass fire, and monitoring and corrective action would have to be taken and should be anticipated by shelter personnel.

Build-up of Fires

When a sustained ignition occurs in a room, there follows a period of heat build-up that eventually leads to total involvement of the room in fire. This is called a "flashover," and it is accompanied by a sudden and drastic surge in temperature.

The period of time required to reach flashover depends on the contents of the room and its size. The higher the fuel loading and the smaller the room, the sooner flashover occurs.[25] In a typical residential room, the time elapsing to flashover is about 15 to 20 minutes following ignition.[26]

Following room flashover, the fire is capable of penetrating other rooms in a building. Horizontal and vertical firespread largely depends on a building's geometry and construction. The presence and integrity of firedoors and firewalls are important in suppressing the spread of the fire. In multistory buildings, the construction of the floors and ceilings is also important. Where they are made of noncombustible materials, vertical fire spread will be limited to stairwells, elevator shafts, and other openings. Use of noncombustible materials can greatly contribute to the effectiveness of firefighting attempts. Other factors that affect the spread through the building are the fuel or fire loading, the position and compartmentalization of hallways, and the location of the initial ignition.

Under building conditions where the buoyant, hot gases of a fire are not confined, fires will usually spread to higher levels. Downward spread from the floor of ignition will subsequently occur only if structural failures expose lower floors to falling embers and debris. Thus downward spread depends on fire loading and structural fire resistance. Provided that the fire resistance ratings of structural components conform to the criteria in the following section, it is unlikely that downward spread of fire will occur.[25]

However, even with good fire resistive construction, fires should not be allowed to develop. Possible blast damage to fire doors and the threat presented by smoke and toxic gases would demand that fires be suppressed as soon as possible after ignition. Fortunately, studies have shown that small self-help teams of untrained men, using portable fire extinguishers, are effective in fighting room fires up to a point just before flashover.[27] After flashover, the only recourse is to attempt to seal off the rooms involved.

Section 3 - Design Countermeasures

Objectives

The objectives of design countermeasures against the threat of fires are to:

- Minimize ignitions of the shelter building by radiation from the thermal pulse of a weapon and from adjacent burning buildings.
- Provide portable fire extinguishers for the use of shelter fire teams enabling them to extinguish incipient fires.

- Minimize spread of fire by appropriate construction directed to containment of fire on the floor of origin.
- Minimize downward spread of fires from the floor of origin.
- Prevent spread of smoke, toxic gases, and heat.
- Restrict shelter building candidates to those occupancies having moderate or lesser fire loadings.

Wherever the following criteria are exceeded by the National Building Code[13] for the type of fire-resistive construction and occupancy selected for the shelter buildings's primary use, that code or any other applicable codes shall govern.

Radiation

Exterior wall openings, and roof openings such as skylights, should be provided with aluminized blinds or reflective drapes of noncombustible composition to provide protection from the thermal pulse of the weapon.[28,29] Ordinary painted metal venetian blinds, when closed, will also suffice, even though the paint will char, provided that they are hung with noncombustible tapes. As a minimum, shielding should be provided on the first floor of the shelter building.

Protection from radiation from adjacent burning buildings should be provided by siting to obtain appropriate separation distances as described in Section 1 of this appendix.

Portable Fire Extinguishers

One 5-gallon stirrup pump type extinguisher with extra length hose (at least 6 feet long) should be provided for each 1,250 sf of shelter area with a minimum of 4 extinguishers per shelter. Also one 5-gallon stirrup pump type extinguisher should be provided for each 5,000 sf of nonshelter area.[29]

Structural Criteria

The minimum fire resistance ratings for structural components of shelter buildings should be that specified for "Ordinary Construction" as defined in Section 707 of the National Building Code, except that

separation distances calculated by the Law Method should govern where exposed facades (or walls) have window openings. Horizontal separation as defined by the National Building Code is not the same as the separation distance used by Law. Rather, under the code, horizontal separation is established for each type of building, then the separation distance between two buildings becomes the sum of their respective horizontal separations.

Table B-3 summarizes the fire resistance ratings for "Ordinary Construction."

Smoke and Toxic Gases

One alternative for protection of the shelter against infiltration of smoke and toxic gases would be to provide an independent, emergency shelter ventilation system designed to provide a positive pressure in shelter spaces of 1/4 to 1/2 inch of water.[25]

The other alternative is to seal the shelter against infiltration. Penetrations of the shelter walls and ceilings by cables, pipes, and ducts should be grouted or equipped with sealants or gland seals to prevent infiltration. Ventilation ducts extending from the normal building ventilation system into the shelter should have vaportight fire dampers installed at the point of entrance to the shelter.[17] These should be automatic, heat-fused dampers capable of being operated manually by shelter personnel from inside the shelter.

The alternative chosen will depend on cost-effectiveness considerations.

Combustible Contents

It is recommended that the maximum combustible fire load for any floor level posing a threat to the shelter should not exceed an average of 15 psf. Fire loads are composed of combustible furnishings, equipment, and structural components. Building occupancy generally governs the fire load. To select candidate shelter buildings, the proposed occupancy of a building can be checked against National Bureau of Standards data on the combustible contents of representative buildings by occupancy.

If candidate buildings are to be equipped with automatic sprinklers, to the extent that such sprinklers exceed the minimum requirements of the codes[13,30] a proportionate increase in the 15 psf maximum average fire

Table B-3

MINIMUM FIRE RESISTANCE RATINGS FOR ORDINARY CONSTRUCTION[1,3]

Component	Horizontal Separation (feet)	Maximum Percentage of Windows to Wall Area	Minimum Fire Resistance Rating
Exterior bearing walls*	0-3	0%	3 hours
	3-20	20	2 hours
	20-30	30	2 hours
	Over 30	40	2 hours
Exterior nonbearing walls*	0-3	0	3 hours
	3-20	30	2 hours
	20-30	40	1 hour
	Over 30	100	None required
Interior bearing walls*			2 hours
Interior partitions enclosing elevator shafts, stairways, and so forth, through floors of buildings four stories or more in height			2 hours
Interior partitions enclosing elevator shafts, stairways, and so forth, through floors of buildings fewer than four stories in height			1 hour
Roof structure			1 hour
Roof covering			Class A or B
Interior finish, maximum flame spread rating in nonshelter areas			75†
Interior finish, maximum flame spread rating in shelter areas			25†

* All exterior walls and interior load-bearing walls will be of approved noncombustible materials.

† Index based on ASTM E-84 Tunnel Test Method.

load may be allowed provided that the building sprinkler system is served by a gravity tank system that may be expected to survive the air blast loading.

Section 4 - Shelter Occupant Countermeasures

Fire countermeasures in a shelter building must be viewed as a purely local problem. Outside assistance could not be depended on, and shelter occupants would have to be prepared to take appropriate self-help measures against the threat of fire. Detailed guidance in this regard has been developed by IIT Research Institute in a report covering shelters in existing buildings.[29] The report is equally applicable to shelters in slanted buildings, and pertinent paragraphs therefrom have been incorporated in this section.

Organization

The shelter fire chief should be selected well before an emergency period and receive special shelter fire fighting training. He should be chosen from the normal peacetime occupants of the building who are familiar with its interior layout, location of utility system controls, and characteristics of its occupancy. In addition, he should possess some firefighting or fire protection background. He should receive training covering all phases of fire prevention, detection, and extinguishment, including planning, equipping, and implementation techniques. He should also be responsible for the necessary equipment and be familiar with its use. In the attack period, he will be charged with staffing, instruction, and supervision of firefighting and fire watch teams, as well as other personnel engaged in fire prevention activities.

The successful suppression of all incipient fires that could occur within fallout shelter areas and other portions of shelter buildings would depend on the availability of sufficient personnel within each shelter who possess the ability to handle such fires utilizing only portable extinguishing appliances.

Fires of this nature could be effectively controlled by the use of two-man self-help teams, with each man equipped with an extinguisher and smoke mask. Therefore, the number of shelter firefighting personnel should be a multiple of the number of portable extinguishing appliances required for any given shelter building. It would appear reasonable to use a basis of three firefighters per extinguisher since this would allow

for three 8-hour shifts and would also permit periodic rotation of firefighting personnel where required to limit total radiation exposure.

All personnel should be given training that includes actual suppression of interior fires utilizing portable extinguishing appliances and smoke masks. In addition, basic instruction should be provided with reference to the types and mode of operation of various types of automatic sprinkler, standpipe and hose, and other extinguishing systems to ensure their maximum utilization when available in shelter buildings.

Shelter Building Vulnerability

Initially, the shelter building should be surveyed to determine its vulnerability to fire and potential countermeasures. The survey should include:

- Identification of fire limiting areas capable of unsuppressed burnout.
- Determination of measures necessary to prevent spread of smoke and toxic gases into shelter areas.
- Potential hazard of fire exposure from adjacent buildings.
- Development of measures necessary to prevent primary ignitions from a weapon's thermal pulse.
- Determination of utility and process systems to be taken out of service in time of emergency.
- Inventory of fire control equipment and facilities.

The results of these surveys should be used by the fire chiefs and shelter managers to develop a fire control operational plan.

A quick, empirical method of assessing fire vulnerability of a shelter building, in terms of firespread potential, has been developed by Varley and Maatman.[29] It is limited to nonoperational, undamaged structures and may be used for an entire building or to draw conclusions about individual floors. Application of this method on an annual basis, and in conjunction with recommendations by professional firemen or fire engineers, would serve three valuable purposes: (1) forewarning the shelter staff of changed building conditions, e.g., fire load and structural modifications; (2) acquainting shelter staff with the building's firefighting

facilities and their condition; and (3) orienting the staff's thinking within a framework of basic fire engineering principles.

Because the shelter building might sustain damage in a nuclear attack, contingencies might arise that could not be foreseen in advance. For example, fire walls, barriers, fire doors, and smoke vents could be damaged and rendered ineffective. For this reason, generalizations about fire behavior that may be inferred from a fire vulnerability survey should be avoided or, at the very least, they should be treated with circumspection. Some fire behavior generalizations to guard against are:

- "Downward movement of CO will probably not occur." This does not mean that such a condition cannot occur. In tests conducted by Waterman[26] fires generated gas pressures that caused CO to penetrate floor levels below the fire. Also Earp[22] states that: "Thus it is quite likely that the occupants of basement shelters in Germany were poisoned by carbon monoxide in the smoke penetrating from the streets or burning buildings above."

- "A fire in the upper stories of a building will burn upwards" implies relative safety for the occupants on lower stories. In fact, if fire barriers are lacking or have been damaged, it is possible for fire to spread downwards.

- "Fire within a shelter space is only a problem of suppression since it will be discovered when incipient" is a dogmatic assumption and is highly dangerous. An "incipient" fire inside a shelter space may progress far enough to generate intolerable levels of CO_2 and CO if its discovery depends on chance observations by occupants. Furthermore, before a small fire can be extinguished, the smoke generated may become intolerable.

Consequently, the shelter manager should base planned remedial action on the somewhat subjective conclusion that (1) any fire on the floor levels above a shelter is potentially dangerous and (2) any fire on the same level as the shelter, either inside or outside, is potentially lethal. The nature of remedial action then becomes obvious - suppress fires as they occur.

Fire Control Plan

Both preattack and postattack operations must be covered in the fire control plan. As a minimum, the preattack plan should include a plan layout of each floor level of the building that indicates:

- Boundaries of fire limiting areas and location of fire control devices such as smoke vents, fire doors, fire walls, and barriers.

- Location of firefighting equipment including sprinkler system control valves and water flow alarm indicators.

- Location of all utility services controls.

- Supplementary instructions as required for operation of the building's utility services.

The postattack portion of the plan should provide for procedures to accomplish such tasks as the following:

- Extinguishment of ignitions that may have been caused by nuclear burst.

- Inspection of the entire shelter area for other possible ignitions.

- Assignment of shelter firefighting teams to survey the shelter building for the purpose of locating and extinguishing fires in nonshelter areas.

- Inspection of the entire shelter building for any other possible ignitions.

- Specific assignment of certain shelter firefighting teams to survey adjacent buildings for the purpose of locating and extinguishing fires.

- Where necessary to the long term shelter operation, restoration of the various utilities to service after examination of the potential safe operability of each.

- Where necessary, removal of any remaining combustibles to locations well away from exterior wall openings to reduce the possibility of their subsequent ignition from potential fires burning in adjacent buildings.

- Establishment of a fire watch routine to maintain the entire shelter building under constant surveillance.

It would be necessary during the postattack operations to coordinate the efforts of the various shelter firefighting teams and fire watch personnel with those of radiation monitoring personnel. This would be

especially important for evaluating the potential safe operating periods available for any fire control and surveillance efforts that were attempted outside the fallout shelter area in the shelter building and in any of the surrounding buildings.

Equipment Required

- One 5-gallon stirrup pump extinguisher (with a hose at least 6 feet long) for each 1,250 sf of shelter area with a minimum of 4 extinguishers per shelter area.
- Smoke masks (U.S. Bureau of Mines approved type), together with spare canisters, provided in number equal to the allowance for stirrup pump extinguishers.
- Gloves and protective clothing for each member of the firefighting teams.
- Such tools as may be available in the shelter building, e.g., sledges, saws, chain falls, rope, and wrenches.

Postattack Fire Surveillance

With fire control activities limited to the self-help level, it is important to establish a continuing fire surveillance program for this period.

Fire Watch in Nonshelter Areas. The problems of maintaining a fire watch tour under fallout radiation conditions could be met in two ways. With respect to personnel, cumulative dosages could be charted and appropriate rotation of fire watches could be accomplished. The other factor that would enhance the feasibility of firewatch tours is proper routing through irradiated areas. Routes could be designed to follow the most shielded portions of each area.

Fire Watch in Shelter Areas. Discovery of a fire within a shelter cannot be left to chance. Because such fires could be potentially lethal, their discovery should be followed by immediate extinguishment. Given the prevalence of tension and apprehension, it would not be wise to relegate this important task to shelter occupants since it would invite conditions of confusion if not outright panic.

In a buttoned-up shelter having no outside source of air, the effects of a fire could be critical. Posting of a continuous fire watch is suggested as the only measure that could adequately meet this situation.

Fire Watch Tour Schedules. Fire watch tours must be scheduled so that the time interval between successive tours would not allow a fire to develop beyond the stage at which it is extinguishable by self-help teams. Therefore, the various functional areas or spaces in the shelter building should be classified by fire hazard in terms of the time interval during which extinguishment is possible. The time interval for each area, i.e., the allowable fire build-up time, then would become the maximum time allowable between successive fire watch tours.

Table B-4 provides allowable fire build-up times for representative building functional areas. Since specific buildings may have unique functional conditions, the table is useful only as a baseline for on-site evaluation and refinement.

Table B-4

ALLOWABLE FIRE BUILD-UP FOR DORMANT AREAS
LOCATED IN FIRE RESISTIVE BUILDINGS*

Area	Allowable Build-up Time (min)
Dining rooms	40
Flammable liquids	None
Heating and mechanical rm. (no combustibles)	120
Janitors' closets	60
Kitchens	12
Laundry rooms	30
Locker rooms (metal lockers)	60
Lodging rooms	30
Metal working areas	90
Motor vehicle areas	20
Offices (metal furniture)	120
Offices and schools (wood furniture)	75
Packing - unpacking	12
Paper (rolls, prints, patterns)	20
Paper (cutting, gluing, folding)	12
Repair shops	30
Sales areas	40
Sewing areas	20
Solid fuel storage (soft coal)	90
Solid fuel storage (wood, scraps, dust)	30
Stationery supplies	20
Theaters and auditoriums (stages without scenery)	60
Trash rooms	12
Wholesale storage (wood crates, wood patterns)	40
Wholesale storage (tight 10' piles, cartons, lt. crates)	30
Wholesale storage (loose 10' piles, cartons, lt. crates)	12
Wood working	30
Upholstering	20

* Values presume uncongested contents and structural surfaces having flame spread not greater than finished wood.[27]

Annex A - Alternative Methods for Developing Building Separation Distances

Computational

The basic expression of the configuration factor ϕ can be obtained from the following diagram wherein dA_1 is an elemental radiator, dA_2 is an elemental receiver, and θ represents the angle between the line-distance, C, connecting the centroids of dA_1 and dA_2 and the normal to each area, respectively.

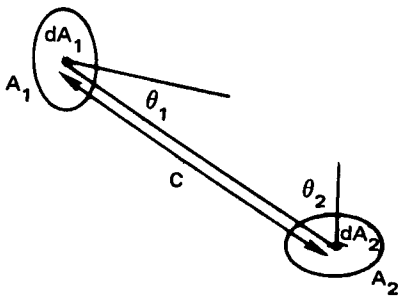

The intensity of radiation received at any point from a radiator is:

$$I = \phi I_o$$

and for our purposes:

$I = 0.3$ cal/cm^2-sec as a maximum

$I = 4$ cal/cm^2-sec for a fuel load equal to or greater than 5 psf

$I_o = 2$ cal/cm^{-2}-sec for a fuel load less than 5 psf.

The energy received by A_2 per unit time from A_1 is:

$$A_1 \cdot \frac{I_o}{\pi} \left(\cos \theta_1\right)\left(\frac{A_2 \cos \theta_2}{C^2}\right)$$

and the intensity of radiation at dA_2 from the entire radiator is then:

$$I = \frac{I_o}{\pi} \int_{A_1} \frac{\cos \theta_1 \cos \theta_2}{C^2} dA_1$$

and since $\phi = I/I_o$:

$$\phi = \frac{1}{\pi} \int_{A_1} \frac{\cos \theta_1 \cos \theta_2}{C^2} dA_1$$

The configuration factor ϕ will be either $\frac{0.3}{4} = 0.075$ (fuel load ≥ 5 psf) or $\frac{0.3}{2} = 0.15$ (fuel load < 5 psf) and orientation angles can be measured; therefore, the distance C can be computed.

Optical Analog[31]

Figure B-11 indicates an optical analog that may be employed to determine the separation distance C. A model of the building facade (the radiator) is constructed of black photographic paper, covered with a diffusing material and then attached to the diffusing screen. The diffusing screen is uniformly illuminated. The interior of Section A is painted white to obtain high reflectivity. The interior of Section B is painted black to prevent reflected light from impinging the photocell. The cell has a sensitive area of about 1 cm^2 and is used together with a galvanometer to measure light intensity. The intensity of light emitted can be held constant by employing a constant voltage transformer. A calibrated scale attached to the galvanometer can then be used to read ϕ directly. Thus, when the photocell is placed close to the radiating area, the configuration factor will be unity, and when placed in the position of the receiving element, the configuration factor can be read directly from the scale. Should there be reflecting surfaces between the radiating surface and the point at which the measurement is to be made, these, with suitable reflectivity coefficients, would have to be included in the illuminated model. When the model of the radiating area is set up, the photo cell is backed off to read 0.15 or .075, depending on fuel load, and the proportional distance C is measured directly between the cell and the radiator.

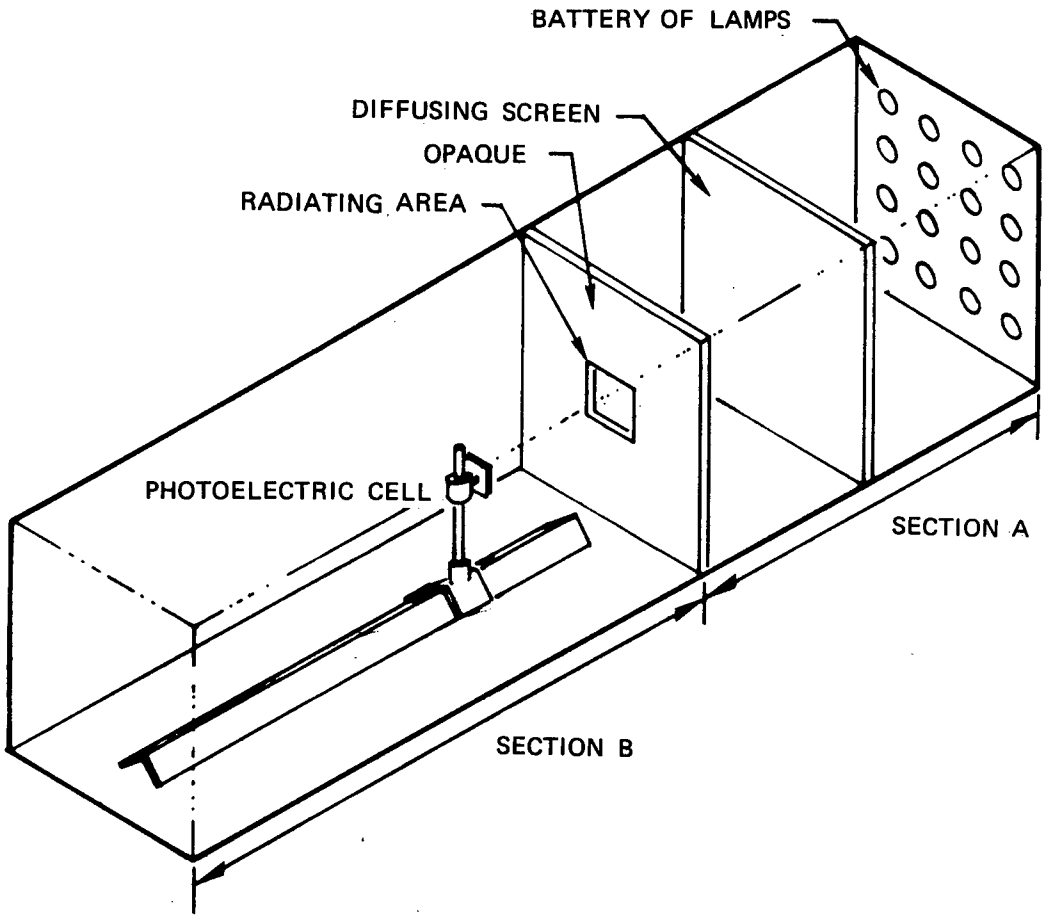

FIG. B-11 APPARATUS FOR DETERMINATION OF THE CONFIGURATION FACTOR[31]

REFERENCES

1. Glasstone, S., Effects of Nuclear Weapons, U.S. Department of Defense and Atomic Energy Commission, 1962 edition (1964 reprinting), Superintendent of Documents, Washington, D.C.

2. Goodale, T. C., M. B. Harkins, and A. B. Willoughby, Feasibility of Active Countermeasures for Thermal Radiation Effects of Nuclear Weapons, Final Report, United Research Services, July 1963 (AD-412 733).

3. Gibbons, Mathew G., Transmissivity of the Atmosphere for Thermal Radiation from Nuclear Weapons, U.S. Naval Radiological Defense Laboratory, San Francisco, California, August 12, 1966 (AD-641 481).

4. Combustible Contents of Buildings, Building Materials and Structures Report, U.S. Department of Commerce, July 25, 1957.

5. Bracciaventi, J., Window and Window Screens as Modifiers of Thermal Radiation Released in Nuclear Detonations, U.S. Naval Applied Science Laboratory, Brooklyn, N.Y., September 12, 1966 (AD-643 019).

6. Fire Aspects of Civil Defense, OCD TR-25, July 1968.

7. Crowley, J. W., et al., Development of Analytical Relationships and Criteria for Blast and Fire Vulnerability of Fallout Shelter Occupants, Systems Sciences Inc. Final Report for OCD Contract No. DAHC 20-67-C-0147, OCD Work Unit 1614B, October 1, 1967 (AD-842 356L).

8. Moll, Kendall, and John McAuliffe, Secondary Ignitions in Nuclear Attack, Stanford Research Institute Report Contract N228 (62479) 65701, OCD Work Unit 2534A, July 1965 (AD-625 173).

9. Brunswig, Hans, Practical Experiences of Fire Protection Services, A critical presentation of the organization technology and tactics of fire protection as employed by a civil defense organization during World War II in Germany, translated by C. E. Harvey and W. C. Truppner, OCD Work Unit No. 4315A, June 1966 (AD-652 618 & 619).

10. Rodden, Robert M., Floyd I. John, and Richard Laurino, Exploratory Analysis of Fire Storms, Stanford Research Institute Report Contract N228 (62479) 65419, for U.S. Office of Civil Defense, May 1965 (AD-616 638).

11. Cohn, B. M., L. E. Almgren, and M. Curless, A System for Local Assessment of the Conflagration Potential of Urban Areas, Gage-Babcock and Associates report prepared for U.S. Office of Civil Defense (OCD-PS-64-74), March 1965 (AD-616 623).

12. Law, Margaret, Heat Radiation from Fires and Building Separation, Department of Scientific and Industrial Research and Fire Offices Committee, Joint Fire Research Organization, Fire Research Technical Paper No. 5, London, 1963.

13. The National Building Code, 1967 Edition, American Insurance Association, New York, N.Y., Chicago, Ill., and San Francisco, Calif.

14. Phung, P. V., and A. B. Willoughby, Prediction Models for Fire Spread Following Nuclear Attacks, URS Corporation, Final Report for OCD Contract No. OCD-PS-64-48, January 1965 (AD-613 359).

15. National Fire Code, Vol. 4, National Fire Protection Association, Boston, Mass., 1966-67.

16. Waterman, T. E., Shelter Habitability in Existing Buildings Under Fire Exposure, IIT Research Institute Report for U.S. Office of Civil Defense, Contract No. N228 (62479) 68355, June 1966 (AD-637 806).

17. Fire Protection Handbook, National Fire Protection Association, 12th ed., Boston, Mass., 1962.

18. Leutz, Herman, "Fireproof Shelters with Secured Ventilating Systems," Proceedings of the Symposium on Protective Structures for Civilian Populations, NAC-NRS, April 19-23, 1965.

19. Herrington, L. P., and J. D. Hardy, "Temperature and Humidity in Relation to the Thermal Interchange Between the Human Body and the Environment," Human Factors in Undersea Warfare, Panel on Psychology and Physiology, Committee on Undersea Warfare, National Research Council, Washington, D.C., 1949.

20. Handbook of Fundamentals, American Society of Heating, Refrigerating, and Air-Conditioning Engineers, Inc., New York, N.Y., 1967.

21. Bond, Horatio, "Fire Casualties of the German Attacks," Fire and the Air War, National Fire Protection Association, Boston, Mass., 1946.

22. Earp, Kathleen F., Deaths from Fire in Large Scale Air Attacks-With Special Reference to the Hamburg Fire Storm, Home Office, Scientific Advisors' Branch, Whitehall, S. W. 1, London, April, 1953.

23. Lee, William, et al., Design of Tests for the Effects of Mass Fires on Shelter Occupants, Isotopes Inc., Palo Alto, Calif., OCD Work Unit 1133B (Contract No. N00228-66-C-0917), September 26, 1966.

24. Broido, A., and A. W. McMasters, Effects of Mass Fires on Personnel in Shelters, Division of Forest Fire Research, Pacific Southwest Forest and Range Experiment Station, U.S. Forest Service, Department of Agriculture, for U.S. Office of Civil Defense (Contract No. DCM-SR-59-7), Technical Paper 50, August 1960.

25. Colvin, C. B., Shelter Remedial Actions Phase III Final Comprehensive Report, Appendix A, URS Corp. Report for Stanford Research Institute, EOSD Project 65-5, November 1967.

26. Waterman, T. E., et al., Prediction of Fire Damage to Installations and Built-up Areas from Nuclear Weapons - Phase III Experimental Studies - Appendices A-G, for National Military Command System Support Center (Contract No. DCA-8), November 1964.

27. Varley, R. B., and G. L. Maatman, Shelter Fire Vulnerability - Specific Fire Limiting Activities for Occupants, IIT Research Institute Report for U.S. Office of Civil Defense (Contract No. OCD-OS-62-210), September 9, 1964 (AD-449 386).

28. Laughlin, K. P., Thermal Ignition and Response of Materials, Project 31.5, Operation Teapot, Civil Effects Test Group, Office of Civil and Defense Mobilization, Battle Creek, Michigan, May 1955.

29. Varley, R. B., and G. L. Maatman, Shelter Fire Vulnerability - Survey and Analysis of Representative Buildings, IIT Research Institute Report for U.S. Office of Civil Defense (OCD-05-62-210), March 17, 1965 (AD-615 391).

30. Uniform Building Code, 1967 edition, International Conference of Building Officials, Pasadena, Calif.

31. Lawson, D. I., and D. Hird, "A Photometric Method of Determining Configuration Factors," British Journal of Applied Physics, 5, 72-4, 1954, Joint Fire Research Organization, Boreham Wood, England.

Standard Methods of Fire Tests of Building Construction and Materials, National Fire Protection Association Standard No. 251, May 1961, (ASTM-E-119).

- Provides methods for determining fire resistance ratings of materials.

Shorter, G. W., et al., "The St. Lawrence Burns," Quarterly of NFPA Vol. 50, No. 4, pp. 300-16, April 1960.

- Gives time-temperature readings from full scale tests in which residences were burned.

Thomas, P. H., "The Size of Flames from Natural Fires," Ninth Symposium on Combustion, New York and London, Joint Fire Research Organization, Boreham Wood, England, Academic Press, pp. 844-59, 1963.

- Flame height computations and graphs are given.

Fire Research 1961, Joint Fire Research Organization, Boreham Wood, England.

- General report that includes method for computation of flame heights emitted from windows.

Proceedings of the Symposium on Protective Structures for Civilian Populations, National Academy of Sciences, National Research Council, April 1965:

- Leutz, Herman, "Possibility of Occurrence of Area Conflagrations and Firestorm with Respect to Fuel Density," p. 31- . Describes method by which a fuel density index can be computed for specific areas and then tabulates values of indexes against probability of occurrence of fire spread, conflagration, or firestorm.

- Leutz, Herman, "Fireproof Shelters and Secured Ventilating Systems," p. 134- . Gives structural and mechanical criteria for the maintenance of tolerable conditions in the shelter when it is exposed to heating from adjacent fires, and ambient atmosphere is charged with CO, CO_2, and other gases of combustion. Note: Use of sand filter to act as heat sink is suggested.

- Smitt, Gosta, "Fire Safe Shelter Design," p. 139- . Gives curves relating temperature development within shelters to varying degrees of shelter wall or ceiling heating from outside fires. Notes that slab temperature reached during fire exposures can have considerable effect on reinforcing steel strength. Cites strength reduction of 50% for 600°C, which is a temperature easily attained in a fire.

McGuire, J. H., "Fire and the Spatial Separation of Buildings," Fire Technology, National Fire Protection Association Quarterly, Vol. 1, No. 4, pp. 278-87, November 1965.

Fire Protection Engineering, NavDocks 2068 (Rev. 9-61), U.S. Naval Facilities Engineering Command, Washington, D.C.

- Fire protection engineering criteria for design, construction, maintenance and operation of buildings, structures, and facilities. Includes building separation curves for combustible and noncombustible buildings.

Appendix C

INITIAL RADIATION CALCULATIONS FOR ENTRANCEWAYS

By C. K. Wiehle

Reproduced, without change, from: Wiehle, C. K., Shelter Entranceways and Openings, prepared by Stanford Research Institute for OCD, final report, September 1967. (AD-662 749)

NOTE: While fully outside entranceways are illustrated, the analysis techniques are useful for all entranceway configurations. No one type should be inferred as the recommended type for all applications.

Appendix C

INITIAL RADIATION CALCULATIONS FOR ENTRANCEWAYS

By C. K. Wiehle

Introduction

Although there are many unknowns concerning both the attenuation of radiation through entranceways and its distribution within the structure, the simplified procedures presented in Refs. 5 and 6 were felt to be adequate for the designs prepared here. Basically, there are three problems associated with the analysis of an entranceway for the initial nuclear radiations. These are the determination of the free-field initial radiation intensities, the maximum permissible dose, and the entranceway attenuation of the radiation. The methods used to calculate these quantities, together with an illustrative example, are given in the following subsections.

Initial Nuclear Radiation

The initial nuclear radiation is defined in Ref. 1 as the radiation emitted within one minute after the detonation of a nuclear weapon, including the prompt radiation. For the purpose of this study, Ref. 1 was used to obtain the intensities of the free-field gamma and neutron radiation at the entranceway opening. Because of the yield-range-dose relationships, it is necessary to specify a yield, range, and HOB (height of burst) before the radiation intensity in the free-field can be calculated. However, even with precise yield-range data, Ref. 1 cautions that any calculation of radiation exposure dose is subject to wide fluctuation in reliability due to variation in weapon design and characteristics. Only the 20 psi overpressure level from a 200-kt weapon yield was considered for the radiation intensity calculations in this study.

Maximum Permissible Radiation Dose

The establishment of a total permissible dose for shelter occupants, although beyond the scope of this study, is a primary factor in the design and cost of entranceways. Even at the modest overpressure level of 20 psi examined in this study, the initial radiation requirement increased the cost of the blast shelter entranceways. The total dose in the shelter

is composed of the initial radiation and residual fallout radiation that penetrates both the entranceway and the shelter proper. For a specific shelter design problem, the relationship between the contributions of the radiation from these two sources can be studied to obtain an economical compromise for the entranceway and shelter design. However, for a study of only the entranceway portion of the shelter system, it is necessary first to establish a permissible dose and then to estimate the entranceway contribution for both initial and residual radiation. For the purposes of this study, it was sufficient to adopt the criterion presented in Ref. 5. Essentially, this limited the total radiation dose in the shelter to 40 rads, with the assumption that the permissible dose was divided equally at 20 rads each for the entranceway and the shelter proper. Further, the entranceway portion was divided equally between initial and fallout radiation, which resulted in a permissible initial radiation dose of 10 rads through the entranceway. To adhere to the criterion mentioned above for a specific shelter would require assuming an accumulated total dose for the free-field fallout radiation and determining its attenuation through the entranceway. However, as noted in the fallout radiation analysis in Appendix 2,* for a study of entranceways only, it was believed sufficient to determine the PF for the blast entranceways in the usual manner (Ref. 20) at a detector point 3 ft inside the shelter entry without calculating the actual radiation dose.

Another factor that is important in describing the permissible radiation dose received by shelterees is the exposed and absorbed dose of nuclear radiation. To describe the effects of nuclear radiation on a biological system adequately, it is necessary to express the free-field radiation exposure dose as an absorbed dose. This has been accomplished by introduction of the rad, which is defined as the absorbed dose of any nuclear radiation that is accompanied by the liberation of 100 ergs of of energy/gram of absorbing material (Ref. 1). Because of the uncertainty of determining the biological effect of nuclear weapons and to simplify the radiation analysis, the absorbed dose in rads was used in this study to judge the adequacy of the entranceways for providing initial radiation protection.

Entranceway Radiation Attenuation

The attenuation of the free-field nuclear radiation intensities through an entranceway can conveniently be separated into three phases for purposes of analysis: the entrance reduction factor, entranceway bend and corridor attenuation, and barrier attenuation.

* Appendix D herein.

Entrance Reduction Factor

The important factors in determining the initial radiation dose within the entranceway are the orientation of the entrance opening relative to the burst point, the entranceway geometry, and the free-field radiation intensity. In general, Refs. 5 and 6 both conclude that the hazard from radiation streaming into the entrance opening would be maximum for a line-of-sight direction along the longitudinal axis of the entrance section between a detector located in the entranceway, usually at the first bend, and the burst point. This would result from the fact that the higher energy gamma rays and neutron particles are more likely to come from a line-of-sight direction than from a scattered direction. Although the effect on radiation dose of the angle between the line-of-sight and the burst point was not investigated, it was possible to examine limited burst positions on the vertical plane through the longitudinal axis of the entrance section. The locations were on the line-of-sight from the detector approximately along the longitudinal axis of the entrance section, on the grazing line-of-sight between the detector and the first step of the entranceway, and for a surface burst location. It was found that the most critical location was for the grazing line-of-sight. In general, as the HOB is increased, the range for a given yield and overpressure also increases to a maximum for some optimum HOB. Since the initial radiation dose is range dependent, it would decrease to a minimum at the optimum HOB for a given yield and overpressure. Although the magnitude of the entrance reduction factor is dependent on the angular deviation from the line-of-sight orientation, the reduction of this factor for the grazing line-of-sight is more than offset by the increase in free-field radiation intensity due to the decreased range; this was not the case for the surface burst location. It may well be that some intermediate angle between those selected may produce a greater entrance section radiation dose, but it was felt sufficient for the purposes of the entranceway designs and cost estimates in this study to use the grazing line-of-sight for the initial radiation analysis.

To determine the fraction of the free-field radiation that would penetrate the entrance section, it is necessary to compute the solid angle fraction subtended by the entrance opening and the detector location. Figure 1-1, obtained from Ref. 20, can be used to calculate the solid angle fraction for rectangular openings. To calculate the entrance reduction factor, R_{fe} for both gamma and neutron radiation, the solid angle fraction is used to enter Figure 1-2, which was obtained from Ref. 6.

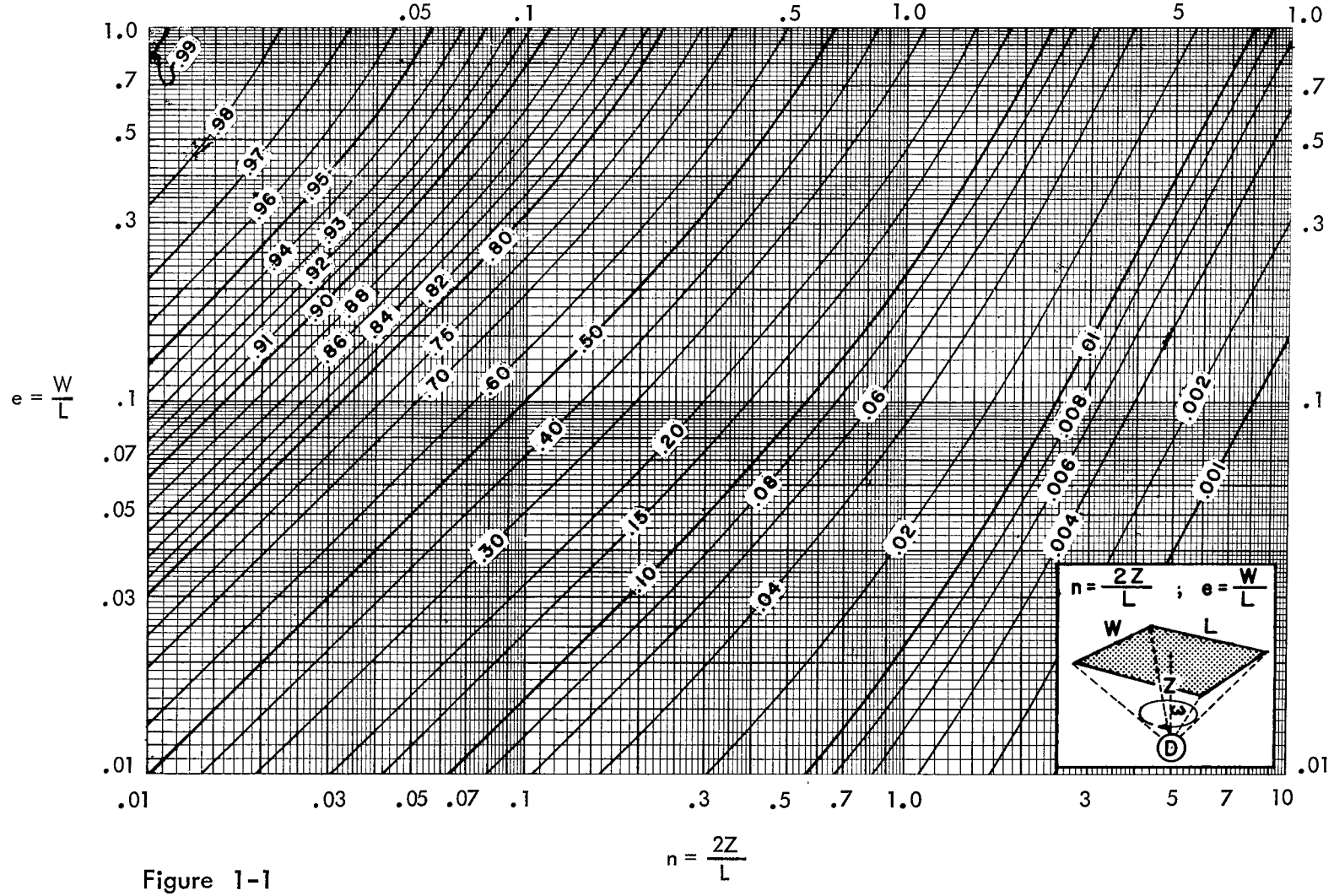

Figure 1-1

VALUES OF SOLID ANGLE FRACTION, ω

SOURCE: Ref.20

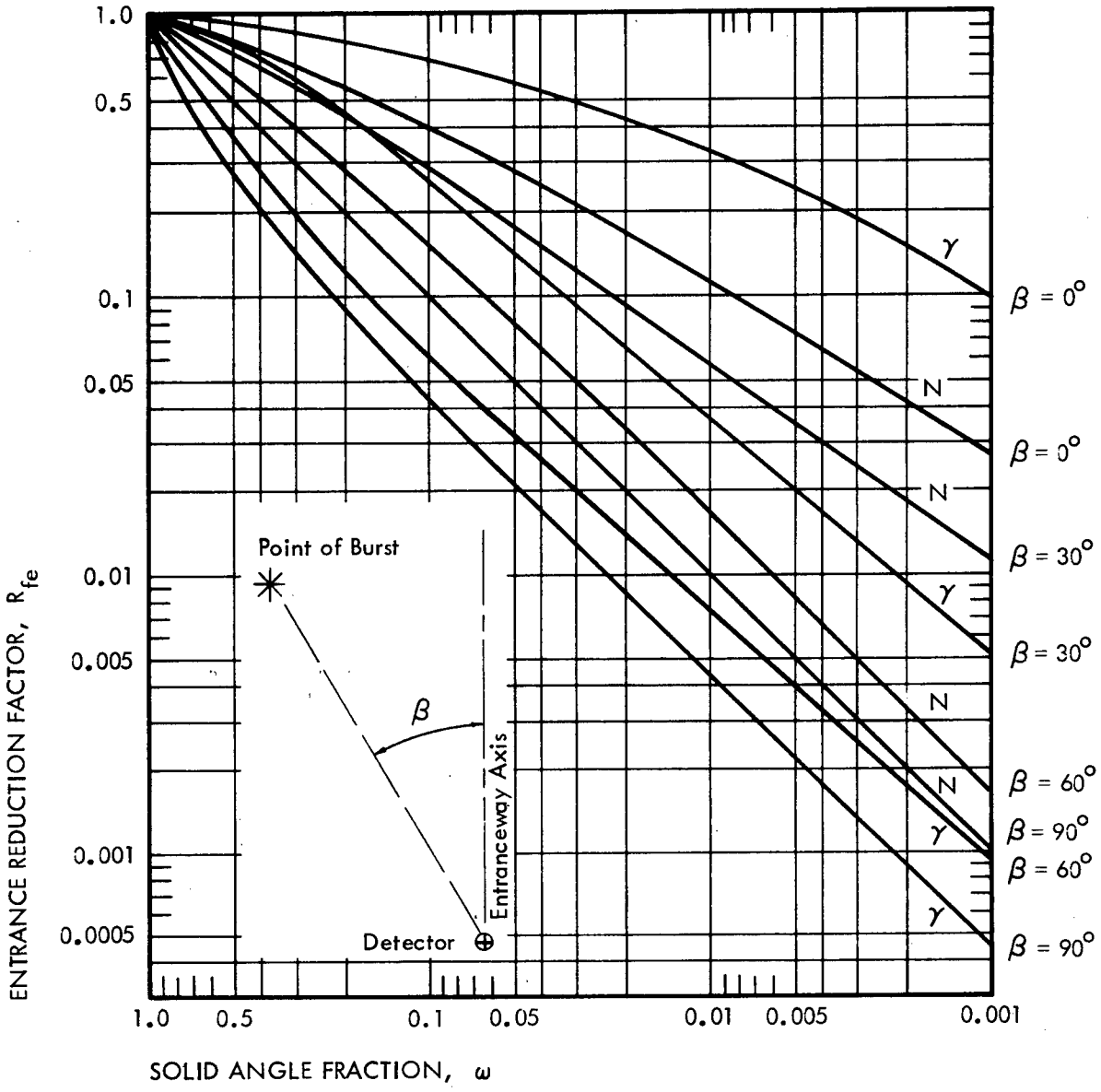

Figure 1-2

ENTRANCE REDUCTION FACTOR FOR INITIAL NUCLEAR RADIATION VERSUS SOLID ANGLE FRACTION AND BURST POINT

SOURCE: Ref. 6.

Entranceway Bend and Corridor Attenuation

Gamma Radiation

As noted in Refs. 15-19, even though considerable analytical and experimental effort has been expended in recent years to study the transmission of gamma radiation through tunnels and bends, detailed calculations for the initial nuclear gamma radiations are both tedious and of uncertain accuracy. For the purposes of this project, the following simplified method presented in Ref. 5 was therefore felt to be adequate. The reduction factor, R_f, for the first 90° bend beyond the entrance section is given by

$$R_{f_1} = 0.1\omega_1$$

where ω_1 = solid angle fraction subtended by the corridor section at the next point of interest

For the second and subsequent 90° bends, the reduction factor is given by

$$R_{f_n} = 0.5\omega_n$$

for n = 2, 3...

Neutron Radiation

Because of the lack of theoretical and experimental information on neutron attenuation in entranceways, it was sufficient for this study to use the simplified procedures presented in Refs. 5 and 6 to determine the length of corridor required for neutron radiation attenuation. The method is based on the concept of the length of corridor required to reduce the neutron dose by one-half. Since neutron attenuation occurs by neutron collision with the corridor walls, it is assumed that the attenuation is a function of the average cross-sectional dimensions of the corridor and not of the bends in the corridor. The experimental evidence indicates that the corridor half-length increases with the neutron energy, although information is lacking for the higher energy levels associated with nuclear weapons. This is accounted for in the method by neglecting any neutron radiation attenuation by wall interaction in the first section of the entranceway and by assuming that most of the higher energy neutrons are not transmitted past the first corridor bend.

It is assumed that the neutron half-length for the corridor beyond the first bend is given by

$$L_{1/2} = 1/2\ K\ (H + W) = 0.366\ (H + W)$$

where $L_{1/2}$ = half length of entranceway corridor, ft

K = 0.732, experimentally determined ratio

H = height of corridor, ft

W = width of corridor, ft

The number of neutron half-lengths for the corridor is given by

$$n = \frac{L}{L_{1/2}}$$

n = number of corridor half-lengths

L = total length of corridor beyond first bend to point of interest, ft

The reduction factor, R_{fc}, for neutron radiation for the corridor beyond the first bend is given by

$$R_{fc} = \frac{1}{(2)^n}$$

Because of a lack of adequate information, the method above does not specifically include a factor for secondary gamma rays resulting from the absorption of thermal neutrons in the corridor walls. In Ref. 5, it is stated that the present degree of conservatism in design should help reduce this hazard.

Barrier Attenuation

Barrier at Entrance

To determine the barrier reduction factor, B, at the outside entrance, Figures 1-3 through 1-5 have been reproduced from Ref. 5. Figure 1-3 shows the barrier reduction factor in relationship to the mass thickness of the shielding material and the angle of incidence for nitrogen capture gamma radiation. The use of nitrogen capture gamma

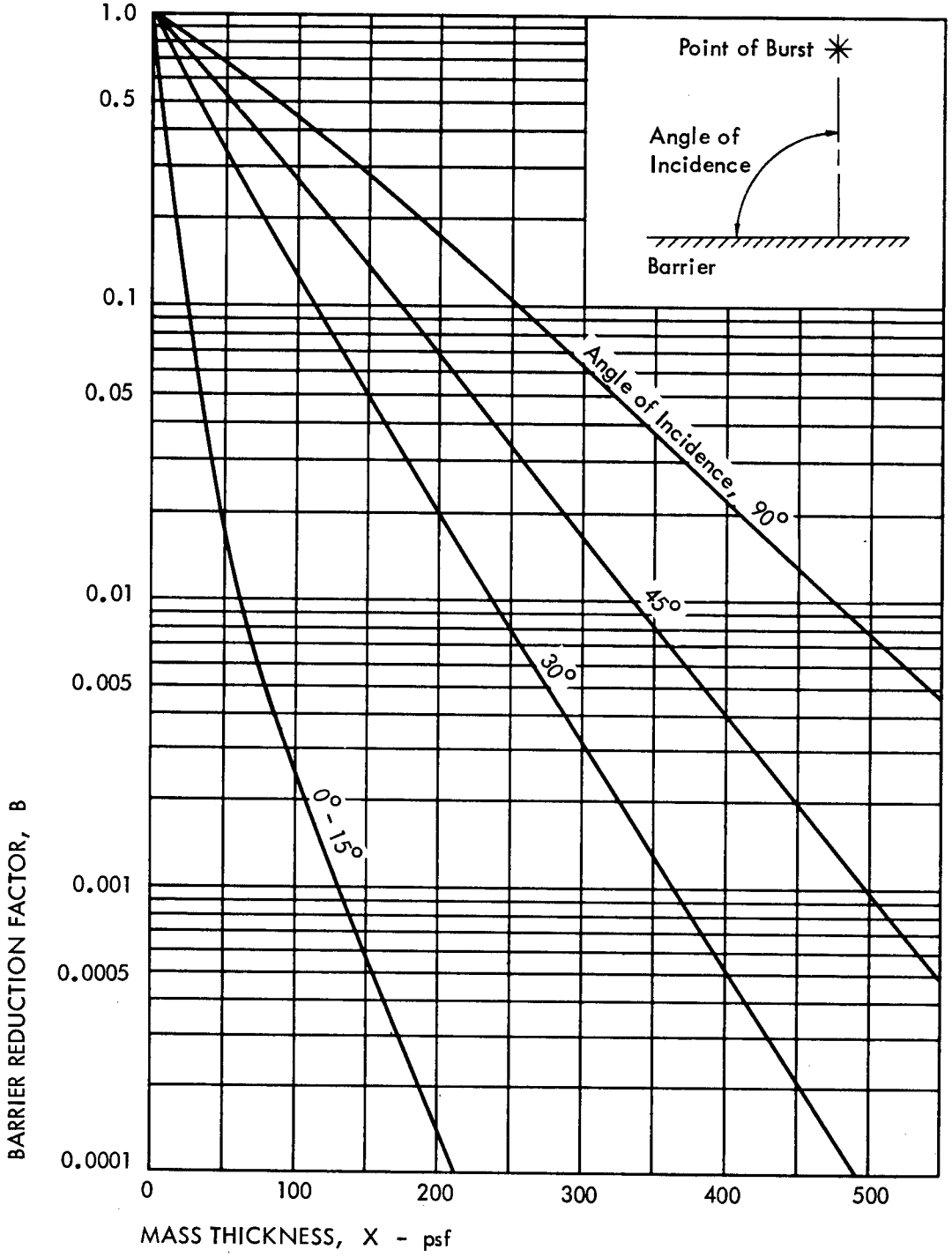

Figure 1-3

BARRIER REDUCTION FACTOR VERSUS MASS THICKNESS FOR NITROGEN-CAPTURE GAMMA RADIATION

SOURCE: Ref. 5

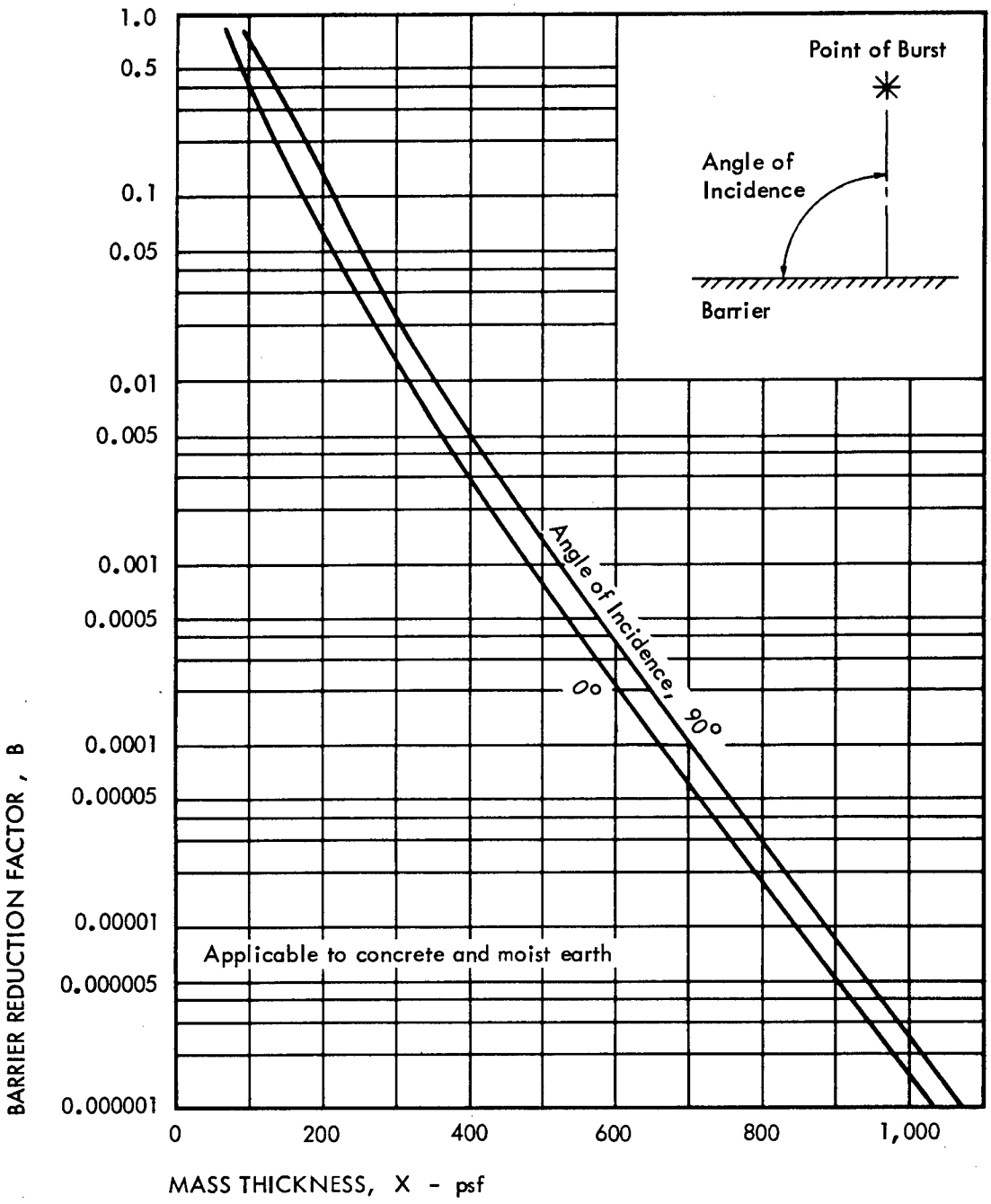

Figure 1-4

BARRIER REDUCTION FACTOR VERSUS MASS THICKNESS FOR 14 Mev NEUTRONS

SOURCE: Ref. 5.

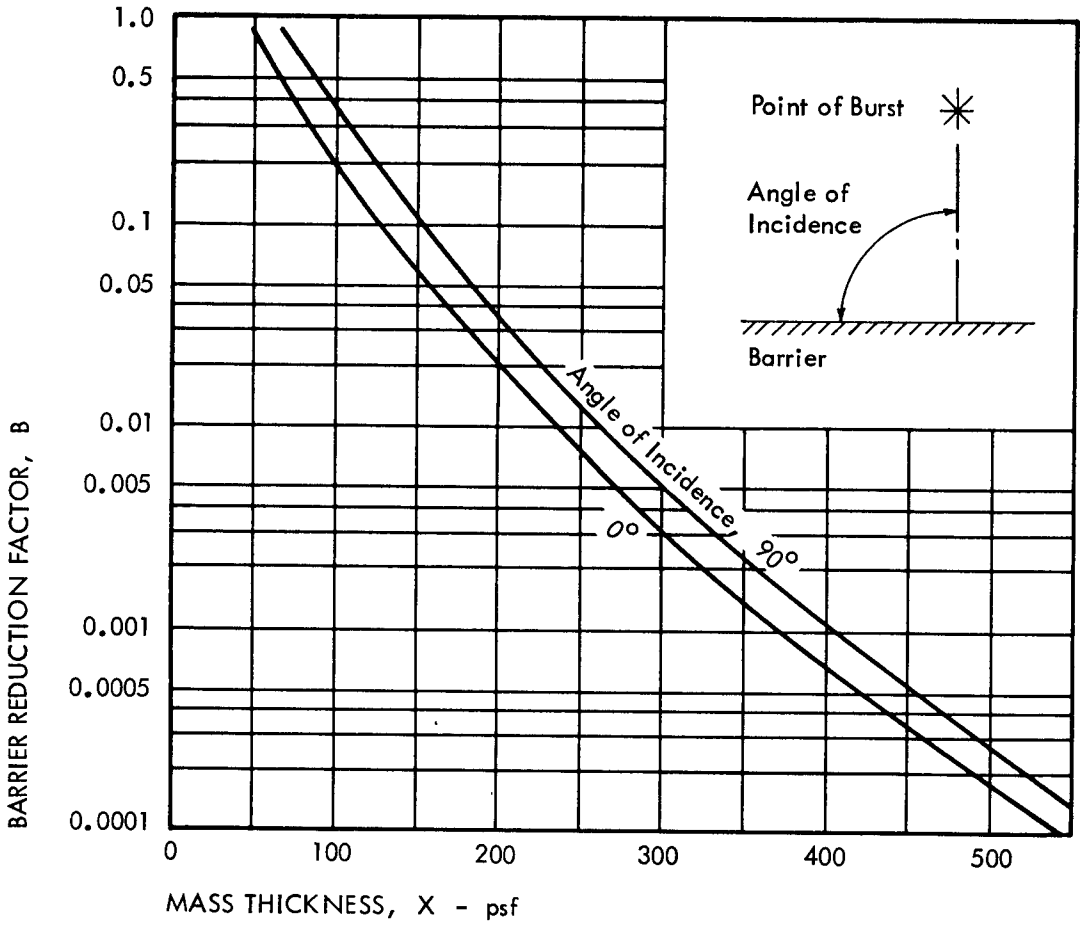

Figure 1-5

BARRIER REDUCTION FACTOR VERSUS MASS THICKNESS FOR 2.5 Mev NEUTRONS

SOURCE: Ref. 5.

radiation for shielding analyses is justified since it is the primary component of the initial gamma radiation at the ranges of interest in this study, and it is recommended as being on the conservative side in Ref. 1. A degree of conservatism for the barrier reduction factor is probably warranted for entranceways due to the previously mentioned neglect of the secondary gamma rays. Figures 1-4 and 1-5 show the barrier reduction factors for fusion yield neutrons ($\sim$ 14 Mev) and fission yield neutrons ($\sim$ 2.5 Mev), respectively.

Barriers Beyond First Corridor Bend

Gamma Radiation. The energy level of gamma radiation, which has been scattered through an angle of 90°, cannot be greater than 0.51 Mev, regardless of the initial energy. Therefore, the recommendation in Ref. 5 that Figure 1-6 be used for gamma ray barrier shielding beyond the first corridor bend, was adopted for this study.

Neutron Radiation. As recommended in Ref. 5, the reduction factors for neutron attenuation through barriers located beyond the first bend were obtained from Figure 1-5 for 2.5 Mev neutrons. The use of the lower average neutron energy level for interior barriers seems justified on the basis of the degradation of the free-field energy level beyond the first 90° corridor bend (Refs. 5 and 19).

Illustrative Example

To obtain the cost data presented in this report, it was necessary to perform an analysis of the attenuation of the initial radiation for the six blast entranceways (Types J and K). To demonstrate the method outlined in the previous sections, a typical initial radiation analysis is presented for entranceway J-1 in Figures 1-7 and 1-8.

Solid Angle Fractions

The solid angle fractions subtended at the various points shown on Figures 1-7 and 1-8 are given in the following tabulation. The values

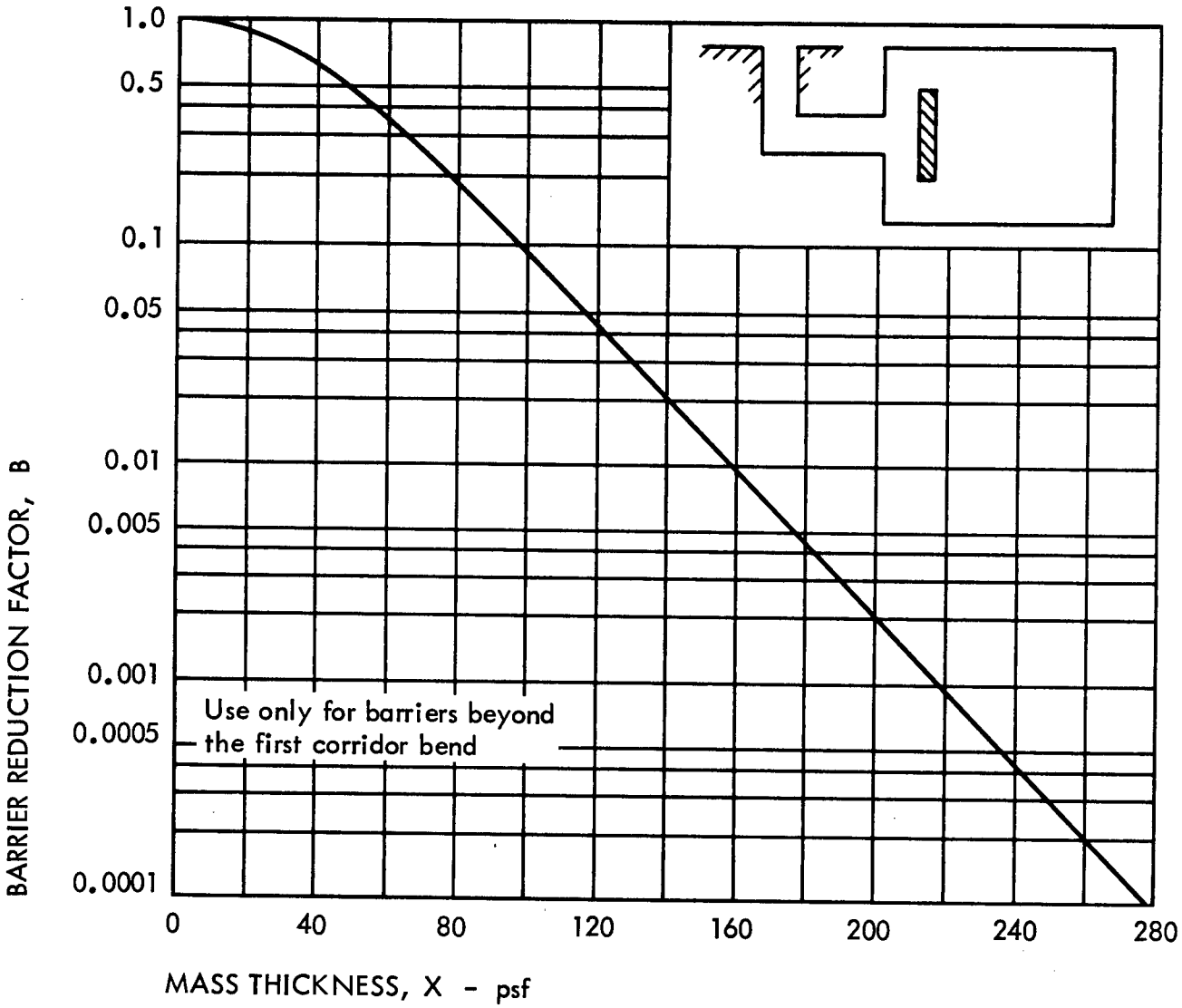

Figure 1-6

BARRIER REDUCTION FACTOR VERSUS MASS THICKNESS
FOR 0.51 Mev GAMMA RAY PHOTON

SOURCE: Ref. 5.

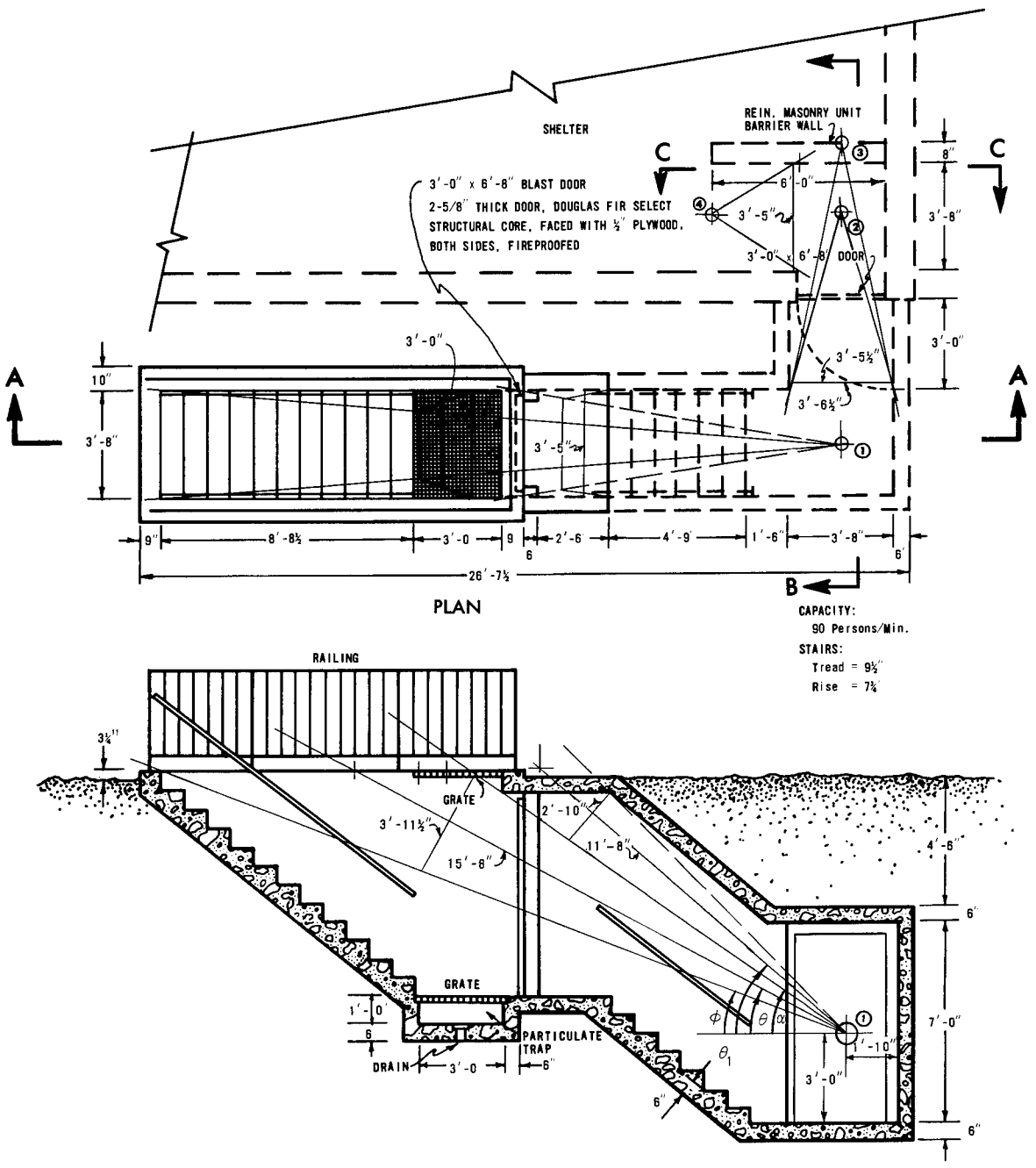

Figure 1-7
UNDERGROUND BLAST SHELTER ENTRANCEWAY, J-1

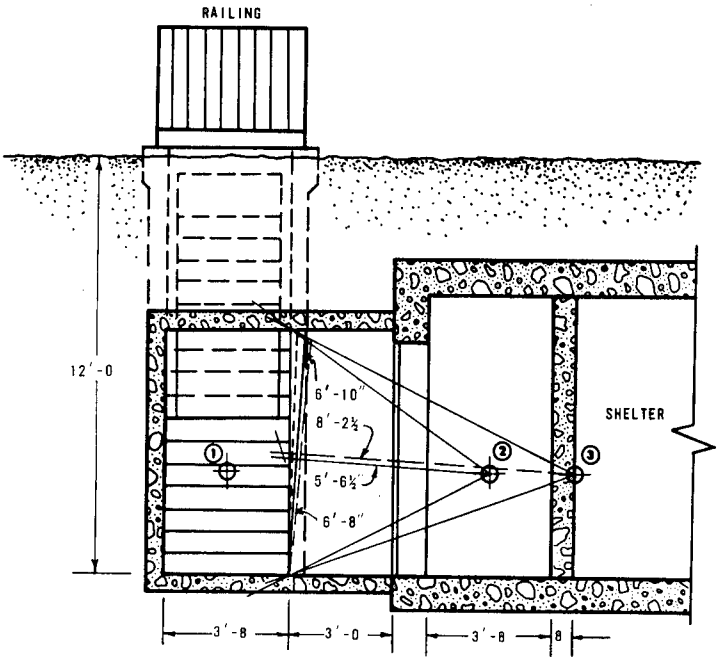

SECTION B-B

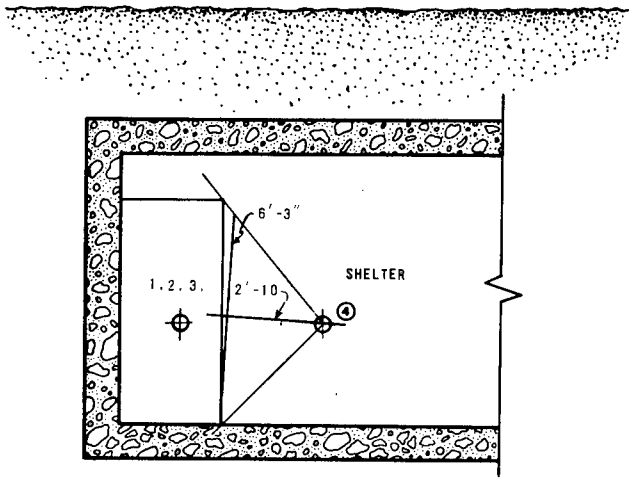

SECTION C-C

Figure 1-8
ENTRANCEWAY J-1, SECTIONS B-B AND C-C

of W, L, and Z were determined graphically as noted on the figures and used to obtain the solid angle fractions, ω, from Figure 1-1:

Point	W	L	Z	e	n	ω
1	3.00	3.96	15.67	0.76	7.91	0.008
2	3.46	6.67	5.54	0.52	1.66	0.10
3	3.54	6.83	8.21	0.52	2.40	0.055
4	3.42	6.25	2.83	0.55	0.91	0.25

where W, L = dimensions of the entrance opening projected on the plane normal to the selected line-of-sight, ft

Z = distance from detector to plane of W and L, ft

$$e = \frac{W}{L}$$

$$n = \frac{2Z}{L}$$

Assumed Weapon Parameters

Peak overpressure, P_{so} = 20 psi
Weapon yield, W = 200 kt
$W^{1/3}$ = 5.85

Free Field Initial Radiation

As noted previously, the worst case orientation for radiation streaming in the entranceways in this study, was found to be for the grazing line-of-sight ϕ, as shown on Figure 1-7.

Slant Range

Knowing the peak overpressure and the angle ϕ, the horizontal range, R, to the shelter entranceway can be determined from Ref. 1 (Para. 3.67):

$$R = 780\ W^{1/3} = (780)(5.85) = 4560 \text{ ft}$$

and the slant range, R_s, is

$$R_s = \frac{4560}{\cos \phi} = 4900 \text{ ft} = 1630 \text{ yd}$$

Free-Field Initial Radiation

Using the appropriate figures and scaling factors from Ref. 1 (Para. 8.27, 8.61, and 11.90), the free-field initial radiation dose can be determined for a 200 kt weapon yield at the slant range of the entranceway as follows:

Gamma radiation = 4500 rads
Neutron radiation = 580 rads

Entranceway Reduction Factors

Gamma Radiation

At Point 1*

From Figure 1-2, for $\omega_1 = 0.008$ and $\beta = (\theta - \phi) = 7^\circ$

$$R_{fe} = 0.15$$

At Point 2

$$R_f = R_{fe} (0.1\omega_2)$$

$$R_f = (0.15)(0.1)(0.10) = 0.0015$$

At Point 3

$$R_f = R_{fe} (0.1\omega_3)B$$

From Figure 1-6, for $X = \frac{8}{12}(150) = 100$ psf

$$B = 0.1$$

$$R_f = (0.15)(0.1)(0.055)(0.1) = 0.00008$$

At Point 4

$$R_f = R_{fe} (0.1\omega_2)(0.5\omega_4)$$

$$= (0.15)(0.1)(0.10)(0.5)(0.25) = 0.00019$$

---

* The barrier reduction factor for the wood blast and entry doors is insignificant and is therefore not included.

Neutron Radiation

At Point 1

From Figure 1-2, for $\omega_1 = 0.008$ and $\beta = 7^\circ$

$R_{fe} = 0.08$

At Point 2

$L_{1/2} = 0.366\ (H+W)$

$= 0.366\ (7.00 + 3.67) = 3.90'$

$L = 7.67'$

$n = \frac{L}{L_{1/2}} = \frac{7.67}{3.90} = 1.97$

$R_{fc} = \frac{1}{(2)^n} = 0.255$

$R_f = R_{fe} \times R_{fc}$

$R_f = (0.08)(0.255) = 0.020$

At Point 3

From Figure 1-5, for X = 100 psf and angle of incidence = 90°

$B = 0.35$

$R_f = (0.08)(0.255)(0.35) = 0.0071$

At Point 4

$L_{1/2} = 0.366\ (7.65 + 3.67)$*

$= 4.14'$

$L = 11.84'$

$n = \frac{11.84'}{4.14} = 2.86$

---

* Average for corridor in entranceway and shelter

$$R_{fc} = \frac{1}{(2)^n} = 0.138$$

$$R_f = R_{fe} \times R_{fc}$$

$$R_f = (0.08)(0.138) = 0.011$$

Initial Gamma Radiation Dose

Through Entranceway

Dose at Point 2

$R_f = 0.0015$

$D_2 = R_f \times D_o$

where D_o = outside radiation dose

D_i = inside radiation dose

$D_2 = (0.0015)\ (4500) = 6.8$ rads

Dose at Point 3

$R_f = 0.00008$

$D_3 = (0.00008)(4500) = 0.4$ rad

Dose at Point 4

$R_f = 0.00019$

$D_4 = (0.00019)(4500) = 0.9$ rad

Through Entrance Roof Slab

Dose at Point 2

From Figures 1-7 and 1-8, W = 2.17', L = 3.42', Z = 11.67'

From Figure 1-1, for e = 0.64, n = 6.82

$\omega_{1A} = 0.009$

From Figure 1-2, for $\omega_{1A} = 0.009$ and $\beta = \theta_1 = \phi = 20°$

$R_{fe} = 0.07$

From Figure 1-3, for X = 1/2 150 = 75 psf, and angle of incidence = $\phi = 21^{\circ}$

B = 0.06

$R_f = R_{fc} \ (0.1\omega_2) \ B$

$R_f = (0.07)(0.1)(0.10)(0.06) = 0.000042$

$D_2 = R_f \times D_o$

$D_2 = (0.00004)(4500) =$ negligible

Dose at Point 4

$R_f = R_{fe} \ (0.1\omega_2)(0.5\omega_4) \ B$

$R_f = (0.07)(0.1)(0.10)(0.5)(.25)(0.06) = 0.000005$

$D_4 =$ negligible

Through Roof Slab over Point 1

Dose at Point 2

$X = (\frac{150}{2}) + (4.5 \times 100) = 525$ psf*

From Figure 1-3, for X = 525 psf and angle of incidence = 21°

$B << 0.0001$

$R_f = B \ (0.1\omega_2)$

$R_f << (0.0001)(0.1)(0.10) << 0.000001$

$D_2 =$ negligible

Therefore gamma radiation dose through roof slab over point 1 is negligible at all points of interest

---

* Assumes an infinite plane barrier with no geometry reduction

Through Entranceway Walls

Dose at Point 4

$X = (1.5 \times 150) + (2.5 \times 100) = 475$ psf

From Figure 1-3, for X = 475 psf and angle of incidence = 0 - 15°

D_4 = negligible

Initial Neutron Radiation Dose

Through Entranceway

Dose at Point 2

$R_f = 0.020$

$D_2 = R_f \times D_o$

$D_2 = (0.020)(580) = 11.6$ rads

Dose at Point 3

$R_f = 0.0071$

$D_3 = (0.0071)(580) = 4.1$ rads

Dose at Point 4

$R_f = 0.011$

$D_4 = (0.011)(580) = 6.4$ rads

Through Entrance Roof Slab

Dose at Point 2

From Figure 1-2, for $\omega = 0.009$ and $\phi = 20°$

$R_{fe} = 0.07$

From Figure 1-4, for X = 75 psf and angle of incidence = $\phi = 21°$

$B = 0.8$

$$R_f = R_{fe} \times B \times R_{fc}$$

$$R_f = (0.07)(0.8)(0.255) = 0.014$$

$$D_2 = R_f \times D_o$$

$$D_2 = (0.014)(580) = 8.1 \text{ rads}$$

Dose at Point 3

$$R_f = R_{fe} \times B \times R_{fc} \times B$$

$$R_f = (0.07)(0.8)(0.255)(0.35) = 0.0050$$

$$D_3 = (0.0050)(580) = 2.9 \text{ rads}$$

Dose at Point 4

$$R_f = R_{fe} \times B \times R_{fc}$$

$$R_f = (0.07)(0.8)(0.138) = 0.0077$$

$$D_4 = (0.0077)(580) = 4.5 \text{ rads}$$

Through Roof Slab Over Point 1

Dose at Point 2

From Figure 1-4, for X = 525 psf and angle of incidence = 21^o

$$B = 0.0007$$

$$R_f = B \times R_{fc}$$

$$R_f = (0.0007)(0.255) = 0.00018$$

$$D_2 = (0.00018)(580) = \text{negligible}$$

Therefore, neutron radiation dose through roof slab over Point 1 is negligible at all points of interest

Through Entranceway Walls

Dose at Point 4

From Figure 1-4, for X = 475 psf and angle of incidence = 0° *

B = 0.001

$D_4 = (0.001)(580) = 0.6$ rads

Summary

The tabulation below summarizes the initial radiation dose.

Source	Type of Radiation	Dose in Rads		
		Point 2	Point 3	Point 4
Entranceway	Gamma	6.8	0.4	0.9
Entranceway	Neutron	11.6	4.1	6.4
Entrance roof slab	Gamma	0	0	0
Entrance roof slab	Neutron	8.1	2.9	4.5
Roof slab at Point 1	Gamma	0	0	0
Roof slab at Point 1	Neutron	0	0	0
Entranceway walls	Gamma	--	--	--
Entranceway walls	Neutron	--	--	0.6
Total radiation dose		27	7	12

From the above tabulation, it is apparent that to reduce the 27 rad dose at Point 2 to a tolerable level in the shelter would require either lengthening the corridor or adding a barrier wall at the shelter entrance. The addition of a 6-ft long barrier wall reduces the dose to 7 rads at the interior face of the wall and to 12 rads at the entrance to the shelter proper. In view of the uncertainties in calculating the free-field nuclear radiation quantities and in the radiation analysis method, the entranceway design is considered adequate for the cost analysis performed

* This assumes the walls are infinite in extent. If the geometry were considered, the reduction factor would be decreased.

in this study. If desired, it would be relatively inexpensive to reduce the radiation dose further by increasing the thickness of the entrance slab, by increasing the length of the barrier wall, or by increasing the length of the corridor between Points 1 and 2. For instance, increasing the thickness of the entrance slab from 6 in. to 9 in. would reduce the radiation dose for Point 4 at the shelter entrance from 12 to approximately 8 rads, but would not significantly increase the total cost of the entranceway.

REFERENCES

1. Glasstone, S., ed., The Effects of Nuclear Weapons, Department of Defense and Atomic Energy Commission, Washington, D.C., February 1964.

5. Newmark, N. M., Design of Openings for Buried Shelters, Contract Report No. 2-67, U.S. Army Engineer Waterways Experiment Station, Vicksburg, Mississippi, July 1963.

6. Stevenson, J. D., and J. A. Havers, Entranceways and Exits for Blast-Resistant Fully-Buried Personnel Shelters, Illinois Institute of Technology Research Institute (for Office of Civil Defense), Chicago, Illinois, September 1965.

20. Office of Civil Defense, Shelter Design and Analysis, TR-20 (Vol. 1), Washington, D.C., May 1964.

Appendix D

FALLOUT SHIELDING ANALYSIS OF ENTRANCEWAYS

By H. L. Murphy

Reproduced, without change, from original publication as Appendix 2 to: Wiehle, C. K., Shelter Entranceways and Openings, prepared by Stanford Research Institute for OCD, final report, September 1967. (AD-662 749)

NOTE: While fully outside entranceways are illustrated, the analysis techniques are useful for all entranceway configurations. No one type should be inferred as the recommended type for all applications.

Appendix D

FALLOUT SHIELDING ANALYSIS OF ENTRANCEWAYS

By H. L. Murphy

The entranceways developed in the project were examined for shielding capability against fallout contaminant from a nuclear detonation, as stated earlier. This somewhat repetitive FSA (fallout shielding analysis) work led to an approach that is presented in this appendix. Entranceways A-2 and C-1 are used for demonstration.

Entranceway pencil drawings to scale were used, since their use permits direct measurement of the many dimensions needed in FSA and thereby saves much working time over a method requiring any calculation of dimensions.

The basic tool was that whose use is currently taught in Office of Civil Defense FSA courses for practicing engineers and architects (Ref. 20). Therein, a careful comparison of Figure 4.6, used for cleared (or contaminated) finite circular areas, with the roof chart (Chart 4) values for a zero mass thickness roof showed identical results for the same solid angle fractions; however, Chart 4 with its entering argument of solid angle fraction (ω) is better suited to entranceway FSA purposes.

Certain assumptions are necessary in entranceway FSA. Some used in this project were:

1. Contamination factors: Fallout contaminant enters the entranceway portal at the "standard" (outdoor) rate per unit (horizontally projected) area, and this is then spread uniformly over all horizontal areas of the entranceway but not beyond the first turn. Using entranceway A-2 (see Figure 2-1) as an example, the contamination factor would be the area of the portal (3.67 X 9.5 ft) divided by the total area of steps and particulate trap under the grating (3.67 X 19.42 ft), or 0.489. To assume that the contaminant would only fall straight down into the entranceway would be nonconservative in PF (protection factor) results and would be assuming zero wind conditions. At the other end, it might be assumed that most if not all of the contaminant would accumulate

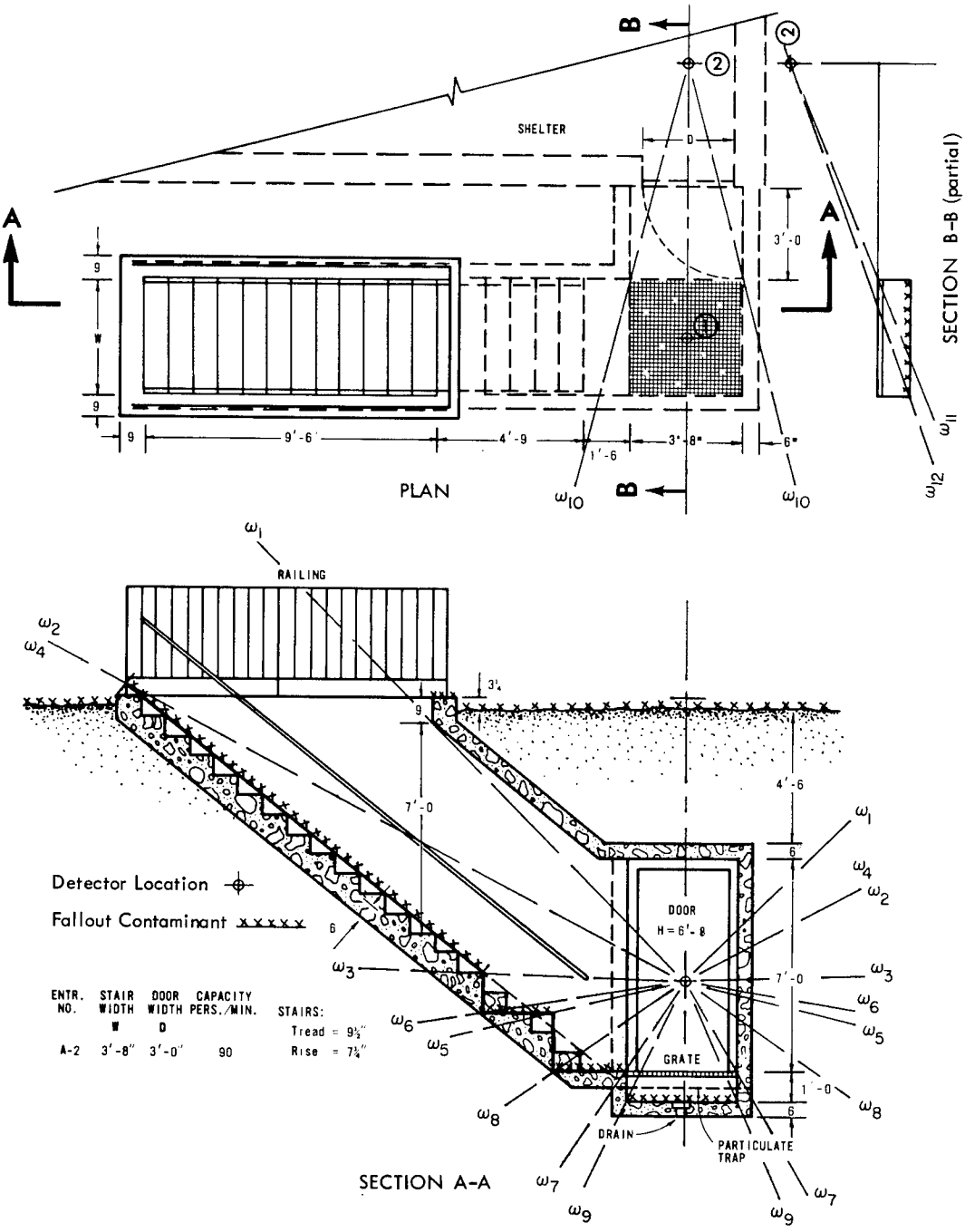

Figure 2-1
WORKED-OUT EXAMPLE 1

on the step at the level of the grating and on the trap under the grating. This assumption is conservative but was not used because shelter occupants could readily sweep the step contaminant through the grating or flush down both step and trap to get rid of the contaminant entirely.

This assumption was modified in entranceways such as B-5 as follows: Each side of the entranceway was separately handled as described for entranceway A-2 down to and including the grating, resulting in a doubling of the assumed contamination under the grating.

Another contamination factor was used in dealing with the steps located above the horizontal plane of the detector; it is discussed in the Worked-Out Example 1.

2. Steel gratings hold no falling contaminant and provide negligible shielding.

3. Doors of ordinary wood or hollow metal construction provide negligible shielding.

4. Detector location is a point although the human body is not.

5. For stairs located above the detector horizontal plane, neither the stairs nor stair nosings, if any, provide significant shielding. This assumption is demonstrated by the examples.

6. Where a contaminated area could both be "seen" (at least partially) by the final detector location and was in a tunnel-like location--for example, the trap under the grating, entranceway A-2--contributions were included for both (a) the contaminated area directly to the final detector location and (b) for the same contaminant being "seen" at a detector location directly above the contaminant, and then through a right-angle (tunnel) turn to the final detector location. This assumption was termed the "tunnel effect" for use in this study. It was sometimes applied as just described; sometimes only the larger of the two contributions (a) and (b) was used; or, for a relatively open entranceway (for example, entranceway D-4), only contribution (b) was used. The rationale was based on the likelihood of gamma radiation scattering off walls in a somewhat long and narrow, relatively confined, tunnel-like situation.

Entranceway A-2 fallout shielding analysis was made using a pencil scale drawing illustrated by Figure 2-1. The computational steps shown in Table 2-1 are explained following the table.

Table 2-1

COMPUTATIONS FOR WORKED-OUT EXAMPLE 1

	ω	W	L	Z	ω	Multipliers	C_o
1.	ω_1	3.67	18	9.3	.0860	-0.5/0.489	-.0036
2.	ω_2	3.67	35.2	9.3	.1095	0.5/0.489	.0046
3.	ω_3	3.67	10.4	3.9	.2213	-0.5 X 0.85	-.0186
4.	ω_4	3.67	40.6	3.9	.2746	0.5 X 0.85	.0238
5.	ω_5	3.67	8.3	1.1	.6223	-0.5	-.0791
6.	ω_6	3.67	13	1.1	.6416	0.5	.0827
7.	ω_7	3.67	3.67	3	.1755	-0.5	-.0169
8.	ω_8	3.67	8.3	3	.2780	0.5	.0284
9.	ω_9	3.67	3.67	4	.1112	1	.0207
10.							C_1 = .0472
11.	ω_{10}	3.67	7	7	.0723	$0.2C_1\omega_{10}$	.0007
12.	ω_{11}	3.67	18.7	4	.2505	-0.5	-.0252
13.	ω_{12}	3.67	21.33	4	.2553	0.5	.0257
							C_t = .0012 X 0.489
							= .0006
							PF $\approx$ 1700

Lines 1-2: Core and peripheral area of a decontaminated, zero mass roof (Chart 10, Case 3). Dividing this one item by the contamination factor permits applying the factor to the overall total contribution, rather than to each step, because it applies to all other contributions except this one.

Lines 3-on: Roof contributions all taken from Chart 4, zero mass thickness.

Lines 3-4: Steps changed to a plane, which is then treated as if horizontal; second contamination factor enters here, in that the plane used has a greater area than the horizontal area of the steps, thus the 0.85 multiplier.

Lines 5-8: Steps below detector horizontal plane, simplified into two steps.

Line 9: Particulate trap contribution to detector location 1.

Line 11: Converts total contribution to detector location 1 through a turn and solid angle fraction into a contribution to detector location 2.

Lines 12-13: Contribution from portion of trap seen from detector location 2.

An entranceway C-1 FSA was made, also using a pencil scale drawing illustrated by Figure 2-2. The computational steps shown in Table 2-2 are explained below.

Table 2-2

COMPUTATIONS FOR WORKED-OUT EXAMPLE 2

	ω	W	L	Z	ω	Multipliers	C_o
1.	ω_1	3.7	4	9	.0278	+0.5 [X_o=75]	.0011
2.	ω_2	3.7	23.5	9	.1022	+0.5 [X_o=75]	.0040
3.							C_1 = .0051
4.	ω_3	3	6.8	3.5	.1770	$0.2C_1\omega_3$	C_{T_A}= .0002
							$PF_A \approx$ 5000
5.	ω_4	3.67	12	6.4	.1207	$0.7\omega_5$ [X_o=100]	.0006
6.	ω_5	2.5	6.67	3.5	.1491		--
7.	ω_6	3.67	17.2	9.3	.0839	0.5 [X_o= 100]	.0021
							C_{T_B} = .0027 x 0.571 = .0015
							$PF_B \approx$ 670

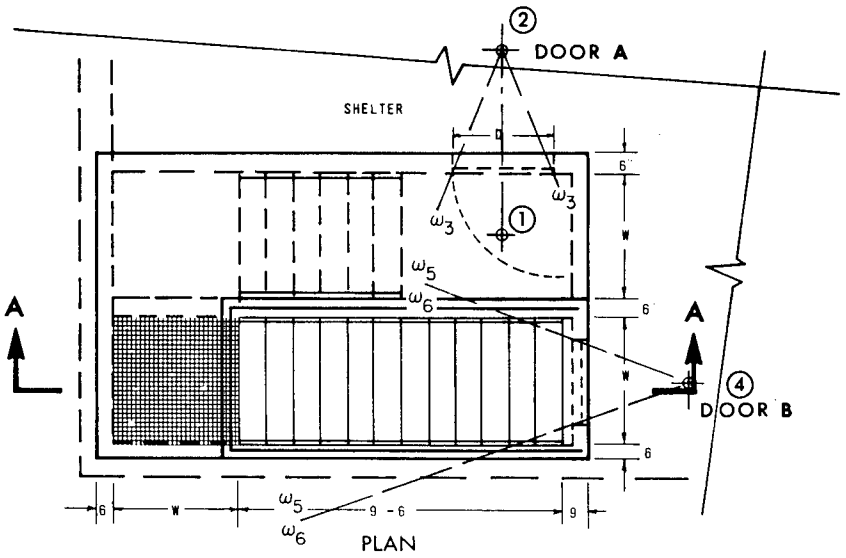

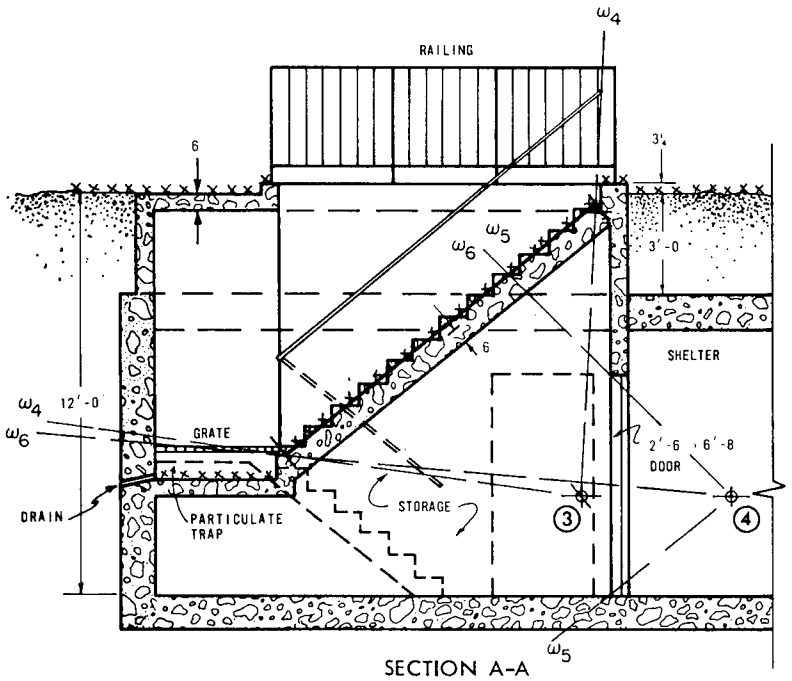

ENTR. NO.	STAIR WIDTH W	DOOR SIZE D	CAPACITY PERS. MIN.	STAIR
C-1	3'-8	3'-0 x 6'-8	90	TREAD 9½

Figure 2-2

WORKED-OUT EXAMPLE 2

Door A

General: Radiation from contamination on stairs must come through the concrete steps, a 6-in. concrete wall acting like an interior partition, and the doorway restriction, or must be reflected through three turns, in either case making this contribution negligible. Similar thinking may be applied to the trap under the grating. Thus, the only contribution left to be considered is that from the contaminated roof above the room where detector location 1 is shown, an ordinary off-center detector location problem. Contributions were all taken from Chart 4.

Lines 1-2: Roof above off-center detector location 1 (ω_1 and ω_2 not shown in Figure 2-2).

Line 4: Turn and solid angle fraction from 1 to 2.

Door B

General: Stairs simplified as in Worked-Out Example 1. Because of tunnel effect, contributions taken directly to detector location 4, and via 3 to 4; that direct to 4 restricted to portion seen through doorway, because any other must come through concrete stairs (used 8-in. or 100 psf, for mass) and through 6-in. more concrete in lintel, thereby becoming negligible. Any contribution from trap under grating is negligible because of both geometry and barriers. Contribution from roof over detector location 1 must come through several heavy barriers, so it is negligible. Contamination factor for steps and trap under grating amounts to 9.5/13.17 and must be combined with a factor for the simplified stairs amounting to 9.5/12, giving a combined factor of 0.571. Contributions were all taken from Chart 4.

Line 5: First right-angle turn is 0.2 and no turn is 1; for this partial turn, 0.7 was used.

Line 7: Ray from stairs to detector location 4 treated as normal to the simplified stairs, thus solution is for a half-roof.

Some of the values in Tables 2-1 and 2-2 are shown to an unwarranted number of decimal places. They are shown that way, however, because (1) all solid angle fractions and all zero mass roof contributions were computer-calculated so that no extra work was involved and (2) such might be useful to anyone trying to check through the computations, for understanding or other reasons.

Near the end of this work, two simplifications used (as in the first example problem solution herein) were subjected to more detailed examination. Computer programs were used for computing solid angle fractions and for computing radiation contributions, both to save professional working time and, more specifically, to carry values out to several decimal places, take differences, and then round off the total to fewer decimal places, all aimed at reducing round-off values wherein "roof" cores were continually subtracted from larger "roof" values. Simplifications examined were:

1. Simplification of the stairs located <u>below</u> the detector horizontal plane to fewer stairs. In Figure 2-1, the total contribution from the actual steps below the detector horizontal plane, including the step at the level of the grating, amounted to 0.0164.* In Worked-Out Example 1 the contribution based on the simplification amounted to 0.0151,* or an error of -8 percent in this one item. In carrying this nonconservative error forward, however, the tunnel turn reduces its effect so much as to leave the overall total contribution unchanged.

2. Simplification of the stairs located <u>above</u> the detector horizontal plane to a sloping, plane, smooth, contaminated surface, then analyzed by rotating the plane of the detector. Each step in Figure 2-1 was analyzed by considering it in five "roof" increments as indicated in the sketch, but the same Z distance was used for each step, as shown by the sketch arrow. The mass thickness of each increment was determined from its scaled thickness (on a scale drawing at 1"=0.1'), using reinforced concrete at 150 pcf. With a core and peripheral roof calculation for each of five increments and for each of 15 steps, 150 roof contributions were calculated. In Worked-Out Example 1, the contribution from the simplification of the stairs above the detector horizontal plane was 0.0052.* The results from the 150 roof calculations was 0.00524,* indicating an error of < 1 percent. Table 2-3 gives

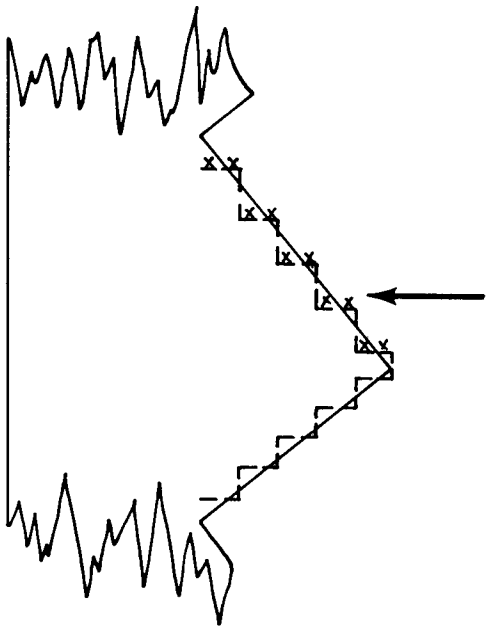

* Value before applying general contamination factor, 0.489.

values obtained for stair widths of 22, 44, and 66 in., and shows gross errors ranging from -9 percent to +10 percent in using the sloping plane approximation. Such errors would be indeed negligible after the radiation contribution values were multiplied by 0.489 (contamination factor), 0.2 (first tunnel turn), and 0.0723 (tunnel solid angle fraction), or a combined multiplier of 0.00707. Unfortunately, time was not available for detailed calculations varying other parameters than stair width.

Table 2-3

CONTRIBUTIONS FOR VARIOUS STAIR WIDTHS

Stair Width	Detailed Computations		Sloping Plane Approximation		
	C_T	$\left[\frac{9.5''}{6''}\right] C_T$	C_o	$0.85\ C_o$	Error
22"	.00166	.00263	.0028	.0024	-9%
44"	.00331	.00524	.0061	.0052	-1%
66"	.00487	.00771	.0100	.0085	+10%

The matter of stair nosings was reviewed briefly during the work. Nosings are required by some building codes, for the particular tread-rise values used. One standard nosing detail, shown in Ref. 38, is a simple one requiring only the sloping of the riser, the effect of which is to increase the tread by 1 in. Such a change would have only a trivial effect on the computations herein; e.g., use of this nosing in the examples in this appendix would mean only that each nosing would move the contaminant out 1 in. from the back of the tread below, leaving the same amount of tread contaminated as was assumed.

REFERENCES

20. Office of Civil Defense, Shelter Design and Analysis, TR-20 (Vol. 1), Washington, D.C., May 1964

38. American Concrete Institute, Manual of Standard Practice for Detailing Reinforced Concrete Structures, ACI 315-51 (Drg. 30), Detroit, Michigan, Jan. 1952

Appendix E

ROOM FILLING FROM AIR BLAST

By J. R. Rempel

PREFACE

This appendix is intended to serve both as a source of immediately applicable methodology and as a guide to the underlying gas dynamic theory. Those interested more in applying the methodology than in derivations and comparisons of calculated and observed results will find the following parts of this appendix of particular importance:

Location	Description
Section IIA	The simplest and fastest method of estimating average pressure in a room as a function of time; adequate for many purposes.
Section IIB3	Two different methods for a step-by-step, hand calculation providing average room pressure as well as dynamic pressure in the opening, valid for all flows through a single opening into a single room when the outside pressure is known as a function of time. Either method may be used but Method F is simpler for inflow, Method D for outflow; they may be combined in use.
Section IIC	Formulas for geometrical extent of the jet created inside the room by inflowing air and for dynamic pressure distribution within it.
Table E-3	A computer program to calculate average pressure within a single room and dynamic pressure in as many as eight openings as functions of time when a single room has openings into several different pressure fields (e.g., a room with front, rear, and side windows struck by a blast on the front wall).
Section IVB	A step-by-step hand calculation of average room pressure and dynamic pressure in each opening during filling of a single room through one or two openings into separate pressure fields.

When using the methodologies noted above, the user may find the meanings of symbols under Notation at the end of this appendix. Subscripts not explained there refer to physical spaces, i.e., subscript 1 indicates quantity is measured outside the room; other odd-numbered subscripts refer to interior of rooms and even-numbered subscripts refer to connecting ducts or openings.

CONTENTS

FIGURES

TABLES

Appendix E

ROOM FILLING FROM AIR BLAST

I Introduction

When a blast wave strikes a building, even should the structure withstand the initial impact, the resulting inflow of air through windows and other openings can be critical in determining the safety of any people sheltered by the structure and in determining the response of the structure itself to the blast impact. Although the physical laws obeyed by moving gases are well known and the course of the inflow in filling the building can in principle be calculated completely, any such calculation is far too lengthy to be practical for most purposes; fortunately, simplifications can be introduced which greatly shorten the labor of estimating effects of the blast inside the building and which give results in good to fair agreement with experiments done with small models. In general, the effect of the inflow is to provide a stream of fast moving air in the shelter space which may (1) endanger shelterees by hurling them against large relatively fixed objects or by hurling objects against them, and (2) provide a back pressure on the inner surfaces of structure walls countering the blast pressures on their outer surfaces.

Several factors enter into the calculation: the pressure outside each wall with openings and the time each opening becomes available, the area occupied by each opening and the volume of each room, the number of connected rooms and the area of each connection, and the ambient pressure and temperature in the building before the blast strikes. Perhaps the first of these to consider is what proportion of the wall exposed to the blast is open. If this fraction is greater than one half, the shock front leading the blast wave will pass into the building only slightly weakened and subsequent inside pressure should be estimated from a knowledge of shock position and the laws of shock reflection. Methods appropriate to this case are only touched upon here. On the other hand, should the fraction be less than one tenth, clearly the filling is not a shock process and the methods treated here are quite pertinent. Unfortunately, in many applications the fraction of open area will lie between these two extremes and, in these cases after the room filling calculation has been completed according to the methods suggested here, some thought must be given independently to the influence of the entering shock front.

When the source of the blast wave is an explosion and the location of the building in relation to the point of explosion is known or postulated, "free field" pressure histories at the building site can be found in standard references,[1,2,15]* and from these histories well known methods[1,3] are available to derive approximate histories on the outside of the walls of the building. Briefly, these methods account for a short-lived peak of pressure created by the impact of the front upon the wall nearest the explosion, the relatively fast erosion of this high pressure to a level which is the sum of the free field pressure plus a drag pressure on the wall due to the high winds behind the blast front. This quasi-steady pressure then decays slowly to zero as the blast wave moves onward past the structure.

Ordinary window glass breaks rather quickly, i.e., within 8 ms (milliseconds) or less when struck by blast overpressure of 1 psi (pound per square inch) or more.[4] Doors may withstand outside pressure longer, or even altogether. The time an opening becomes available with respect to the first impact of the blast upon the building becomes, then, the breaking time plus the time required by the wave to travel from the wall nearest the explosion to the opening. If the opening is in the wall nearest the explosion, travel time is of course zero. Strictly, the decay of the blast wave overpressure which occurs during this time must be taken into account, but when the blast arises from a nuclear explosion of yield greater than a few kt (kilotons) this decay is slight and negligible; that is, a single "free field" pressure history for all openings may be assumed.

It should be emphasized that the methods given here are simplified and their use can lead only to estimates. They are intended to provide: (1) calculations applicable to hand computation by those untrained in gas dynamics and (2) approximate results useful until more careful calculations are made. Only in the case of the simplest structural configurations and the simplest pressure history shapes can limits of error be suggested for these results. Such cases will be the subject of the discussion immediately below.

II Classical Nuclear Blast Wave Incident upon a Single Room

A. Estimation of Inside Pressure History

The "classical" blast wave from nuclear explosions consists of a steep pressure front or rise followed by a long-lasting decay phase during which the pressure in the wave falls to zero. It is accompanied by high winds giving rise to dynamic pressure against objects in the stream. Striking a wall at normal or near normal incidence, it creates a high pressure

---

* References are listed at the end of this Appendix.

zone at the surface, which however is rapidly eroded as relief waves move across the wall face from the edges. As a first approximation in the calculation of room filling, this reflected phase can usually be neglected. Following the decay of the high reflected pressure, the quasi-steady pressure (free field plus dynamic) remains against the wall for hundreds of milliseconds to several seconds, depending on explosive yield. Generally filling is complete before this quasi-steady pressure has fallen more than a few percent; hence, as a first approximation the outside pressure may often be considered constant and, if only a single wall with opening is exposed to the blast, the time ΔT (in milliseconds) to complete filling may be computed as the ratio $\frac{V}{2A}$, where V is room volume in cubic feet and A is area of opening in square feet.† The average room pressure at any time t during the filling process is then simply the fraction of the quasi-steady outside pressure given by the ratio $\frac{t}{\Delta T}$. For the purposes of this calculation, areas of several openings in the same wall should be added together to form the quantity A.*

In case there are two or more walls with openings exposed to the blast and each such wall sustains a different outside pressure history (as will happen, for example, when the drag coefficient is different for two walls), the calculation is more complicated but first estimates of filling time and average inside pressure during filling may be found by adding interior pressures calculated as if each wall alone were exposed. As an example, consider a room of volume 30'x10'x10' = 3000 ft^3 in which the front wall has total openings of 36 ft^2 and side walls have total openings of 60 ft^2. The ratios $\frac{V}{2A}$ for the front and side walls are 41.7 and 25 ft, respectively. If the quasi-steady overpressure on the front wall is 10 psig (pounds per square inch - gauge) and on the side wall 8 psig and if further the side wall opening becomes available 10 ms after the first blast impact, then the average inside pressure will be approximately as shown in Figure E-1 by the heavy line OAFG. In other words the room will fill in approximately 24 ms. Lines OAC and DE represent filling rates through front and side walls,respectively; and ordinates of OAC and DE are added to form the line OAFG. Of course after the average inside pressure exceeds 8 psi there will be outflow through the side wall; to allow for this loss the line FG has been placed between the outside pressure at the side wall (8 psig) and the outside pressure at the front wall (10 psig). The ordinate at FG is closer to 8 psig than to 10 psig because the area of the opening in the side wall is greater than that in the front wall. The line FG is intended to represent the final quasi-equilibrium pressure in the room.

---

* The experimental justification of most of the procedures described in this section is demonstrated later in Figures E-4, E-5, E-6 and E-8.

† Empirical relationship, dimensionally inconsistent. Meanings of symbols as used in this Appendix are defined as introduced and under "Notation" at end of Appendix.

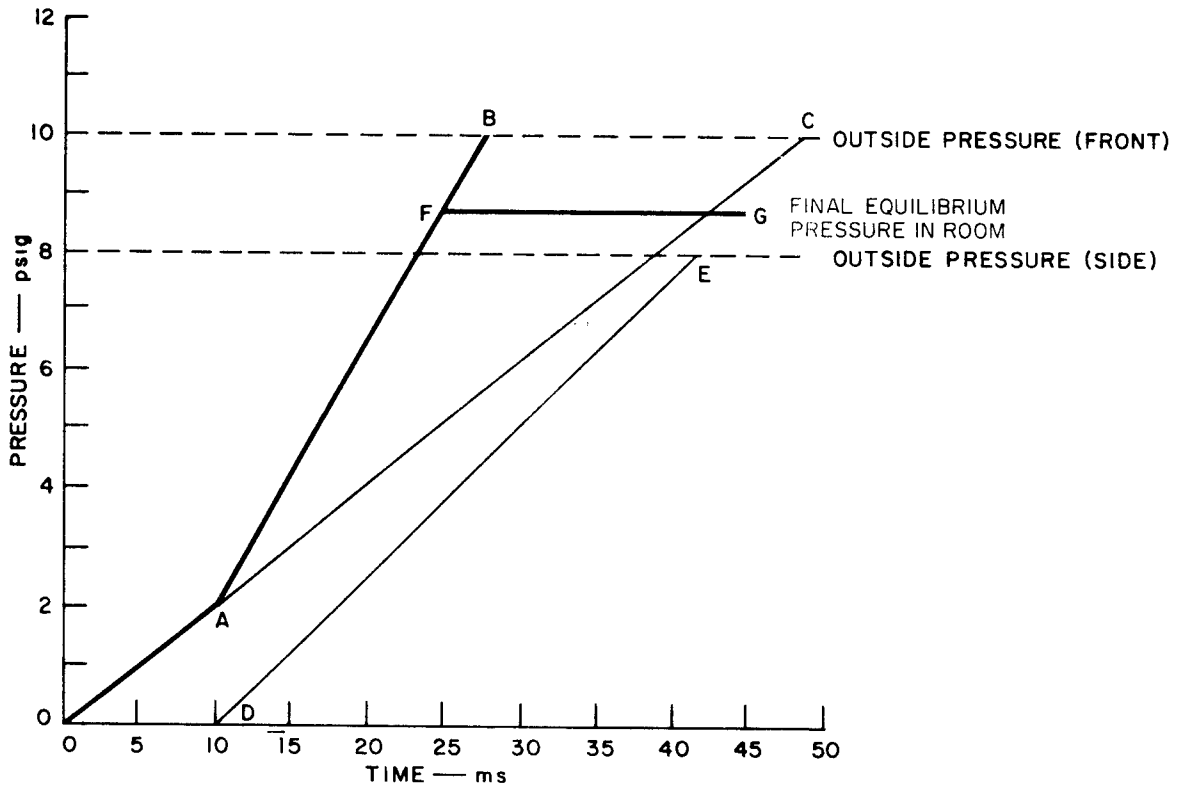

FIGURE E-1 APPROXIMATE FILLING RATES THROUGH TWO WALLS

These simple calculations do not apply when the reflected pressure lasts an appreciable length of time, or when the wave is non-classical such as it would be were a precursor present. Under these conditions the more detailed methods set forth below must be followed.

B. General Case

Justification for use of the simple methods noted above rests upon experience with a step-by-step calculation and comparison of its results with experiments. This calculation applies the principles of steady isentropic flow in ducts in successive, small time intervals. Conditions computed for the end of one time step become initial conditions for the next step. Conservation of energy, momentum and mass along with the assumption that the air behaves as a perfect gas with constant specific heats determine the thermodynamic variables, pressure, temperature and density, as well as the wind speed through the opening. Unique expressions lending themselves to simple calculation cannot be given for the laws of conservation of energy and momentum, and alternate forms leading to somewhat different results will be stated. All such expressions rely upon certain approximations to the conservation laws and these approximations usually introduce errors into the results in comparison with which the approximations arising in the assumptions of isentropy, perfect gas behavior and constant specific heats are negligible.

1. Inflow. Figure E-2 shows the idealized room with a single opening struck head-on by a blast wave. Three regions are noted: the outside ①, the doorway ② which serves as a duct connecting the outside with the room ③. In order to make the calculations tractable, uniformity of conditions in each of the two regions ① and ③ and over the cross section of region ② is assumed; furthermore, during each small time interval Δt, steady conditions are assumed in each region. During the aforementioned quasi-steady state outside the building these assumptions are probably valid for region ① but they clearly introduce error if the reflection or diffraction phase lasts an appreciable time, for during that episode relief waves are moving into the region from the edges of the building as well as from the doorway itself causing rapid fluctuations in wind speed and pressure. (Some account is taken of changes in pressure during the diffraction episode by the standard techniques of estimating outside pressure.) Similar remarks can be made concerning regions ② and ③, but if we are content to deal with "average" pressure and speed in those two regions, we may apply the step-by-step isentropic analysis. However, our present methods do not provide for any apportionment of gaseous energy in region ③ between streaming kinetic energy and internal energy; for simplicity of calculation it will be treated as entirely internal at all times, which will cause overestimation of pressure and neglect of winds within the chamber. In evaluating the wind threat, the speed and dynamic pressure in the duct ② must be regarded as the upper bounds on wind speed and dynamic pressure in region ③. Later, methods will be given for estimating change in dynamic pressure as the wind moves into the room.

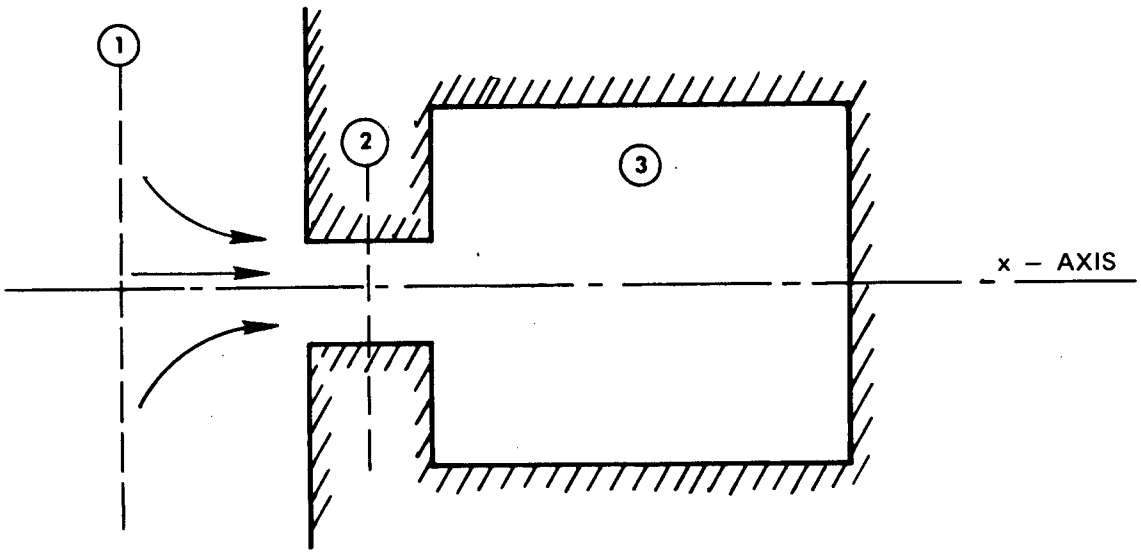

FIGURE E-2 THE FILLING CHAMBER

In writing the conservation equations, two views can be taken of conditions in region ①. On the one hand pressure, density and wind speed may be those of the free field behind the blast front or, on the other hand, the air upstream of the opening may be treated as stagnate at a pressure above free field either by the amount of the reflected pressure or by the amount of the product of the drag coefficient and dynamic pressure. Provided drag coefficients are known, the second view is more simply applied, especially when the blast front does not meet the wall head-on. In what follows, the pressure, P_1, and density, ρ_1, in region ① will be those of stagnate air outside the wall. The work done in moving a mass element Δm in region ① through a small distance Δx toward region ② is:

$$P_1 A_1 dx = P_1 \Delta V_1 = \frac{P_1}{\rho_1} \cdot \Delta m$$

where A_1 is the cross sectional area, and ΔV is the volume occupied by Δm in region ①. The mass element carries with it the internal energy it had in region ①, i.e.,

$$\frac{1}{\gamma - 1} \cdot \frac{P_1}{\rho_1} \cdot \Delta m,$$

where γ is the ratio of specific heat at constant pressure to the specific heat at constant volume. (The perfect gas equation of state is assumed; see Ref. 5.) If the flow into the room is steady, energy conservation requires that the same total energy, specifically, the sum

$$\frac{1}{\gamma - 1} \cdot \frac{P_1}{\rho_1} \cdot \Delta m + \frac{P_1}{\rho_1} \cdot \Delta m = \frac{\gamma}{\gamma - 1} \cdot \frac{P_1}{\rho_1} \cdot \Delta m$$

be given up within region ② during the same time interval. Furthermore mass conservation asserts that the mass element moving through region ② toward region ③ equal Δm. The work done in region ② in pressing the mass element toward region ③ is

$$\frac{P_2}{\rho_2} \cdot \Delta m$$

and the internal energy in the element is

$$\frac{1}{\gamma - 1} \cdot \frac{P_2}{\rho_2} \cdot \Delta m$$

where the subscript ② denotes conditions in region ②. Since the air is flowing into the room, however, the element in ② also carries (streaming) kinetic energy of amount

$$\frac{1}{2} u_2^2 \Delta m$$

where u designates particle or material speed. Thus, if conditions are not changing too fast, we can write (cancelling out the factor Δm):

$$\frac{\gamma}{\gamma - 1} \cdot \frac{P_1}{\rho_1} = \frac{\gamma}{\gamma - 1} \cdot \frac{P_2}{\rho_2} + \frac{1}{2} u_2^2 \qquad (1)$$

To apply conservation of linear momentum we consider a control surface, shown dashed in Figure E-3. Neglecting gravitational forces, the x-component of the force integrated over this surface must equal the rate of flow of the x-component of momentum out of the volume plus the rate of increase of x-momentum within the volume.[6] Neglecting frictional and viscous effects, the only force on the surface is the thermodynamic pres-

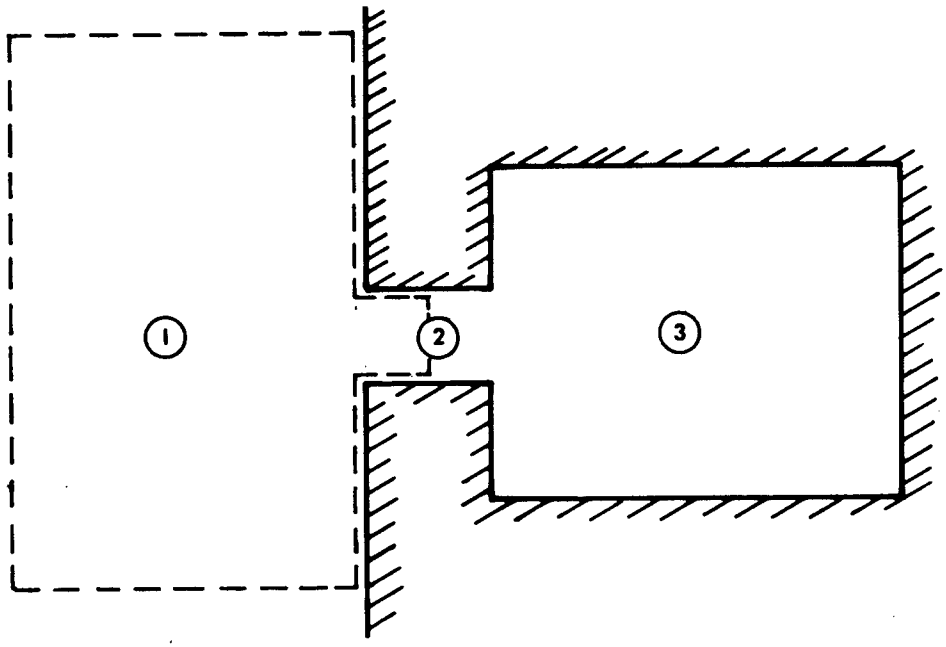

FIGURE E-3 FIRST CONTROL SURFACE

sure, exerted normal to the surface in an inward direction. Across the throat of the duct this pressure is taken to be P_2; everywhere else on the surface it is approximately P_1. (Around the entrance to the duct pressure on the wall will be less than P_1, but the mass flow rate turns out not to be highly sensitive to corrections made for this effect and, in order to simplify calculation, uniform pressure P_1 will be assumed. The mass speed u_2 however would be reduced by this correction.) During the quasi-steady episode momentum within the surface will change only slowly and we assume that it is in fact constant during each successive time increment Δt. (This assumption is clearly false during the shock diffraction episode due to the presence of fast moving reflected shock fronts within the surface. During the quasi-steady episode the assumption neglects the relief wave spreading into the stagnate air outside the opening.) Thus, carrying out the integration over the surface, we find

$$\int P \cos \theta \, da = (P_1 - P_2) A_2$$

In this integral θ is the angle between the inward normal to the surface and the positive x-direction and da is an element of area on the control surface. The total momentum in the positive x-direction passing through the surface is simply

$$\rho_2 u_2^2 A_2$$

Hence, momentum conservation reduces to

$$P_1 - P_2 = \rho_2 u_2^2 \tag{2}$$

Finally we note that even in the presence of moderately strong or weak shocks the isentropic equation of state of a perfect gas is accurate enough for this approximate calculation; hence

$$\rho_2 = \rho_1 \left[\frac{P_2}{P_1}\right]^{1/\gamma} \tag{3}$$

(See Ref. 7).

Given P_1 and ρ_1, Eqs. (1), (2), and (3) may be solved for P_2, ρ_2, and u_2.* The result can be written as:

---

* For diatomic gases like air, γ=1.4; see Ref. 8.

$$\frac{2\gamma}{\gamma + 1} \left[\frac{P_2}{P_1}\right]^{1/\gamma} = \frac{P_2}{P_1} + \frac{\gamma - 1}{\gamma + 1} \tag{4}$$

which is independent of ρ_1. If $y = \frac{P_2}{P_1}$, $A = \frac{\gamma - 1}{\gamma + 1}$

and $B = \frac{2\gamma}{\gamma + 1}$, Eq. (4) can be put in the form

$$By^{\frac{1}{\gamma}} = y + A \tag{5}$$

When A and B have the values stated above, Eq. (5) has two solutions, one of which is y = 1 and the other is y = 0.1912. The second solution is the only one of interest here and will be designated y_o.

To continue the calculation ρ_1 must be known. This value can be found from the Rankine-Hugoniot relations and knowledge of the strength and angle of incidence of the original shock front (Ref. 1,2), or it can, with enough accuracy for incident shock strengths less than 15 psi, be computed from ambient conditions using the isentropic equation of state, i.e.,

$$\rho_1 = \rho_o \left[\frac{P_1}{P_o}\right]^{1/\gamma} \tag{6}$$

where P_o and ρ_o are ambient pressure and density, respectively. With ρ_1 known, air density and pressure in the opening can be calculated from:

$$\rho_2 = \rho_1 \, y_o^{\,1/\gamma} \tag{7}$$

$$P_2 = y_o \, P_1 \tag{8}$$

from which wind speed becomes:

$$u_2 = \left[\frac{P_1 - P_2}{\rho_2}\right]^{\frac{1}{2}} = \left[\frac{P_1 \, (1 - y_o)}{\rho_1 \, y_o^{\,1/\gamma}}\right]^{\frac{1}{2}} \tag{9}$$

The mass flow into the room (3) can be written

$$\Delta m = \rho_2 \, u_2 \, A_2 \Delta t$$

$$= \left[P_1 \, (1 - y_o) \, y_o^{\frac{1}{\gamma}} \, \rho_1 \right]^{\frac{1}{2}} A_2 \, \Delta t \qquad (10)$$

If V_3 is the volume of the room and the prime is used to denote conditions in the room at the beginning of time step Δt, then average density in the room ρ_3 at the end of Δt can be written as:

$$\rho_3 = \rho_3' + \frac{\Delta m}{V_3} \qquad (11)$$

To find pressure in the room at the end of the time step we assume that all the energy lost in region (1) appears as an increase of internal energy of the gas in the room, i.e.,

$$\frac{\gamma}{\gamma - 1} \cdot \frac{P_1}{\rho_1} \cdot \Delta m = \frac{1}{\gamma - 1} \cdot \left(P_3 - P_3' \right) \; V_3$$

which can be solved to give P_3 in terms of known quantities:

$$P_3 = \frac{\gamma \, P_1}{\rho_1} \cdot \frac{\Delta m}{V_3} + P_3' \qquad (12)$$

At any time air temperature T_3 within the room can be calculated from the perfect gas law:

$$T_3 = \frac{P_3}{R \rho_3}$$

where R is the gas constant[5] for air in the appropriate units (e.g., in metric units R = 0.3028 joule/g^{o}C). The quantity T_3 can reach high values as a result of the compression existing behind the shock and within the room; however, if airflow to the outside (outflow) is maintained, the relaxation of pressure following the passage of the front will return room gas temperatures to safe levels before injury to occupants is likely. Only the long lasting increase in room temperature resulting from fires will normally be a threat to the shelterees.

Conditions existing in the chamber at the beginning of a time step are used in the foregoing calculations only in Eqs. (11) and (12) and do not influence duct parameters because transients have been omitted from consideration. Transient phenomena, for example, determine the direction of flow; that is, if $P_1 > P_3$, flow is inward as discussed above, but otherwise flow is outward. Repeated neglect of signals originating from the room leads to an accumulation of error in the calculation of average pressure as can be seen from comparisons between calculation as above and measurement shown in Figures E-4, E-5, and E-6. The experiments[9] were carried out in a 24-inch shock tube; the configuration of each model chamber is shown in an inset in the figure; and the foregoing calculation produces Curve F of the figures. The curves in Figures E-5 and E-6 labelled "external history (A)" are measurements in the free stream by means of a pitot tube oriented with respect to the stream to conform with the orientation of the opening in the model room; "external history" in Figure E-4 is side-on overpressure in the unobstructed shock tube.[9] In each case the calculation initially yields pressure in agreement with observation but eventually shows room pressure during filling in excess of measurement, although the maximum difference is 20% or less. Magnitude of Δt for these calculations was one-quarter the transit time of a sound signal across the room.

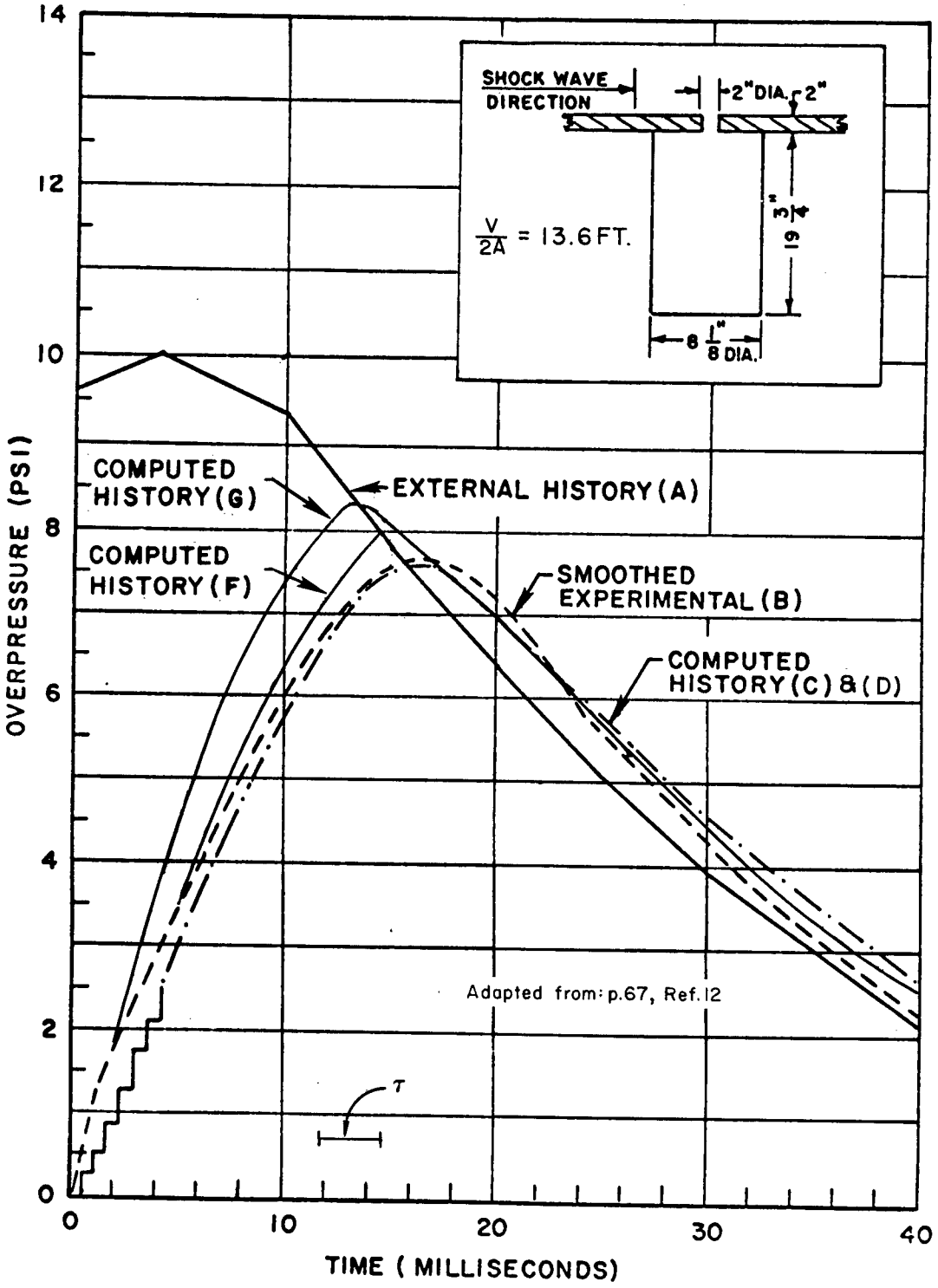

FIGURE E-4 FILL HISTORIES FOR SIDE-ON INCIDENCE

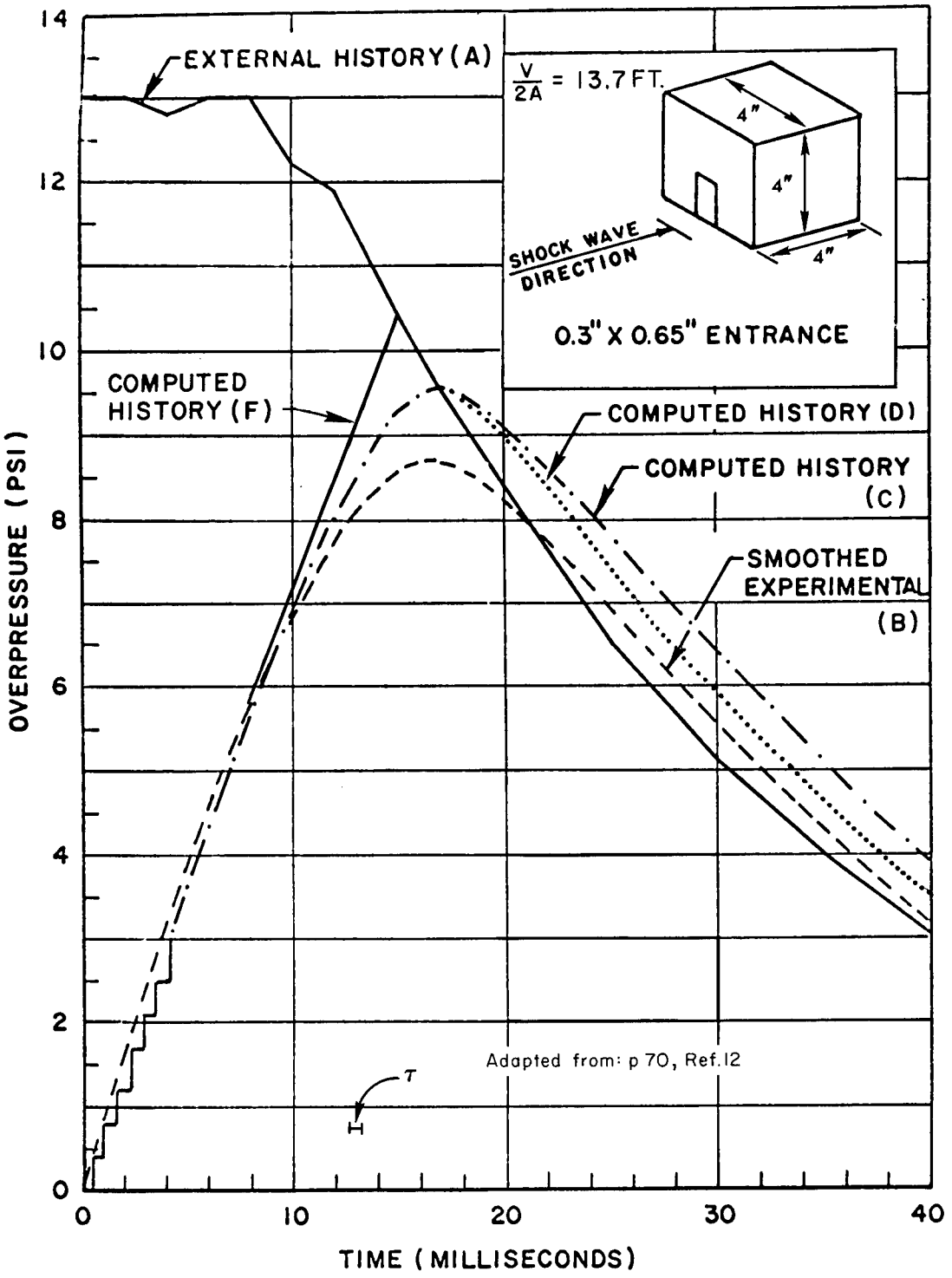

FIGURE E-5 FILL HISTORIES FOR A FACE-ON MODEL

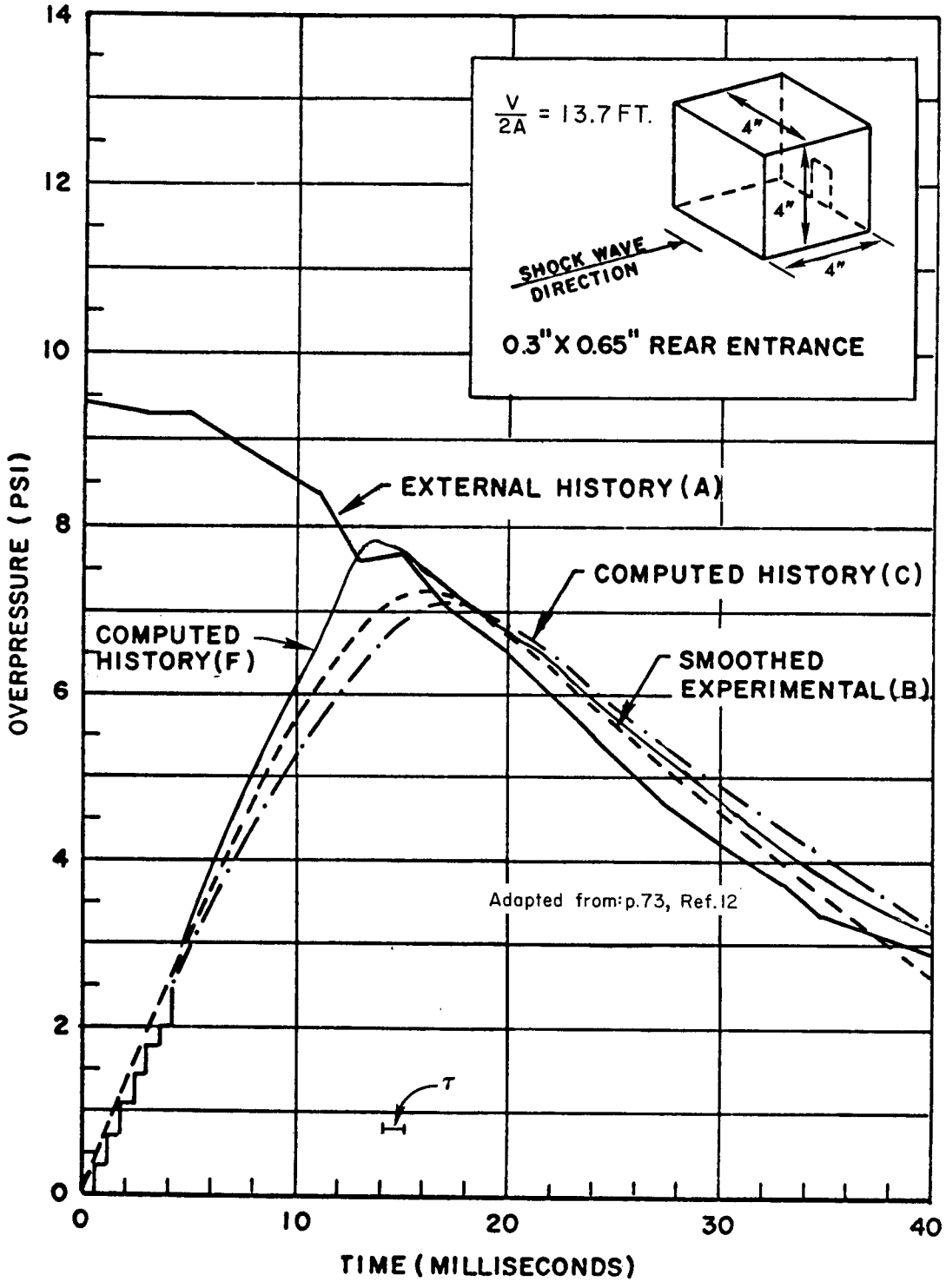

FIGURE E-6 FILL HISTORIES FOR A REAR FILL MODEL

Choice of the size of Δt is somewhat arbitrary except that (1) values much greater than sound transit time will give a false idea of the degree of irregularity in the fill process and (2) enough steps should be taken to make it possible for the influence of variations in P_1 to be shown in the results. The length of the bar labelled "τ" in Figures E-4, E-5, and E-6 represents the sound transit time across the longest room dimension.

The existence of significant theoretical errors in our treatment of flow into a room by quasi-steady analysis is clearly revealed by considering the single control surface formed by superposition of that shown in Figure E-3 and that indicated with dashed lines in Figure E-7. Such a surface coincides with the inner surfaces of the room and passage and extends into quiescent air outside. Under our hypotheses there is no flow through this surface anywhere and no change of momentum within it, yet the surface integral of the x-component of pressure over the boundaries does not vanish.

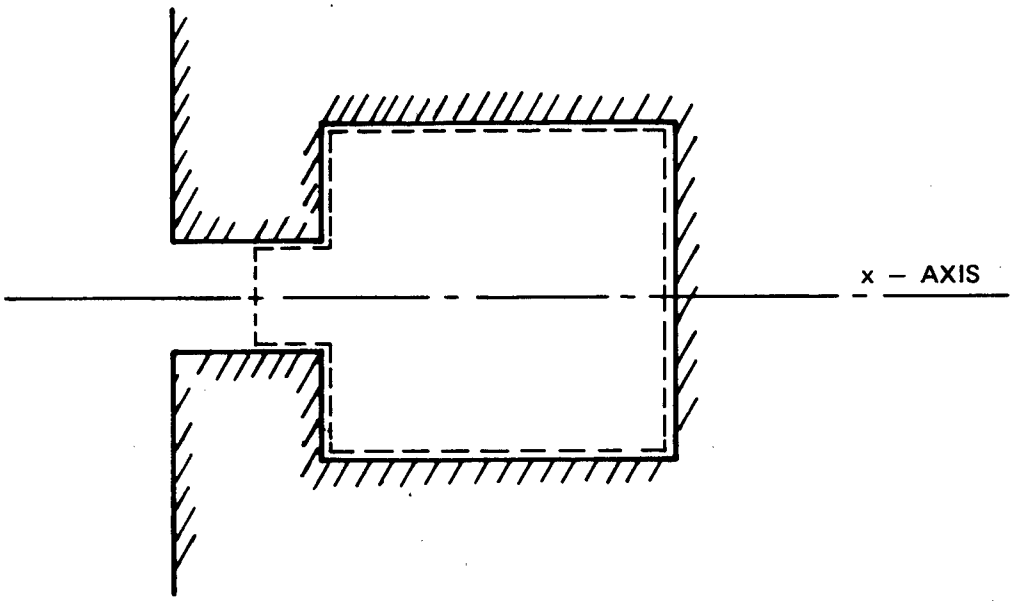

FIGURE E-7 SECOND CONTROL SURFACE

This absurdity can be avoided in one or both of two ways. A term may be added to the right side of Eq. (2) to account for the changing flow pattern within the control surface shown in Figure E-3 or a term may be added to the left side of Eq. (2) to account for the possible nonuniformity of pressure over the boundaries of the surface. As the room begins to fill, a rarefaction wave moves back into the high pressure gas outside the first doorway bringing more and more gas into motion toward the opening. In other words, the neglect of the rate of change with time of the momentum within the control surface outside the room may be at least one cause of the contradiction noted above. Any attempt to calculate a correction for this effect would certainly add to the complexity of these simplified procedures; furthermore, the degree of agreement between observations and theory of Method F (shown in Figures E-4, E-5, and E-6) suggests that the added effort to account for the rarefaction wave may not be needed to achieve the desired degree of accuracy.

Some writers[10,11,12,17] use the equation

$$P_2 = P_3' \tag{13}$$

instead of Eq. (2). Justification for Eq. (13) is based on analogy with the treatment of flow into a large chamber steadily being evacuated.[13] Equation (13) of course provides continual coupling between flow conditions and conditions in the room.

Using Eq. (13) we derive the pressure buildup inside the room in the following way. Substituting Eq. (3) into Eq. (1), then replacing P_2 with P_3' according to Eq. (13) and solving the resulting equation for u_2, we find:

$$u_2 = \left[\frac{2\gamma}{\gamma-1} \cdot \frac{P_1}{\rho_1} \left(1 - \left(\frac{P_3'}{P_1} \right)^{1-1/\gamma} \right) \right]^{1/2}$$

from which we calculate the mass inflow in the time increment Δt:

$$\begin{aligned} \Delta m &= K \rho_2 u_2 A_2 \Delta t \\ &= K \rho_1 \left(\frac{2\gamma}{\gamma-1} \cdot \frac{P_1}{\rho_1} \right)^{1/2} \left(\frac{P_3'}{P_1} \right)^{1/\gamma} \left[1 - \left(\frac{P_3'}{P_1} \right)^{1-1/\gamma} \right]^{1/2} A_2 \Delta t \end{aligned} \tag{14}$$

Whenever Eq. (13) is employed, empirical corrections must be made to reduce the calculated inflow rate or the calculation will not yield realistic values for room pressure in small experimental models; the simplest correction is the discharge coefficient,[13] represented by the factor K

in Eq. (14). Investigators at the IIT Research Institute[17] have found it necessary to use the value $K = 0.7$ to reconcile computed pressure rises in small models with those measured; Curves D in Figures E-4 and E-5 have been produced by a calculation based on Eq. (13), with $K = 0.7$ during inflow and $K = 1.00$ during outflow.

The value of the discharge coefficient is usually discussed in connection with boundary layer thickness and the Reynolds number.[13] It should be noted therefore that the relatively good agreement between the observed room pressures and Curves D was obtained in very small models and not in full-sized rooms. To provide an estimate of the influence of the value of K on calculated pressure rise, Curve G, based on the value $K = 1.00$ during both outflow and inflow, has been entered in Figure E-4. In the flow into full-sized rooms, presumably, the Reynolds number will be larger and the discharge coefficient more nearly equal to 1.00 than in the flow into small models.

Finally, the pressure increment during the interval Δt is found by substitution of Eq. (14) into Eq. (12):

$$P_3 - P_3' = K \gamma P_1 \left[\frac{2\gamma}{\gamma - 1} \cdot \frac{P_1}{\rho_1} \right]^{\frac{1}{2}} \left(\frac{P_3'}{P_1} \right)^{\frac{1}{\gamma}} \left[1 - \left(\frac{P_3'}{P_1} \right)^{1 - \frac{1}{\gamma}} \right]^{\frac{1}{2}} \frac{A_2 \, \Delta t}{V_3} \qquad (15)$$

Melichar[11,12] omits both the factors K and γ before the right-hand side of Eq. (15), which is equivalent numerically to making $K = 0.7$ and $\gamma = 1.4$. He attempts to justify this procedure on theoretical grounds unconnected with boundary layer theory.[12] Some of his numerical results are shown as Curves C in Figures E-4, E-5, E-6, and E-8. Melichar employs a value of Δt equal to the transit time of sound across the room.

Pursuing the analogy between room filling and steady flow into a chamber held at constant pressure, we expect to encounter the phenomenon of choking as the ratio of room pressure to outside pressure drops below the critical value.[13] For a given set of reservoir conditions, i.e., for each pair of values P_1 and ρ_1, the critical pressure ratio is that for which isentropic flow into the room achieves the maximum mass rate and for which the flow speed equals local sound speed. Therefore, to find this critical ratio, we can differentiate Eq. (14) with respect to P_3'/P_1, set the result equal to zero and solve for $(P_3'/P_1)_{crit.}$, which yields;

$$\left(\frac{P_3'}{P_1} \right)_{crit.} = \left(\frac{2}{\gamma + 1} \right)^{\frac{\gamma}{\gamma - 1}}$$

For every value of P_3' below the critical value as given above, mass flow into the room will be that obtained by substituting the critical ratio into Eq. (14), i.e.:

$$(\Delta m)_{\text{choked}} = K\left[\gamma\ \rho_1\ P_1\left(\frac{2}{\gamma+1}\right)^{\frac{\gamma+1}{\gamma-1}}\right]^{\frac{1}{2}} A_2\ \Delta t$$

Because the mass flow rate is limited in this way independently of the value of P_3' it is called "choked" flow. Flow obeying Eq. (14) is called "unchoked" or "subsonic." Numerically, when $\gamma = 1.4$ the critical ratio equals 0.5283; thus, assuming ambient pressure is 14.7 psia,* the critical outside pressure is

$$\frac{14.7}{0.5283} = 27.83 \text{ psia or } 13.13 \text{ psig}^{\dagger}$$

Peak overpressure in none of the experiments reported in Figures E-4, E-5, and E-6 rose above 13.13 psig; hence, according to the foregoing theory, choked flow should not have occurred.

A similar degree of comparison between calculation and measurement is found in the results shown in Figure E-8 stemming from a 27 ft^3 model exposed to a large chemical explosion, except that the transient fluctuations associated with the entering shock front are more easily discerned in the larger model than in the small shock tube models. The parameter values used in the calculations summarized in Figure E-8 were:

$P_o = 13.58$ psia	ambient pressure
$\rho_o = 0.0672$ lb/ft^3	ambient density
$\gamma = 1.4$	ratio of specific heats
$A_2 = 0.821$ ft^2	area of opening
$V_3 = 27.0$ ft^3	volume of model room

The fraction of the impacted wall area occupied by the opening is slightly less than one-tenth.

From the results shown in Figures E-4, E-5, E-6, and E-8, some estimate can be made of the validity of the greatly simplified method of computing pressure rise in a filling room set forth in Section IIA. In each figure, the value of V/2A in feet has been entered. A constant pressure

---

* Pounds per square inch, absolute.

† Pounds per square inch, gauge.

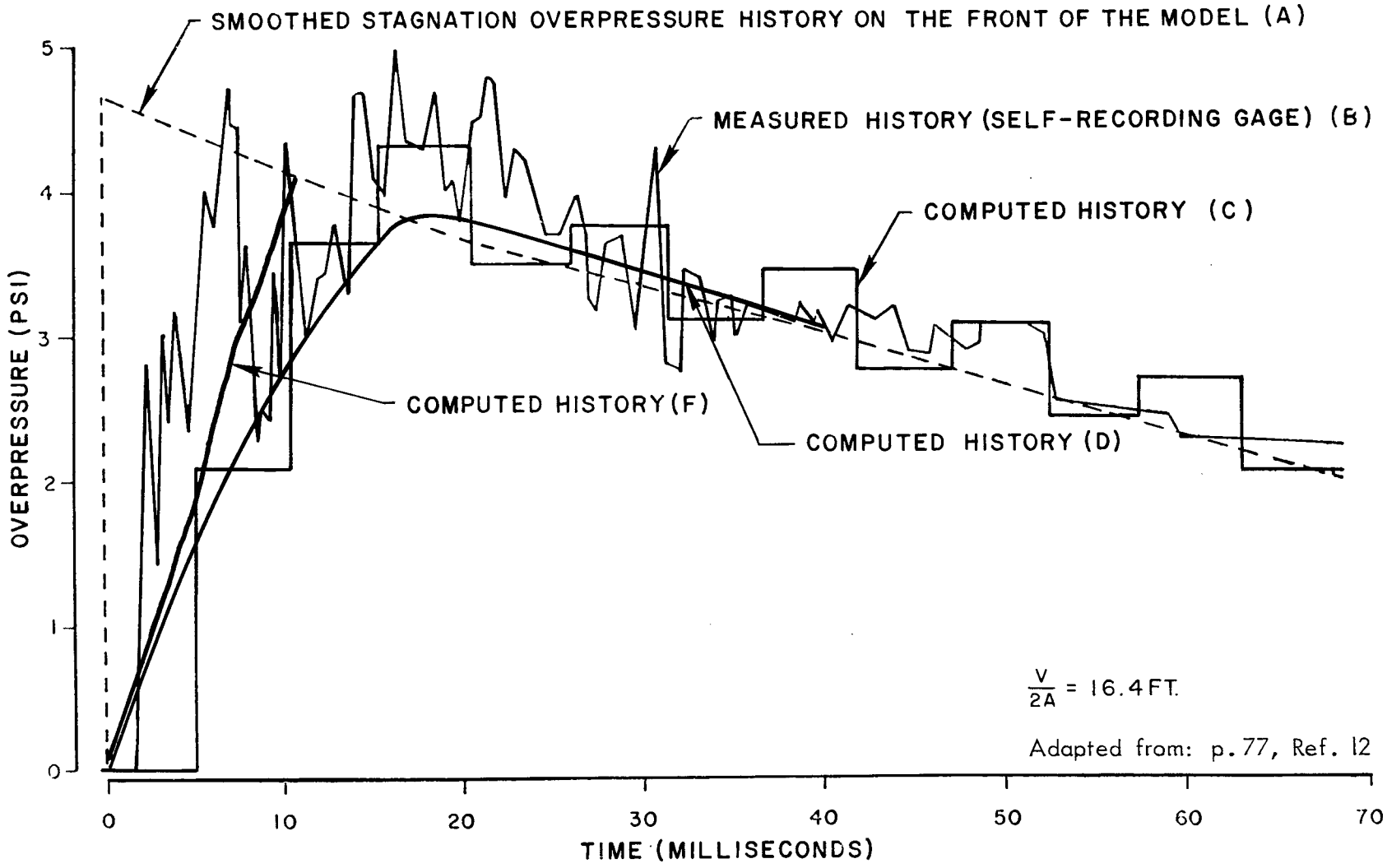

FIGURE E-8 COMPARISON OF THE COMPUTED VERSUS THE EXPERIMENTAL FILL HISTORY OF THE MODELED CHAMBER TESTED IN PROJECT DISTANT PLANE

rise from zero time and zero overpressure to a pressure equal to outside pressure at a time equal to V/2A msec overestimates the fill pressure and underestimates the fill time in the small models but seems to give results in good agreement with both calculation and measurement in the three-foot cube model reported in Figure E-8, although the presence of important oscillations (caused by shock waves) in the pressure record in the large model makes clear assessment difficult. It should be noted also that the fraction of the wall struck by the blast that is occupied by the opening (opening fraction) is over 9 percent in the large model while only 1.2 percent in the small four-in. cube models. The straight line estimate explained in Section IIA would appear to be good also in Figure E-4 for which model size is intermediate and opening fraction is almost 6 percent.

The data from the models suggest that the simplified method of estimating pressure rise in a room set forth in Section IIA is adequate when outside pressure decay is slow as in a free-field nuclear blast wave. As will be noted later, when there exists an important diffraction phase in the blast wave interaction with the structure, more sophisticated methods may be justified.

2. Outflow. All the experimental records discussed so far show that room pressure eventually exceeds outside pressure by a small amount. If all openings are into the same outside pressure field and if the fall of outside pressure is steady and slow, this overshoot is not likely to be of practical importance. However, as will be seen later, if a room has openings that are affected by different outside pressure histories, a significant outward pressure may develop on one or more walls of the room. To calculate this pressure, the rate of outflow of air through each opening must be found.

To compute inflow we treated the exterior atmosphere and the aperture leading into the room as parts of a system of ducts through which quasi-steady flow was maintained. Pressure increase within the room was computed as resulting from the transfer of mass and energy from the large outside reservoir into the room. Outflow may be treated in the same way, except that the direction of flow is opposite. For outflow, Eqs. (1) and (2) still apply, but the air in the duct now originates in the room and the adiabatic expansion law, Eq. (3), must be replaced by

$$\rho_2 = \rho_3' \left[\frac{P_2}{P_3'} \right]^{\frac{1}{\gamma}} \tag{16}$$

Equations (1), (2), and (16) may be combined to form an equation identical to Eq. (5) except that now

$$B = \frac{2\gamma}{\gamma + 1} \cdot \frac{\rho_3'}{\rho_1} \left[\frac{P_1}{P_3'} \right]^{\frac{1}{\gamma}}$$

But, as before, $y = \frac{P_2}{P_1}$ and $A = \frac{\gamma - 1}{\gamma + 1}$

In this form, Equation (5) has two solutions in the range $1 > y > 0$ whenever $\gamma = 1.4$ and

$$\frac{\rho_3'}{\rho_1} \left[\frac{P_1}{P_3'}\right]^{\frac{1}{\gamma}} > 1$$

or,

$$\frac{P_1}{\rho_1^{\gamma}} > \frac{P_3'}{\rho_3'^{\gamma}} \qquad (17)$$

These two solutions merge into a single solution at $y = \left[\frac{B}{\gamma}\right]^{\frac{\gamma}{\gamma - 1}}$

if

$$\frac{P_1}{\rho_1^{\gamma}} = (0.9094) \frac{P_3'}{\rho_3'^{\gamma}}$$

Furthermore, if $\gamma = 1.4$, Equation (5) has two solutions but only one in the range of $0 \leq y \leq 1$ whenever

$$\frac{P_3'}{\rho_3'^{\gamma}} \geq \frac{P_1}{\rho_1^{\gamma}} > (0.9094) \frac{P_3'}{\rho_3'^{\gamma}} \qquad (18)$$

Whenever

$$\frac{P_1}{\rho_1^{\gamma}} < (0.9094) \frac{P_3'}{\rho_3'^{\gamma}} \qquad (19)$$

no solution to Equation (5) exists.

Since the quantity $\frac{P}{\rho^{\gamma}}$ is constant along an isentrope and increases with entropy, when Inequality (17) is true during outflow, specific entropy outside is greater than or equal to specific entropy within the room.

The specific entropy (i.e., entropy per unit mass) in the room at any time during filling can be formally calculated as follows.

First we note that temperature of air in the room rises during the whole inflow period, as can be seen by treating Δm as a true differential and writing Equation (12) as:

$$dP_3 = \frac{\gamma P_1}{\rho_1 V_3} \cdot dm$$

From the perfect gas law

$$P_3 V_3 = m_3 R T_3$$

(where m_3 is the mass of air in the room, and R the gas constant for air) we write

$$dP_3 = \frac{R T_3}{V_3} \cdot dm + \frac{m_3 R}{V_3} \cdot dT_3$$

$$dP_3 = \frac{P_3}{m_3} \cdot dm + \frac{m_3 R}{V_3} \cdot dT_3 = \frac{\gamma P_1}{\rho_1 V_3} \cdot dm$$

$$\frac{1}{V_3}\left[\frac{\gamma P_1}{\rho_1} - \frac{P_3}{\rho_3}\right] dm = \frac{m_3 R}{V_3} \cdot dT_3$$

or

$$\left[\gamma T_1 - T_3\right] dm = m_3 \, dT_3 \qquad (20)$$

Clearly, at the start of filling $T_1 > T_3$, hence at the start $dT_3 > 0$. Moreover Equation (20) shows that T_3 can increase above T_1 while $dm > 0$ until T_3 approaches γT_1. Thus as temperature outside (T_1) falls due to the adiabatic relaxation behind the shock front, inflow and rising inside temperature continue.

In an isentropic process involving a certain mass of ideal gas the quantity $\frac{\rho}{T^{1/(\gamma - 1)}}$ is constant; or, taking differentials,

$$\frac{d\rho}{\rho} = \frac{dT}{\gamma T - T}$$

Rewriting Equation (20) as

$$\frac{dm}{m_3} = \frac{dT_3}{\gamma T_1 - T_3}$$

and dividing numerator and denominator by V_3 and noting that density $\rho_3 = \frac{m_3}{V_3}$, we find

$$\frac{d\rho_3}{\rho_3} = \frac{dT_3}{\gamma T_1 - T_3}$$

In other words the process of room filling during the time period t to t + dt results in a temperature increase dT_3 that bears the relation

$$\frac{dT_3}{(dT_3)_{isentropic}} = \frac{\gamma T_1 - T_3}{\gamma T_3 - T_3}$$

to the temperature increase in an isentropic process providing the same density increase. When $T_1 > T_3$, $\frac{dT_3}{(dT_3)_{isentropic}} > 1$

Now the entropy change dS in a process at constant density is

$$dS = \frac{c_v dT}{T}$$

where c_v is specific heat at constant volume. If we imagine a return to the isentrope (after an increment of filling) by a process at constant density or volume, the specific entropy change within the room resulting from the filling increment becomes

$$dS_3 = \frac{c_v}{T_3} \left[dT_3 - (dT_3)_{isentropic} \right]$$

or,

$$dS_3 = \frac{c_v \gamma}{T_3} \left[\frac{T_1 - T_3}{\gamma T_1 - T_3} \right] dT_3 \qquad (21)$$

which on substitution of the quantity dT_3 from Eq. (20) becomes

$$dS_3 = \frac{c_v \gamma}{T_3 m_3} (T_1 - T_3) dm \qquad (22)$$

Therefore, during inflow (i.e., when $dm > 0$) specific entropy within the room will increase until $T_3 = T_1$ or $P_3 = P_1$, whichever occurs first.

Because of the passage of the shock front, air outside has greater than ambient specific entropy. Hence, initially before inflow begins

$$\frac{P_1}{\rho_1^\gamma} > \frac{P_3}{\rho_3^\gamma}$$

but Eq. (22) shows that the inflow process, according to the theory applied here, creates entropy within the room. Should enough entropy be so created, Inequality (19) may eventually be satisfied and solution of the outflow equations presented here may be impossible. The rise in specific entropy within the room as a result of inflow is:

$$\Delta S_3 = c_v \gamma \int_{t=0}^{P_3=P_1} \frac{T_1 - T_3}{T_3 m_3} \frac{dm}{dt}\, dt$$

where t = time and T_1, T_3, and m_3 are functions of time. From Eq. (20) we know that T_3 rises asymptotically toward γT_1 until $P_1 = P_3$; thus T_3 may be larger than T_1. For a given function $P_1(t)$ [which determines $T_1(t)$, $T_3(t)$, and $m_3(t)$], the maximum specific entropy within the room will be reached when

$$T_3 = T_1$$

If we assume that at this time inflow is still under way, then

$$P_1 > P_3$$

which implies, when $\gamma > 1$, that

$$P_1^{1-\frac{1}{\gamma}} > P_3^{1-\frac{1}{\gamma}}$$

or

$$P_1^{\frac{1}{\gamma}-1} < P_3^{\frac{1}{\gamma}-1}$$

Now from the equality of the temperatures at this time, the perfect gas law implies

$$\frac{P_1}{\rho_1} = \frac{P_3}{\rho_3}$$

Multiplying both sides by the last inequality above, we find

$$\frac{P_1^{\frac{1}{\gamma}}}{\rho_1} < \frac{P_3^{\frac{1}{\gamma}}}{\rho_3}$$

or

$$\frac{P_1}{\rho_1^{\gamma}} < \frac{P_3}{\rho_3^{\gamma}}$$

Hence, in general, the possibility may not be ruled out that Inequality (19) will be satisfied. Whether the outflow equations as presented here have a solution will depend on the nature of the function $P_1(t)$. If outflow is to be calculated, then to provide an initial disparity between specific entropy outside and inside, the inflow period must be treated using the initial density behind the shock front and computed from the Hugoniot relation:[1]

$$\rho_{1o} = \rho_o \frac{(\gamma+1)P_{1o} + (\gamma-1)P_o}{(\gamma-1)P_{1o} + (\gamma+1)P_o} \tag{23}$$

Subsequent outside air densities may be calculated from the adiabatic law:

$$\rho_1 = \rho_{1o}\left[\frac{P_1}{P_{1o}}\right]^{\frac{1}{\gamma}} \tag{24}$$

In Eqs. (23) and (24), ρ_{1o} and P_{1o} refer to the air density and absolute pressure immediately behind the shock front. When peak pressure at an opening is reached by reflection of an incident shock wave from a wall, Eq. (24) is not correct regardless of whether P_{1o} is taken as peak incident absolute pressure or peak reflected absolute pressure, but the error in using Eq. (24) is small. We will arbitrarily consider ρ_{1o} and P_{1o} as representing conditions behind the free-field shock front. Use of Eqs. (23) and (24) may make it possible to satisfy the reverse of Inequality (19).

Should such still not be possible, other calculational methods must be used for the outflow phase, such as that proposed by Melichar[11,12] or that reported by IIT Research Institute.[17] These methods equate duct pressure P_2 with outside pressure during outflow; the IIT investigators then fit observed outflow pressure data by choosing values for the discharge coefficient and for the ratio of inside to outside pressure at the time of flow reversal.

3. Outline of Hand Calculation. In constructing from the foregoing equations a calculational scheme for estimating the parameters of flow into and out of a single room with a single opening we start with a series of values of P_1, one for each time step. These may be obtained by linear interpolation from a given table of outside pressure as a function of time and each value should pertain to the center of the time interval. The size of the time interval, Δt, itself is arbitrary, but it should be no greater than the quantity τ; presumably up to a limit, greater accuracy results from smaller values of Δt. The size of Δt may be changed during the calculation when the rate of change of flow parameters changes. We also need values for ambient pressure P_o and density ρ_o.

Two methods of calculation are shown below. The first is that used to produce Curves F in Figures E-4, E-5, E-6, and E-8, namely, that based on Eqs. (1), (2) and (3) for inflow or Eqs. (1), (2) and (24) for outflow, and in the outline below it is called Method F. This method has the advantage of great simplicity and of not requiring knowledge of empirical constants; however, as will be explained later, values of wind speed and dynamic pressure computed by it are subject to doubt in some cases and for that reason a method given by IIT Research Institute is included also. The latter method is responsible for Curves D in the figures and, therefore, in the outline below it is called Method D. As noted earlier, Method D is numerically equivalent to the calculation used by Melichar.[11,12]

Average pressure inside a room and dynamic pressure in the single opening to an outside reservoir whose pressure variation in time is known may be calculated as functions of time by the sequential application of the steps stated below. Each cycle through a series of steps completes the calculation for one time interval. The first three steps are executed only during the first cycle; subsequent passes begin with step (4), as indicated in the outline. Step (5) is a branch point to separate sequences for inflow and outflow, chosen according to a criterion given in step (5). There are further branches (a) to Method D or F, chosen at the discretion of the user at each time, and (b) under Method D to choked or unchoked flow, determined by stated criteria. Throughout the outline, the quantity γ has been set equal to 1.4.

(1) Set $P_3' = P_o$ and $\rho_3' = \rho_o$ and $t = 0$.

(2) Compute

$$\rho_{1o} = \rho_o \frac{6P_{1o} + P_o}{P_{1o} + 6P_o}$$

where P_{1o} is the absolute pressure immediately behind the shock front.

(3) Choose value of Δt (see opening paragraph of this Section IIB3).

(4) Determine outside pressure at the current time; i.e., determine P_1, from the known reservoir pressure history (pressure variation with time). During first time interval $P_1 = P_{1o}$.

(5) Determine direction of flow; i.e., if $P_1 > P_3'$, flow is inward; go to step (6). Otherwise flow is outward; go to step (28).

Inflow

(6) Compute $$\rho_1 = \rho_{1o}\left[\frac{P_1}{P_{1o}}\right]^{0.7143}$$

Branch to selected Method below for step number (7D) (Method D) or step (7F) (Method F).

Method D (Inflow)

(7D) If $P_3'/P_1 \leq 0.5283$ inflow is choked; go to step (8D). Otherwise inflow is unchoked; go to step (18D).

Choked Inflow

(8D) $$\Delta m_{choked} = K\left[1.4\,\rho_1 P_1 \left(\frac{2}{2.4}\right)^{\frac{2.4}{0.4}} F^*\right]^{1/2} A_2\,\Delta t$$

$$= 0.6847\,K\,[\rho_1 P_1 F]^{1/2} A_2\,\Delta t$$

Using the recommended value[17] of K = 0.70 this becomes

$$\Delta m_{choked} = 0.4793\,[\rho_1 P_1 F]^{1/2} A_2\,\Delta t$$

(9D) $P_2 = P_3'$

(10D) $$\rho_2 = \rho_1\left[\frac{P_2}{P_1}\right]^{0.7143}$$

---

* The factor F will often be necessary for consistency of units. For example, if u_2 is to be in ft/sec and P_1 is in lb/in^2 and ρ_1 in lb/ft^3, then F = 32. X 144. = 4,608.

(11D) $$u_2 = \frac{\Delta m_{choked}}{\Delta t\ A_2\ \rho_2\ K}$$

(12D) $$P_3 = P_3' + 1.4\ \frac{P_1}{\rho_1}\ \frac{\Delta m}{V_3}$$

If desired, dynamic pressure q_2 at the opening may be found from:

(13D) $$q_2 = \frac{1}{2}\ \frac{\rho_2 u_2^2}{F}$$

(14D) $$\rho_3' = \rho_3$$

(15D) $$P_3' = P_3$$

(16D) Advance time by amount Δt and return to step (4).

Unchoked Inflow

(18D) $$P_2 = P_3'$$

(19D) $$\rho_2 = \rho_1 \left[\frac{P_2}{P_1}\right]^{0.7143}$$

(20D) $$u_2^2 = 7 \left[\frac{P_1}{\rho_1} - \frac{P_2}{\rho_2}\right] F$$

(21D) $$\Delta m_{unchoked} = \rho_2\ u_2\ A_2\ \Delta t$$

(22D) $$P_3 = P_3' + 1.4\ \frac{P_1}{\rho_1}\ \frac{\Delta m_{unchoked}}{V_3}$$

(23D) $$\rho_3 = \rho_3' + \frac{\Delta m_{unchoked}}{V_3}$$

(24D) If desired, dynamic pressure, q_2, in the opening may be found from:

$$q_2 = \frac{1}{2}\ \rho_2\ \frac{u_2^2}{F}$$

(25D) $P_3' = P_3$

(26D) $\rho_3' = \rho_3$

(27D) Advance time by amount Δt and return to step (4).

Method F (Inflow)

(7F) $P_2 = 0.1912\ P_1$

(8F) $\rho_2 = \rho_1 \left[\frac{P_2}{P_1}\right]^{0.7143} = 0.3067\ \rho_1$

(9F) $u_2^2 = 7 \left[\frac{P_1}{\rho_1} - \frac{P_2}{\rho_2}\right] F = 2.637 \left[\frac{P_1}{\rho_1}\right] F$

(10F) $\Delta m_3 = u_2\ \rho_2\ A_2\ \Delta t = 0.498\ (P_1\ \rho_1\ F)^{1/2}\ A_2 \Delta t$

(11F) $P_3 = P_3' + 1.4\ \frac{P_1}{\rho_1}\ \frac{\Delta m_3}{V_3}$

(12F) $\rho_3 = \rho_3' + \frac{\Delta m_3}{V_3}$

(13F) If desired, the dynamic pressure, q_2, in the doorway may be calculated:

(14F) $q_2 = \frac{1}{2}\ \rho_2\ \frac{u_2^2}{F} = 0.4044\ P_1$

(15F) $\rho_3' = \rho_3$

(16F) $P_3' = P_3$

(17F) Advance time by amount Δt and return to step (4).

Outflow

(28) Branch to selected Method below for step (29D) (Method D) or step (29F) (Method F).

Method D (Outflow)

(29D) If $P_1/P'_3 \leq 0.5283$, outflow is choked; go to step (30D). Otherwise outflow is unchoked; go to step (39D).

Choked Outflow

(30D) $$\Delta m_{choked} = -0.6847\ K\ [\rho'_3 P'_3 F]^{1/2}\ A_2 \Delta t$$

For K = 1.0 this becomes[17]

$$\Delta m_{choked} = -0.6847\ [\rho'_3\ P'_3\ F]^{1/2}\ A_2 \Delta t$$

(31D) $$P_2 = P_1$$

(32D) $$\rho_2 = \rho'_3 \left[\frac{P_2}{P_1}\right]^{0.7143}$$

(33D) $$u_2 = \frac{\Delta m_{choked}}{\Delta t\ A_2\ \rho_2\ K}$$

(34D) $$P_3 = P'_3 + 1.4\ \frac{\Delta m_{choked}}{V_3}\ \frac{P'_3}{\rho'_3}$$

(35D) $$\rho_3 = \rho'_3 + \frac{\Delta m}{V_3}$$

(36D) $$P'_3 = P_3$$

(37D) $$\rho'_3 = \rho_3$$

(38D) Advance time by amount Δt and return to step (4)

Unchoked Outflow

(39D) $$P_2 = P_1$$

(40D) $$\rho_2 = \rho'_3 \left[\frac{P_2}{P'_3}\right]^{0.7143}$$

(41D) $$u_2^2 = 7\left[\frac{P_1}{\rho_1} - \frac{P_2}{\rho_2}\right] F$$

(42D) $\Delta m_{unchoked} = -\rho_2 \, u_2 \, A_2 \, \Delta t$

(43D) $P_3 = P'_3 + 1.4 \dfrac{\Delta m_{unchoked}}{V_3} \dfrac{P'_3}{\rho'_3}$

(44D) $\rho_3 = \rho'_3 + \dfrac{\Delta m_{unchoked}}{V_3}$

(45D) $P'_3 = P_3$

(46D) $\rho'_3 = \rho_3$

(47D) Advance time by amount Δt and return to step (4).

Method F (Outflow)

(29F) $B = \dfrac{7}{6} \dfrac{\rho'_3}{\rho_1} \left[\dfrac{P'_3}{P_1} \right]^{0.7143}$

(30F) Solve $By^{0.7143} = y + A$ for y.

(31F) $P_2 = yP_1$

(32F) $\rho_2 = \rho'_3 \left[\dfrac{P_2}{P'_3} \right]^{0.7143}$

(33F) $\Delta m = -\rho_2 \, u_2 \, A_2 \, \Delta t$

(34F) $P_3 = P'_3 + 1.4 \dfrac{P_1}{\rho_1} \dfrac{\Delta m}{V_3}$

(35F $\rho_3 = \rho'_3 + \dfrac{\Delta m}{V_3}$

(36F) $P'_3 = P_3$

(37F) $\rho'_3 = \rho_3$

(38F) Advance time by amount Δt and return to step (4).

The theoretical differences between the two methods outlined above are striking. At the present time there is not enough experimental evidence from full-sized rooms to permit a clear judgment between them. If the room fills slowly, that is, the filling time is long compared with the transit time of sound across the room, then the analogy underlying Method D should be good; but even so there is doubt about the correct value of the discharge coefficient, K. The possible influence of K on the calculated room pressure is large, as can be seen from the difference between Curves D and G in Figure E-4. If the filling is rapid, perhaps Method F should be preferred. However, as will be seen in the following paragraphs, this Method can lead to anomalous values of wind speed through the opening.

C. Wind Speed and Dynamic Pressure

Other flow parameters of interest are wind speed and dynamic pressure. The present simple methods yield values of these parameters only in the doorway, but, ordinarily, values at the doorway may serve as upper bounds for the whole room.

Unfortunately, measurements of wind speed and dynamic pressures in shock-filling rooms are even fewer than observations of room pressure. The differences among the predictions of speed among the several calculational methods are large, but the values of dynamic pressure are often in fair agreement. For estimates of the acceleration of objects in the stream, the dynamic pressure is the only pertinent parameter.

During both inflow and outflow wind speed may be calculated from Eq. (9) and, if the isentropic assumption is made, Eq. (6). Dynamic pressure, q_2, is customarily defined as

$$q_2 = \frac{1}{2} \rho_2 u_2^2$$

Using Eq. (9) this can be written:

$$q_2 = \frac{1}{2} \quad P_1 \quad (1 - y_o) \tag{25}$$

Because of the neglect of transient effects, Eqs. (9) and (25) do not reflect the influence of changes in the room pressure, and values calculated from them may be unrealistic. Peak speeds found from Eq. (9) for the experiments reported in Figures E-4, E-5, E-6, and E-8 are supersonic, i.e., above local sound speed in the doorway.

Because of its use of the choking analogy Method D never calculates supersonic speeds; but it does neglect transient shock fronts which could alter the flow substantially in fast filling rooms.

Table E-1 contains the several calculated values of peak speed and dynamic pressure corresponding to each of the experiments reported in Figures E-4, E-5, E-6, and E-8. The table suggests that use of Method F may result in overestimate of that important criterion for damage potential, dynamic pressure. As noted above, because signals from the filling room into the outside reservoir are neglected, Method F in addition to overestimating peak dynamic pressure may overestimate the time-average dynamic pressure in the doorway.

There are no direct observations of wind speed in the opening to compare with calculations. Coulter,[9] however, had reported (1) measurements of the acceleration of an $\frac{1}{8}$ inch diameter nylon ball placed in the doorway of a small model struck head-on by a weak shock wave, and (2) measurements of the motion of smoke columns inside these models during shock filling. With the help of acceleration coefficients derived (theoretically and experimentally) by Bowen and others[14] we can compute motion of the nylon sphere from Eq. (25). Coulter allowed a shock front of overpressure equal to 4.89 psig to strike a reflecting plate in which an entrance 1 x 4 inches was cut. Since the chamber behind the opening had a volume to opening area ratio (V/A) equal to 1.33, filling was essentially complete in 1.33/2 = 0.667 ms, during which time there was little or no decay of the incident wave. If we assume ambient pressure equal to 14.7 psi, reflection at

Table E-1

PEAK VALUES OF OTHER FLOW PARAMETERS

Method / Experiment	C*		F		G	
	q_2(psi)	u_2(fps)	q_2	u_2	q_2	u_2
Fig. E-4	7.98	1045.	9.93	1650.	8.02	985.
Fig. E-5	10.2	1180.	11.2	1680.	10.2	1110.
Fig. E-6	7.79	972.	9.74	1640.	7.80	972.
Fig. E-8	4.08	747.	7.37	1634.		

* Correct adiabatic law has been substituted for the inverted form appearing in Melichar's FORAST code.[11]

normal incidence of a 4.89 psi shock produces a reflected overpressure equal to 11.1 psi.[1] Hence the value of P_1 in Eq. (25) becomes 11.1 + 14.7 = 25.8 psi, and

$$q_2 = \frac{1}{2} \times 25.8 \ (1 - 0.1912)$$

$$= 10.5 \text{ psi}$$

or

$$q_2 = 48100 \text{ lb/sec}^2 \text{ ft}$$

In this expression "lb" is a unit of mass.

A still object in a stream of moving air is accelerated according to the formula

$$\frac{dv}{dt} = \alpha \, q \qquad (26)$$

where α is an acceleration coefficient characteristic of the object and q is the dynamic pressure as defined here. Eq. (26) continues to hold for the moving object as long as its speed is small compared to air speed. Bowen and others[14] suggest a value of $\alpha = 0.138 \text{ ft}^2/\text{lb}$ for a 1/8 inch diameter steel sphere. Since α is inversely proportional to mass, the corresponding value for a nylon sphere of the same size is approximately

$7.87 \times 0.138 = 1.09$ ft^2/lb (specific gravity of iron equals 7.87). Hence acceleration of the nylon sphere should be, according to Eq. (26),

$$\frac{dv}{dt} = 1.09 \times 48100 = 52200 \text{ ft/sec}^2$$

and the final speed of the sphere when filling is complete 667 μsec after impact becomes:

$$v = 52200 \times 667 \times 10^{-6} = 34.8 \text{ ft/sec}$$

and the displacement is $s = \frac{1}{2} \times 52200 \times (667)^2 \times 10^{-12} = 0.0116$ ft = 0.14 inch. Coulter measured terminal speed after 700 μsec as 29.8 ft/sec. Observed displacement in this same time was approximately 0.10 inch, which means the ball did not move far from the center of the doorway during the period of observation and was subjected to only slightly attenuated peak dynamic pressure.

Corresponding to Eq. (25), Method D produces the following equation for the calculation of dynamic pressure in the opening:

$$q_2 = \frac{7}{2} P_1 \left[\left(\frac{P_3'}{P_1} \right)^{\frac{1}{\gamma}} - \frac{P_3'}{P_1} \right] \qquad (27)$$

The value of q_2 in Eq. (27) is not constant in time even when P_1 does not change appreciably. For simplicity, we may assume P_3' varies linearly from 14.7 psia to P_1 over the filling time 0.667 ms. Again, we take $P_1 = 25.8$ psia and find the following variation of dynamic pressure with time:

time (ms)	0	0.2	0.4	0.6	0.667
P_3' (psia)	14.7	18.0	21.35	24.7	25.8
q_2 (psi)	8.97	6.80	4.15	1.08	0.00

The tabulation shows a nearly linear variation of q_2. Integrating Eq. (26) approximately, we find the final value of speed to be:

$$v = 1.09 \frac{f_t^2}{lb} \cdot \frac{1}{2} \times 8.97 \frac{lb}{in^2}\ 0.667 \times 10^{-3}\ sec\ 144 \frac{in^2}{ft^2}\ 32 \frac{ft}{sec^2}$$

$$= 15.0 \frac{ft}{sec}$$

which is about half the observed value. The relatively better agreement with experiment furnished by Method F than by Method D may reflect the fact that the shock filling in this case is "fast."

However, it would seem that any relatively good agreement between calculated and observed acceleration in this example was fortuitous, since Coulter's photographs of events in the chamber make it clear that the diffraction episode very nearly coincided with the calculated filling time, that is, air flow during the period of observation was more a shock related process than a case of quasi-steady adiabatic flow. Some support for this view comes from the second set of wind observations reported by Coulter: motion of smoke in the same kind of chamber used for measurements of the motion of the nylon ball. Most of Coulter's observed values of wind speed and dynamic pressure from smoke motion are one or two orders of magnitude lower than comparable values calculated by the methods presented here. However, Coulter could not by this smoke method measure speeds in the doorway and, in fact, as filling went on his observations were restricted to regions farther and farther from the core of the flow.

Vertex Corporation[10] and Melichar[11,12] have applied the theory of steady subsonic jets to estimate the attenuation and spreading of the incoming stream of high speed air. Melichar describes the early period after shock impact as including jet evolution but his method of estimating duration of this preliminary stage requires consideration of shock front patterns. Presumably flow speeds and dynamic pressure during evolution are less than those quantities in the fully established jet, so use of quasi-steady state conditions is conservative for our purposes. According to Melichar, the steady jet consists of four regions, illustrated in Figure E-9 (reproduced from Ref. 12). In the conical core whose base is the opening into the chamber, horizontal speed and density uniformly equal the speed and density in the opening. The tip of this core extends into the room between 3 and 6 times the opening diameter. Vertex Corporation[10] assumes that the flux of horizontal momentum is constant from one vertical section through the jet to another and gives the equivalent of the following formula for the radius of the jet:

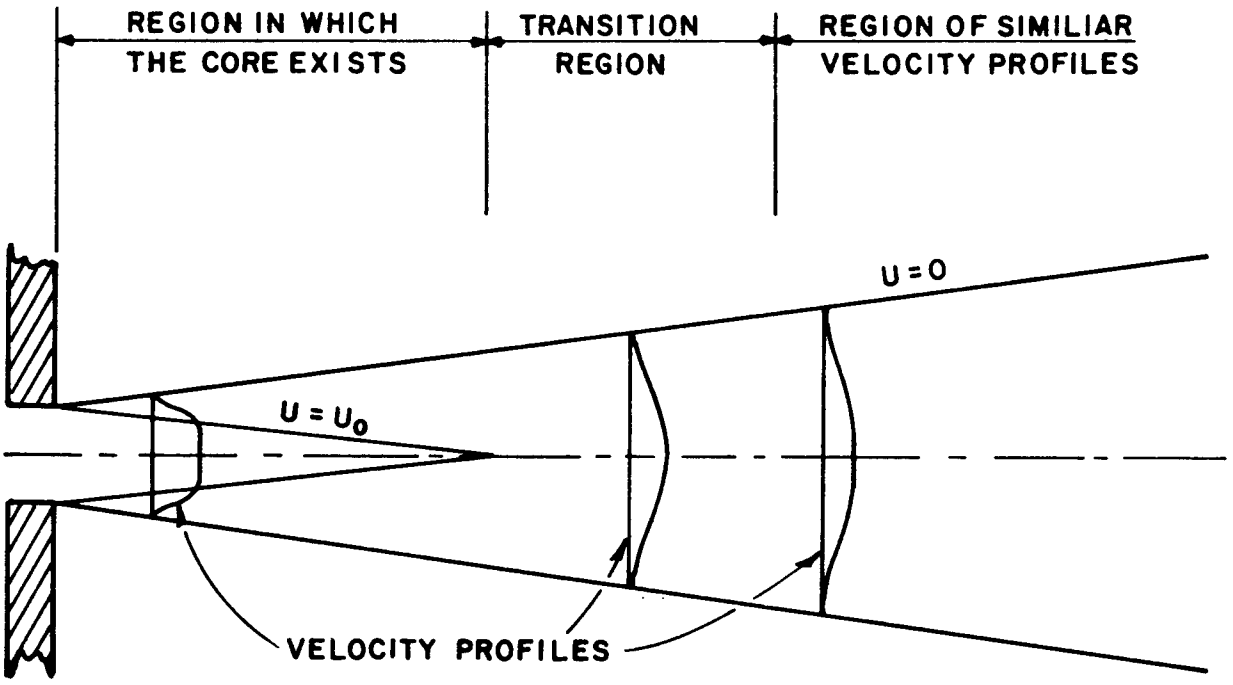

Source: p.33, Ref.12

FIGURE E-9 · SCHEMATIC OF JET FLOW

$$R = 0.178 \left[\ell + 5.6 \ (A/\pi)^{1/2}\right] \tag{28}$$

where ℓ = distance along jet axis from (circular) opening of area A.

Vertex also suggests that doors may be considered circular openings for the purposes of this estimate. Now, if the flux of horizontal momentum is constant at all cross sections through the jet, and if

$$I = \int_o^R \rho \ u^2 \ 2\pi \ rdr = 2 \int_o^R q \ 2\pi \ rdr \tag{29}$$

(where r is radial distance from jet axis, ρ density, u horizontal particle speed) then I is independent of ℓ. Melichar provides speed profiles, i.e., u as a function of r and ℓ, for one value of pressure differential across the orifice and suggests that ρ be taken constant throughout the jet. Vertex approximates the function u = u(r) as:

$$u = u^* \cos^2 \left[\frac{\pi}{2} \frac{r}{R}\right] \tag{30}$$

where u* is the speed on the jet axis. Vertex further assumes

$$u^* \left[\ell + 5.6 \ (A/\pi)^{1/2}\right] = \text{constant}$$

which is only very approximately true according to curves reproduced by Melichar, but which allows one to calculate u in terms of speed in the opening, since at the opening $\ell = 0$. Vertex does not assume ρ independent of r and ℓ but provides formulas for ρ as a function of T and for T as a function of r and ℓ.

For a first estimate of dynamic pressure in the jet, an equation for average dynamic pressure $\bar{q}$ across the jet will be derived from Eq. (29).

If q_2 is the dynamic pressure in the opening then by equating the value of I at the doorway to its value downstream we can write:

$$q_2 A = \bar{q} \pi R^2$$

$$= \bar{q} \pi \left[0.178 \left(\ell + 5.6 \sqrt{\frac{A}{\pi}} \right) \right]^2$$

$$\bar{q} = \frac{q_2 A}{\pi} \frac{1}{\left[0.178 \left(\ell + 5.6 \sqrt{\frac{A}{\pi}} \right) \right]^2} \tag{31}$$

when Eq. (31) has been applied and presumably "safe" areas in a shelter found, then more detailed consideration must be given to the possible enhancement in those areas of the value of q along the axis of the jet. It is suggested that values of u* be found from Melichar's curves[12] and air density in the jet be taken equal to the average in the room at the time considered.

The theory of steady jets, upon which the foregoing considerations are based, stems ultimately from observations of continuous flow through small orifices in large reservoirs kept at constant pressure into an essentially infinite reservoir, also kept at constant pressure. In the present case flow is into a relatively confined space. Indefinitely continued expansion and attenuation of the jet cannot be expected. In fact there is a strong possibility that in some situations even the expansion relatively near the doorway itself will be reduced in amount. Circulatory flow patterns with relatively little turbulent mixing could be set up in small rooms with large openings. This is a subject needing further study by civil defense investigators.

III Multiple Rooms

Although the algebra becomes increasingly cumbersome as rooms are added, the foregoing principles of calculation can be applied to a series of connected rooms. For example, two rooms are represented in Figure E-11 for which two control surfaces may be employed. Through the smaller the momentum flux is due to flow through the first doorway and the resulting momentum equation may be written as:

$$A_2 (P_1 - P_2) = \rho_2 u_2^2 A_2 \tag{32}$$

Using the larger control surface we find:

$$(P_1 - P_3') A_2 + (P_3' - P_4) A_4 = \rho_4 u_4^2 A_4 \quad (33)$$

Method G employs the two equalities below during filling:

$$P_2 = P_3' \quad (34)$$

$$P_4 = P_5' \quad (35)$$

Equations governing flow into the first of the two connected rooms can be written as follows:

$$\frac{\gamma}{\gamma-1} \cdot \frac{P_1}{\rho_1} = \frac{\gamma}{\gamma-1} \cdot \frac{P_2}{\rho_2} + \frac{1}{2} u_2^2 \quad (36)$$

$$\rho_2 = \rho_1 \left(\frac{P_2}{P_1}\right)^{\frac{1}{\gamma}} \quad (37)$$

To these two equations one of the two possible pressure relations represented by Eqs. (32), or (34) must be added to form a complete system from which P_2, u_2, and ρ_2 for the time interval under consideration may be calculated.

Under Methods F and G, the equations governing flow into the first of two rooms are identical to those from which the filling of a single room is computed. Calculation of flow into the second or inner room is more complicated however.

Because observed pressure buildup in two connected rooms has not generally followed simple calculations based on an assumption of uniform pressures over the control surfaces of Figure E-10, provision will be made in the analysis at the outset for a correction term Δ. The quantity Δ will be chosen to reconcile momentum balances based on inner and outer control surfaces such as those shown in Figures E-3 and E-7, that is,

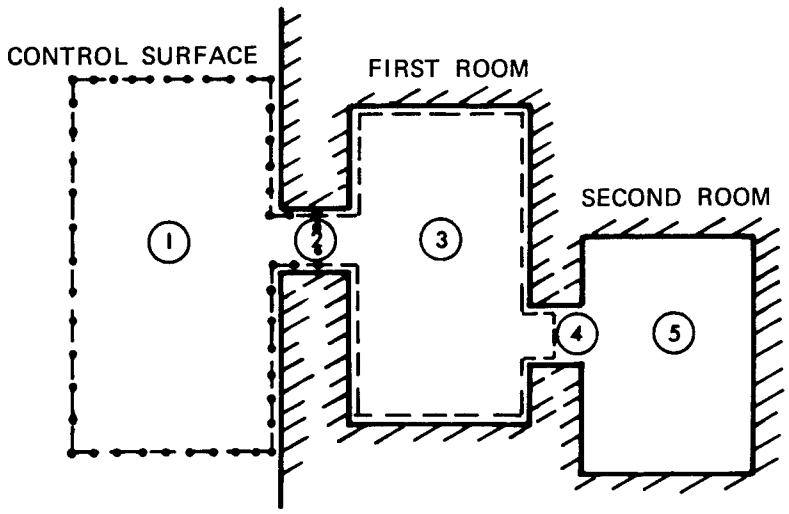

FIGURE E-10 CONTROL SURFACE USED IN CALCULATING FLOW INTO SECOND ROOM

$$(P_3' - P_2)\ A_2 + \Delta = (P_1 - P_2)\ A_2$$

or,

$$\Delta = (P_1 - P_3')\ A_2 \tag{38}$$

Generalizing, we will take the correction terms, Δ, equal to the pressure differential across the duct times the area of the duct. Thus, the corrected Eq. (33) becomes:

$$(P_3' - P_4)\ A_4 = \rho_4\ u_4^2\ A_4 \tag{39}$$

During filling of the second room, there will be an average wind moving through the first room into the second doorway. If u_3 is the speed of this wind and A_3 is the cross sectional area of the first room, then, in view of the quasi-steady state assumption, conservation of energy implies

$$\frac{\gamma}{\gamma-1}\cdot\frac{P_3'}{\rho_3'} + \frac{1}{2}\ u_3^2 = \frac{\gamma}{\gamma-1}\cdot\frac{P_4}{\rho_4} + \frac{1}{2}\ u_4^2 \tag{40}$$

and conservation of mass implies

$$\rho_3\ u_3\ A_3 = \rho_4\ u_4\ A_4 \tag{41}$$

and the assumption of isentropy leads to

$$\rho_4 = \rho_3'\left(\frac{P_4}{P_3'}\right)^{\frac{1}{\gamma}} \tag{42}$$

Eqs. (39), (40), (41), and (42) make it possible to compute by Method F the four unknowns:

$$\rho_4,\ u_4,\ P_4 \text{ and } u_3$$

The resulting solution for P_4 can be put in a form similar to that used in computing P_2

$$\frac{2\gamma}{\gamma+1}\left(\frac{P_4}{P'_3}\right)^{1/\gamma} = \frac{P_4}{P'_3} + \frac{\gamma-1}{\gamma+1}\left[1 - \left(\frac{A_4}{A_3}\right)^2\left(\frac{P_4}{P'_3}\right)^{2/\gamma}\right] + \frac{\gamma-1}{\gamma+1}\left[\frac{A_4}{A_3}\left(\frac{P_4}{P'_3}\right)^{1/\gamma}\right]^2 \frac{P_4}{P'_3} \tag{43}$$

If $y = \frac{P_4}{P'_3}$

$$A = \frac{\gamma-1}{\gamma+1}\left\{\left[1 - \left(\frac{A_4}{A_3}\right)^2\left(\frac{P_4}{P'_3}\right)^{2/\gamma}\right] + \left[\frac{A_4}{A_3}\left(\frac{P_4}{P'_3}\right)^{1/\gamma}\right]^2 \frac{P_4}{P'_3}\right\}$$

and $B = \frac{2\gamma}{\gamma+1}$

then Eq. (43) can be written as

$$B\, y^{1/\gamma} = y + A \tag{44}$$

where in general $A = A(y)$; however, since $P_4 \leq P'_3$ and usually $A_4 \ll A_3$, the dependence of A on y is weak; i.e.:

$$A \cong \frac{\gamma-1}{\gamma+1} \tag{45}$$

Use of Eq. (45) is equivalent to neglecting the average wind speed in the first room in Eq. (40).

After the duct parameters, i.e., ρ_2, P_2, u_2, ρ_4, u_4, and, if desired, u_3, have been found from the foregoing equations, then the new room pressures P_3 and P_5 and densities ρ_3 and ρ_5 are calculated:

$$\Delta m_5 \left(\frac{\gamma}{\gamma-1} \cdot \frac{P'_3}{\rho'_3} + \frac{1}{2} u_3^2 \right) = \frac{1}{\gamma-1} (P_5 - P'_5) V_5 \qquad (46)$$

where $\Delta m_5 = u_4 \rho_4 A_4 \Delta t$, mass increment in second room

$$\frac{\gamma}{\gamma-1} \cdot \frac{P_1}{\rho_1} \cdot \Delta m = \frac{1}{\gamma-1} (P_3 - P'_3) V_3 + \frac{1}{\gamma-1} (P_5 - P'_5) V_5 \qquad (47)$$

where $\Delta m = u_2 \rho_2 A_2 \Delta t$, mass increment in first room

$$\rho_5 = \rho'_5 + \frac{\Delta m_5}{V_5} \qquad (48)$$

$$\rho_3 = \rho'_3 + \frac{\Delta m - \Delta m_5}{V_3} \qquad (49)$$

Outflow from both the first and second rooms is treated with similar basic equations except Eq. (37) is replaced by

$$\rho_2 = \rho'_3 \left(\frac{P_2}{P'_3} \right)^{1/\gamma} \qquad (50)$$

and Eq. (42) by

$$\rho_4 = \rho'_5 \left(\frac{P_4}{P'_5} \right)^{1/\gamma} \qquad (51)$$

Again, in the computation of outflow parameters in the first doorway (i.e., ρ_2, P_2 and u_2) Eqs. (32), (36), and (37) are used as set forth above when only a single room was considered. For outflow through the second doorway, two cases should be distinguished: (1) there is inflow through the first doorway and (2) flow through the first doorway is outward. These conditions affect the form of Eqs. (33) and (40). In case (1), $u_3 = 0$, and Eq. (40) simplifies to:

$$\frac{\gamma}{\gamma-1} \cdot \frac{P'_3}{\rho'_3} = \frac{\gamma}{\gamma-1} \cdot \frac{P_4}{\rho_4} + \frac{1}{2} u_4^2 \qquad (52)$$

but Eq. (33) must contain two correction terms, Δ_3 and Δ_5, to account for excess force against the righthand and lefthand walls, respectively, of the first room:

$$(P_1 - P_3') A_2 - \Delta_3 + (P_3' - P_4) A_4 + \Delta_5 = \rho_4 u_4^2 A_4 \qquad (53)$$

where $\Delta_3 = (P_1 - P_3') A_2$ and $\Delta_5 = (P_5' - P_3') A_4$. Thus Eq. (53) becomes:

$$P_5' - P_4 = \rho_4 u_4^2 \qquad (54)$$

Combining Eqs. (51), (52), and (53), we find:

$$By^{1/\gamma} = y + A$$

where

$$y = \frac{P_4}{P_5'} \qquad (55)$$

$$B = \frac{2\gamma}{\gamma+1} \cdot \frac{\rho_5'}{\rho_3'} \cdot \frac{\rho_3'}{\rho_5'} \qquad (56)$$

$$A = \frac{\gamma-1}{\gamma+1} \left[\frac{P_3' + \Delta_5}{P_5'} \right] = \frac{\gamma-1}{\gamma+1} \qquad (57)$$

In case (2), there is net flow through the first room (i.e., $u_3 \neq 0$) Eq. (40) is unchanged but the analog of Eq. (33) is:

$$(P_1 - P_3') A_2 + (P_3' - P_4) A_4 + \Delta_5' = \rho_4 u_4^2 A_4 \qquad (58)$$

where

$$\Delta_5' = (P_5' - P_3') A_4 - (P_1 - P_3') A_2 \qquad (59)$$

This value of Δ_5' is computed by equating the force tending to drive the air out of the second room, i.e., $(P_5' - P_4) A_4$

to the momentum flux stopped in the first room and the outside reservoir, i.e.:

$$(P_1 - P_3') A_2 + (P_3' - P_4) A_4 + \Delta_5' .$$

Solving Eqs. (40), (41), (51), and (58), we find again that

$$By^{1/\gamma} = y + A$$

where x and B are given by Eqs. (55) and (56), but now

$$A = \frac{\gamma+1}{\gamma-1}\left\{(1-\alpha^2)\left[\frac{P_1 - P_3'}{P_5'}\cdot\frac{A_2}{A_4} + \frac{P_3' + \Delta_5'}{P_5'}\right] + \alpha^2 y\right\} \tag{60}$$

and

$$\alpha = \frac{A_4}{A_3}\cdot\frac{\rho_5'}{\rho_3'}\cdot y^{1/\gamma} \tag{61}$$

Substituting Eq. (59) into Eq. (61),

$$A = \frac{\gamma+1}{\gamma-1}\left\{(1-\alpha^2) + \alpha^2 y\right\} \tag{62}$$

Since, ordinarily, $A_3 \gg A_4$, and $y < 1$, $\alpha^2 \ll 1$, from which we conclude:

$$A \approx \frac{\gamma+1}{\gamma-1} \tag{63}$$

An alternative expression for A in case (2) can be found by writing the excess force on the wall against which the outflow from the second room is directed as the pressure differential across the duct times the duct area:

$$\Delta_5'' = (P_5' - P_3')\ A_4 \tag{64}$$

Substituting Δ_5'' from Eq. (64) for Δ_5' in Eq. (60), we compute for the constant term

$$A = \frac{\gamma+1}{\gamma-1}\left\{(1-\alpha^2)\left[\frac{P_1 - P_3'}{P_5'}\cdot\frac{A_2}{A_4} + 1\right] + \alpha^2 y\right\} \tag{65}$$

for which small α becomes

$$A = \frac{\gamma+1}{\gamma-1}\left[\frac{P_1 - P_3'}{P_5'}\cdot\frac{A_2}{A_4} + 1\right] \tag{66}$$

One final case remains to be considered, namely, outflow through the first doorway combined with inflow through the second. Conditions in the second doorway are computed by solving Eq. (40) with $u_3 = 0$, Eq. (42) and

$$(P_1 - P_3')\ A_2 + (P_3' - P_4)\ A_4 = \rho_4\ u_4^2\ A_4 \tag{67}$$

These equations lead to Eq. (44) in which

$$y = \frac{P_4}{P'_3}$$

$$B = \frac{2\gamma}{\gamma+1}$$

$$A = \frac{\gamma-1}{\gamma+1}\left[\left(\frac{P_1}{P'_3} - 1\right)\frac{A_2}{A_4} + 1\right]$$

In summary then we see that in every case an equation of the form $By^{1/\gamma} = y + A$ must be solved for y. This equation is encountered also in the first doorway if Method F is used. In Table E-2 the meanings of y, A, and B for each case are listed. Since conditions in the first doorway under Method F are independent of conditions inside, the definitions for the first duct appear separately.

In Figure E-11 results of a calculation carried out by Method F for two rooms are compared with measurement of average pressure in the first room. The two rooms consisted of two small models such as those illustrated in Figures E-5 and E-6 placed back to back with a connecting door exactly like the outside door. The experiment was performed in a shock tube in which the wave struck the first doorway head-on. Also in Figure E-11 appears the result of a calculation treating the whole volume of the two model rooms as if it were in a single room. In Figure E-12 measured and calculated results for the second room in the model appear. At least in this one example, all three calculated pressure rises, i.e., in the first room, in the second room, and in the whole volume of both rooms treated as a single room, are quite similar and there appears to be no advantage in using the complicated procedures for computing the fill of two connected rooms.

The calculated histories shown in Figures 11 and 12 have not been carried beyond the time of equilibrium between inside and outside pressures.

Figure E-13 shows pressure history calculated by Method D ignoring the wall between rooms. The outflow phase (when calculated pressure exceeds input pressure) especially appears to be without justification. For this calculation the discharge coefficient has been set equal to 0.7 on inflow and 1.0 for outflow.*

---

* CAVFIL, a FORTRAN program written at IIT Research Institute, was used to make the computation

Table E-2

MEANINGS OF y, A, AND B IN THE EQUATION $By^{1/\gamma} = y + A$
WHEN METHOD F IS USED

First doorway

Inflow

$$y = \frac{P_2}{P_1}$$

$$B = \frac{2\gamma}{\gamma + 1}$$

$$A = \frac{\gamma - 1}{\gamma + 1}$$

Outflow

$$y = \frac{P_2}{P_3'}$$

$$B = \frac{2\gamma}{\gamma + 1} \cdot \frac{\rho_3'}{\rho_1} \cdot \frac{P_1}{P_3'}$$

$$A = \frac{\gamma - 1}{\gamma + 1} \cdot \frac{P_1}{P_3'}$$

Second doorway

Inflow Both Doors

$$y = \frac{P_4}{P_3'}$$

$$B = \frac{2\gamma}{\gamma + 1}$$

$$A = \frac{\gamma - 1}{\gamma + 1} \left[1 - \left(\frac{A_4}{A_3} y^{1/\gamma} \right)^2 (1 - y) \right]$$

Table E-2 (concluded)

Outflow Both Doors

$$y = \frac{P_4}{P_5'}$$

$$B = \frac{2\gamma}{\gamma + 1} \cdot \frac{\rho_5'}{\rho_3'} \cdot \frac{P_3'}{P_5'}$$

$$A = \frac{\gamma + 1}{\gamma - 1} \left[1 - \alpha^2 (1 - y)\right]$$

$$\alpha = \frac{A_4}{A_3} \cdot \frac{\rho_5'}{\rho_3'} y^{1/\gamma}$$

or alternatively

$$A = \frac{\gamma + 1}{\gamma - 1} \left\{(1 - \alpha^2) \left[\frac{P_1 - P_3'}{P_5'} \cdot \frac{A_2}{A_4} + 1\right] + \alpha^2 y\right\}$$

Inflow First Door/Outflow Second Door

$$y = \frac{P_4}{P_5'}$$

$$B = \frac{2\gamma}{\gamma + 1} \cdot \frac{\rho_5'}{\rho_3'} \cdot \frac{P_3'}{P_5'}$$

$$A = \frac{\gamma - 1}{\gamma + 1}$$

Outflow First Door/Inflow Second Doorway

$$y = \frac{P_4}{P_3'}$$

$$B = \frac{2\gamma}{\gamma + 1}$$

$$A = \frac{\gamma - 1}{\gamma + 1} \left[\left(\frac{P_1}{P_3'} - 1\right) \frac{A_2}{A_4} + 1\right]$$

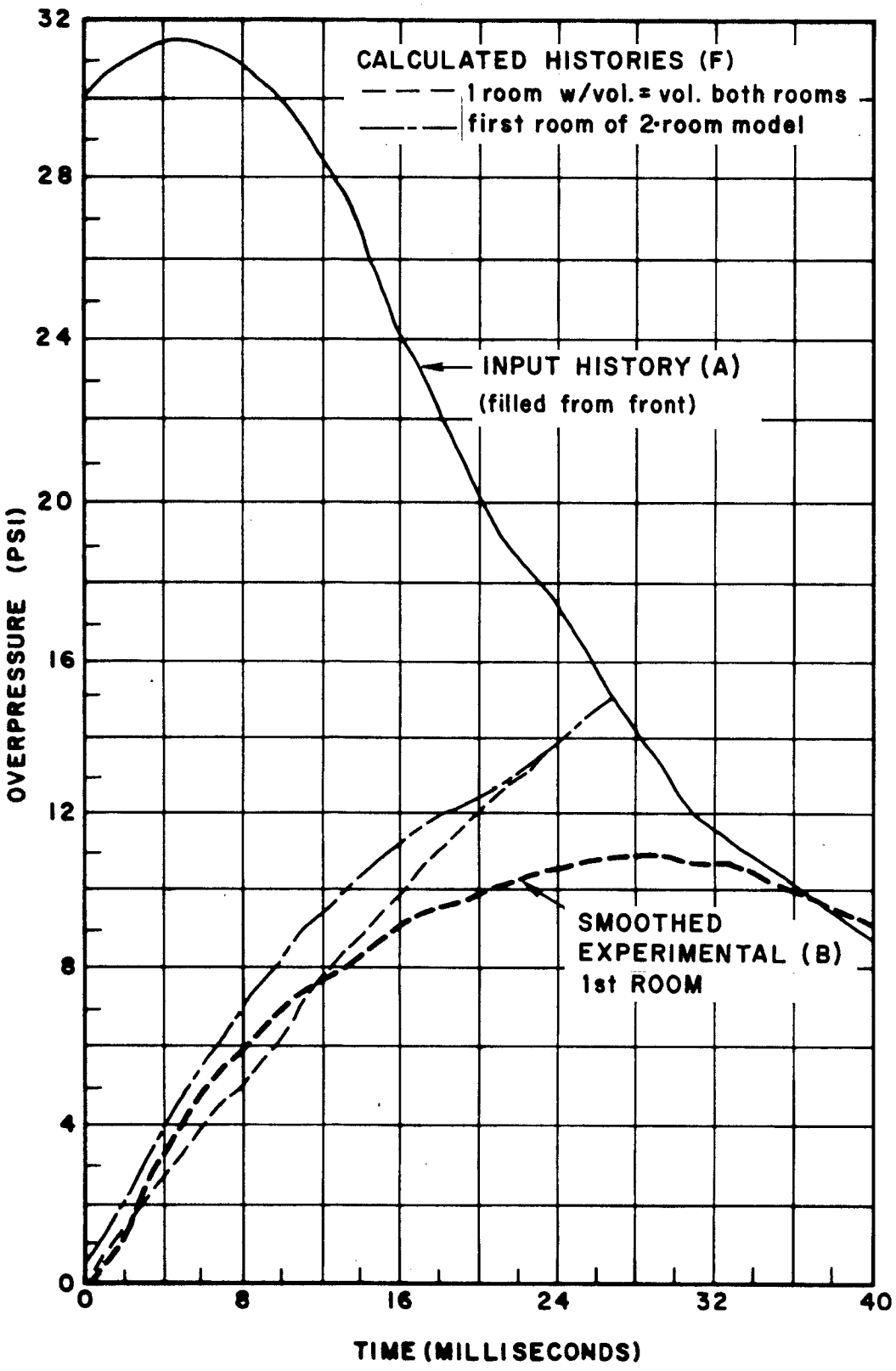

FIGURE E-11 COMPARISON OF OBSERVATIONS IN THE FIRST ROOM OF A TWO-ROOM MODEL WITH CALCULATIONS BY METHOD F

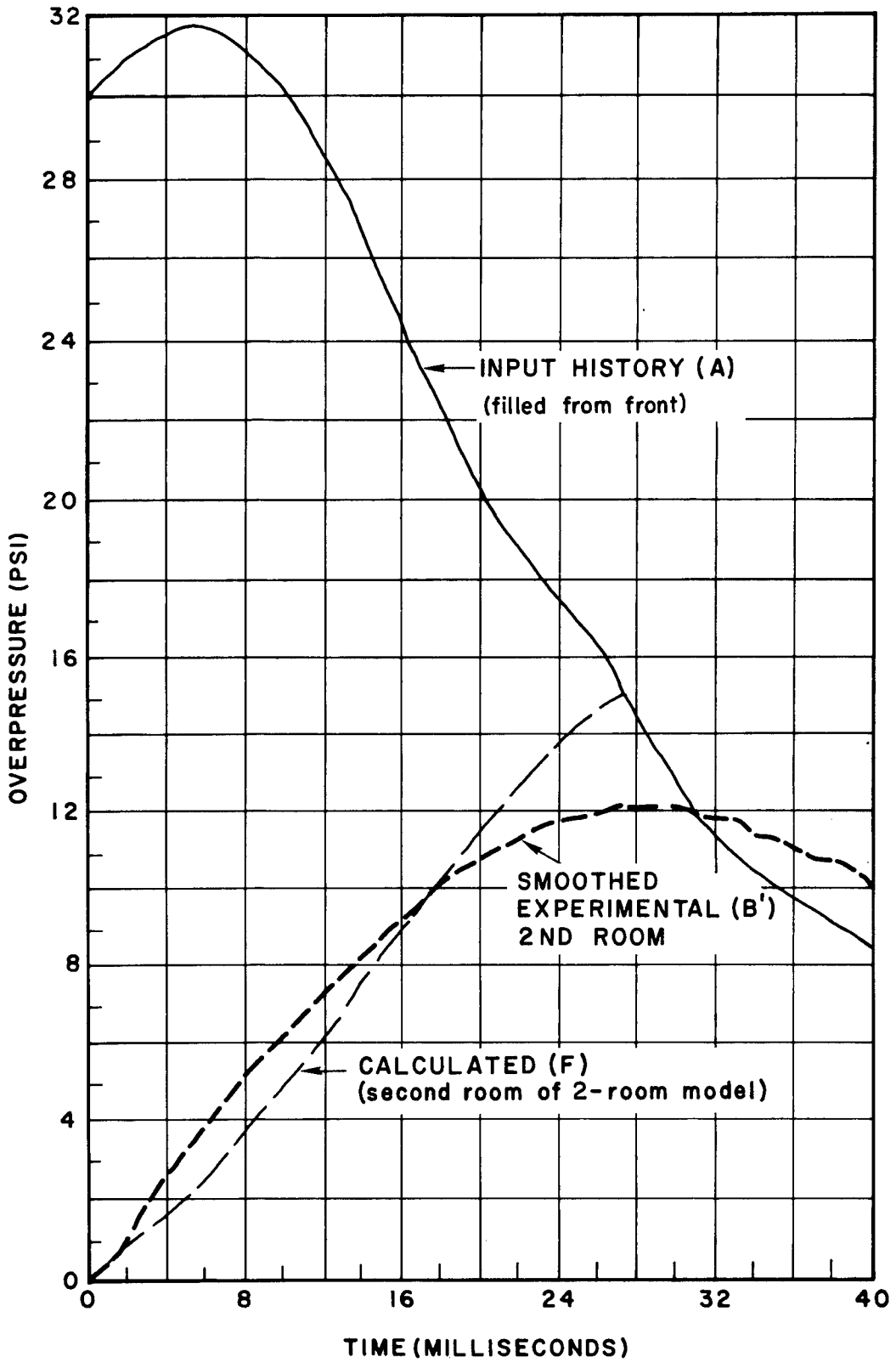

FIGURE E-12 COMPARISON OF OBSERVATIONS IN THE SECOND ROOM OF A TWO-ROOM MODEL WITH CALCULATIONS BY METHOD F

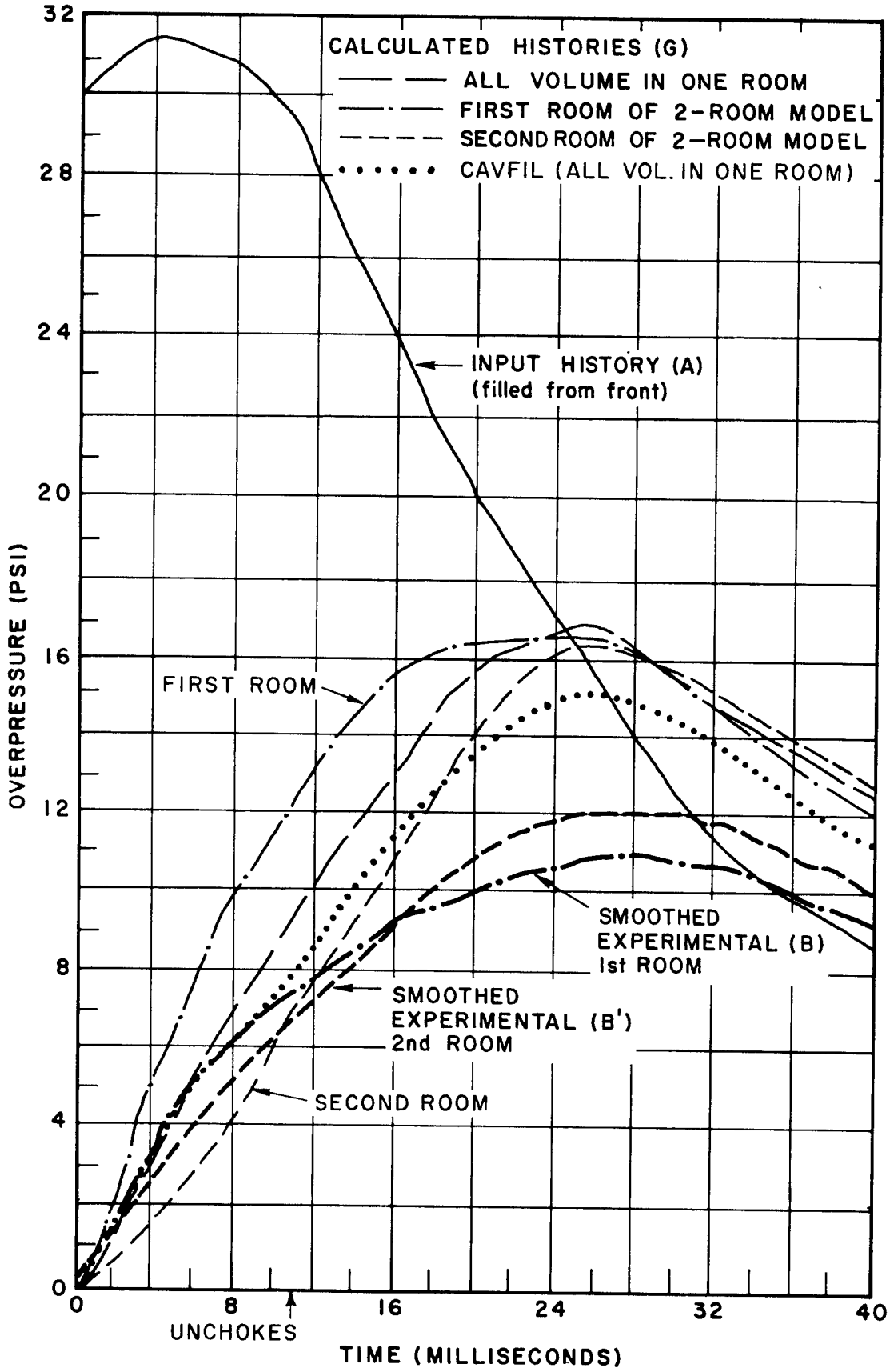

FIGURE E-13 COMPARISON OF OBSERVATIONS IN TWO-ROOM MODEL WITH CALCULATIONS OF METHOD G

The outside pressure, labelled "input history" in Figures E-11, E-12, and E-13, was measured in a separate experiment. It is in fact the stagnation pressure reported by a pitot gauge, placed in a shock tube having no other obstructions, when the incident wave was essentially identical to the wave which impacted the cube.[19] The source of the curve labelled "external history" in Figure E-5 is similar. Thus the short-lived reflected wave has been justifiably neglected in these "external histories."

IV Openings into Different Pressure Fields

The simple methods considered under the heading General Case in Section II above can easily be extended to the case of simultaneous flow into a single room through several openings, each of which is exposed to a separate outside pressure history. This situation will arise, for example, when a nuclear blast wave sweeps over a building, striking one of the four walls head-on, two side-on and exposing the fourth to the wake of the wave. The roof would be struck partially head-on if the explosion were an air burst, or side-on if the burst were on the ground. Head-on impact produces a strong but brief reflected wave followed by a quasi-steady wind and an associated strong drag force superimposed upon the static pressure. When impact is not head-on, only the drag and static pressures are ordinarily taken into account. References 1 and 3 contain discussions of methods of estimating outside pressure in these cases.

A. Computer Program

A computer program has been written in time-share FORTRAN to calculate average pressure as a function of time inside an open room exposed to a nuclear blast wave. Dynamic pressure in each opening may be obtained also. Characteristics of the room, the wave and ambient conditions are typed by the operator in response to typed questions. Provision is made for a maximum of eight openings and the delays between wave front arrival at the leading face of the building and each opening must be supplied. Only three different pressure histories, however, are available for assignment to each opening: the history associated with head-on impact, and two others which contain only the static pressure behind the front and a drag force. Three different drag coefficients must be specified, one for the history associated with head-on impact and one each for the two remaining histories. In order to relate each opening to one of the three possible histories a "location code" is specified for each opening. This code is the number 1 for the head-on history and the numbers 2 and 3 for the remaining two histories.

Duration of reflected pressure ("clearing time") against the wall struck head-on is not calculated in the program but must be entered by the operator. Other details of blast history are however calculated according to algorithms based on descriptions given in References 1 and 3.

The operator may choose certain features of the presentation of the program output. He may have outside (or "input") pressure histories at each opening listed (pressures as functions of time); he may limit program output to peak room pressures (both static and dynamic) or he may choose to have only the history in the room during pressure build-up presented. Finally he must indicate whether or not he wants dynamic pressure histories in each opening presented.

It should be pointed out that the state of knowledge at this time does not justify great reliance upon all parts of the numerical solution to any given problem. Values of dynamic pressure in particular have not been compared with measurements. However, calculated values are conservative for purposes of damage assessment. Calculated values of room pressure during outflow through one or more openings probably do not accurately reflect the relatively small actual pressure differential between inside and outside.

The program algorithm is based on Method F. A partial value of Δm_3 is calculated for each opening corresponding to each time step Δt and inside pressure P_3'. The sum of the partial values for all openings becomes Δm. The equation

$$By^{1/\gamma} = y + A$$

is solved during outflow in a subroutine. When two solutions for $y < 1$ exist the larger is chosen.

A listing of the computer program appears in Table E-3.

B. Numerical Example

As an indication of how the foregoing general procedures may be modified to account for several openings a brief numerical example will be carried out here.

Consider a volume contained in two rooms connected to each other by an open doorway and consider each room connected to the outside by a single doorway, as shown in Figure E-14. The blast wave that sweeps over the structure will be characterized by a free field overpressure of 10 psig,

```
      COMMON G2,G3,L3
      LOGICAL L1,L2,L3,L4,L5
      DIMENSION P(100),T(100),O(100,8),A(8,2),N(8),Q2(8)
     &,POUT(8)
      PRINT,"AMBIENT AIR PRESSURE (PSI)"
      INPUT,P0
      PRINT,"AMBIENT AIR DENSITY (LB/CF)"
      INPUT,RH00
      PRINT,"ROOM VOLUME (CF)"
      INPUT,V3
      PRINT,,"NUMBER OF OPENINGS (NOT MORE THAN 8)"
      INPUT,NWIN
      PRINT,"AREAS OF EACH OPENING (SOFT)"
      INPUT,(A(I,1),I=1,NWIN)
      PRINT,"LOCATION CODE FOR EACH OPENING"
      INPUT,(N(I),I=1,NWIN)
      PRINT,"DELAY IN ENTRY AT EACH OPENING (MSEC)"
      INPUT,(A(I,2),I=1,NWIN)
      PRINT,"CLEARING TIME (MSEC)"
      INPUT,TC
      PRINT,"DRAG COEFFS: FRONT, SIDE AND REAR"
      INPUT,CDFF,CDFS,CDFR
      PRINT,"PEAK FREE FIELD OVERPRESSURE (PSI)"
      INPUT, PS0
      PRINT, "DURATION OF POSITIVE PHASE (SEC)"
      INPUT, T0
      TC=TC/1000.
      PRINT,"WANT PEAK VALUES ONLY (.TRUE. OR .FALSE.)"
      INPUT,L1
      IF(L1)GO TO 3
      PRINT,"INTERVAL BETWEEN VALUES OF OUTPUT (MSEC)"
      INPUT,TI
      TI=TI/1000.
      PRINT,"WANT  DECLINE OF ROOM PRESSURE (.TRUE. OR .FALSE.)"
      INPUT,L2
      GO TO 5
    3 TI=T0/99.
      L2=.FALSE.
    5 L3=.FALSE.
      PRINT,"WANT OUTSIDE PRESSURE (.TRUE. OR .FALSE.)"
      INPUT,L5
      IF(L5)PRINT 26
      PR=2.*PS0*(7.*P0+4.*PS0)/(7.*P0+PS0)
      PD0=2.5*PS0*PS0/(7.*P0+PS0)
      PSC=PS0*(1.-TC/T0)*EXP(-TC/T0)
      PDC=PD0*(1.-TC/T0)*(1.-TC/T0)*EXP(-2.*TC/T0)
      PC=PSC+PDC
      NT=T0/TI+1
      IF(NT.LE.100)GO TO 13
      PRINT,"***VECTOR OVERLOADED - TIME INTERVAL TRUNCATED"
      NT=100
   13 G=1.4; G2=1./G ; G3=1.-G2 ; G4=2./G3
      G5=G+1. ; G6=2.*G/G5 ; G7=(G-1.)/G5 ; G8=G/(G-1.)
      G9=.1912**G2
      GP0=2.*G*P0 ; GPS=2.*G*(PS0+P0)
      RH010=RH00*(GP0+G5*PS0)/(GP0+(G-1.)*PS0)
      RH011=RH010*(GPS+G5*(PR-PS0))/(GPS+(G-1.)*(PR-PS0))
      C=SQRT(G*P0*32.*144./RH00)
      DO 7 I=1,NWIN
      Q2(I)=0.
      A(I,2)=A(I,2)/1000.
    7 CONTINUE
      P30=P0 ; RH030=RH00
      TT=0. ; T0=0.
      TAU=2.*(V3**(1./3.))/C
      DT=TAU/10.
      DDT=DT
    9 IF(TI-2.*DDT)10,11,11
   10 DDT=DDT/2.
      GO TO 9
   11 IST0P=TI/DDT+1
      DDT=TI/IST0P
      MC=-1
      DO 990 J=1,NT
      IF(J.GT.100)GO TO 992
      DO 99 I=1,IST0P
      MC=MC+1
      MD=2 ; II=I
      IF(MC.NE.0)GO TO 62
      II=I-1 ; MD=1
   62 TT=T0+II*DDT
      IF(TT.GT.T0)GO TO 99
      R=TT/T0 ; RR=1.-R
      PD=PD0*RR*RR*EXP(-2.*R)
      PS=PS0*RR*EXP(-R)
       DM=0. ; W=0.
       DO 500 K=1,NWIN
       M=N(K) ; DLY=A(K,2)
       IF(DLY.GT.TT)GO TO 500
       PS1=PS0+P0
       RH012=RH010
       GO TO (15,16,17),M
   15  CDF=CDFF
       IF(TT-TC)20,20,21
   20  P11=(TC-TT)*(PR-PC)/TC+PC
       RH012=RH011
       PS1=PR+P0
       GO TO 30
   16  CDF=CDFS
       GO TO 21
   17  CDF=CDFR
   21  P11=PS+CDF*PD
   30  POUT(K)=P11
       P11=P11+P0
       RH01=RH012*((P11/PS1)**G2)
       IF(P11-P30)36,35,37
   35  U22=0.
       GO TO 39
   36  JSIGN=-1
       AA=G7*P11/P30
       BB=G6*RH030*P11/(RH01*P30)
       Z=P11/(RH01**G)
```

```
      Y=.9094*P30/(RH030**G)
      IF(Y.GT.Z)G0 T0 60
      CALL EQ(AA,BB,P2)
      IF(.N0T.L3)G0 T0 303
      NT=J
      G0 T0 19
 60   PRINT,"Y.GT.Z" ; G0T0 999
303   P2=P2*P30
      RH02=((P2/P30)**G2)*RH030
      X=P11/RH01
      G0 T0 38
 37   JSIGN=+1
      P2=.1912*P11
      RH02=G9*RH01
      X=P11/RH01
 38   U22=G4*(X-P2/RH02)*32.*144.
      IF(U22)40,39,39
 40   PRINT,"U22 NEGATIVE",U22
      G0 T0 999
 39   U2=SQRT(U22)*JSIGN
      Q2(K)=.5*U22*RH02/(32.*144.)
      G0 T0 (500,65),MD
 65   DDM=U2*RH02*A(K,1)*DDT
      DM=DM+DDM
      W=W+P11*DDM/(G3*RH01)
500   C0NTINUE
      P3=P30+(G-1.)*W/V3
      RH03=RH030+DM/V3
      P3A=P30
      P30=P3 ; RH030=RH03
      IF(.N0T.L2 .AND. P3.LT.P3A)G0 T0 80
      G0 T0 (19,99),MD
 80   NT=J
      G0 T0 19
 99   C0NTINUE
 19   T0=TT
      P(J)=P30-P0
      T(J)=TT
      IF(L5)PRINT 27,J,(P0UT(K),K=1,NWIN)
      D0 18 L=1,NWIN
      Q(J,L)=Q2(L)
      Q2(L)=0.
 18   C0NTINUE
      IF(L3)G0 T0 992
990   C0NTINUE
      IF(L1)G0 T0 991
      G0 T0 992
991   PRINT 50,T(NT),P(NT),(Q(I,K),K=1,NWIN)
 50   F0RMAT(1HO,30X,11HPEAK VALUES//1H 6HTIME- ,E11.4,X,
     &3HSEC,4X,10HPRESSURE= ,E11.4,X,4HPSIG//
     &18H DYNAMIC PRESSURES,X,5H(PSI)/8(1H E11.4/))
      ST0P
992   PRINT 22
      D0 993 I=1,NT
      PRINT 51,I,T(I),P(I)
993   C0NTINUE
 22   F0RMAT(1HO,15X,9HTIME(SEC),5X,14HPRESSURE(PSIG))
 51   F0RMAT(1H ,I10,5X,E11.4,5X,E11.4)
      PRINT,"WANT VALUES 0F DYNAMIC PRESSURE (TRUE 0R FALSE)"
      INPUT,L4
      IF(.N0T.L4)G0 T0 999
      PRINT 23
      D0 994 I=1,NT
      PRINT24,I,(Q(I,K),K=1,NWIN)
994   C0NTINUE
 23   F0RMAT(1HO,15X,22HDYNAMIC PRESSURES(PSI)//)
 24   F0RMAT(1H I10,3X,8(F5.2,2X))
 26   F0RMAT(1HO,15X,23H0UTSIDE PRESSURES(PSIG)/)
 27   F0RMAT(1H ,I10,3X,8(F6.2,X))
999   ST0P
      END
      SUBR0UTINE E0(A,B,X)
C SØLVES THE EQUATI0N B*(X**G2)=X+A F0R X
      C0MM0N G2,G3,L3
      L0GICAL L3
      X0=(B*G2)**(1./G3)
      F1=X0+A
      F2=B*(X0**G2)
      IF(F1-F2)1,2,3
 3    PRINT,"N0 S0LN IN E0"
      L3=.TRUE.
      RETURN
 2    IF(X0-1.)4,5,5
 5    PRINT,"N0 S0LN IN E0 LT 1"
      L3=.TRUE. ; RETURN
 4    X=X0 ; RETURN
 1    N=0
      IF(X0-1.)8,42,7
 7    N=1
 8    F1=1.+A
      IF(F1-B)9,10,11
 9    N=N+3 ; G0 T0 12
 10   N=N+1 ; G0 T0 12
 11   N=N+5
 12   G0 T0 (40,5,40,42,39,5),N
 39   XU=1. ; XL=X0 ; G0T0 21
 40   XU=X0 ; XL=0. ; G0 T0 21
 42   XU=1. ; XL=0. ; G0 T0 21
 21   XM=(XU+XL)/2.
      R=(XU-XL)/XU
      IF(R-0.001)22,23,23
 23   F1=XM+A
      F2=B*(XM**G2)
      IF(F1-F2)24,22,25
 24   XU=XM
      G0 T0 21
 25   XL=XM ; G0 T0 21
 22   X=XM
 99   RETURN
      END
```

Table E-3 (concluded)

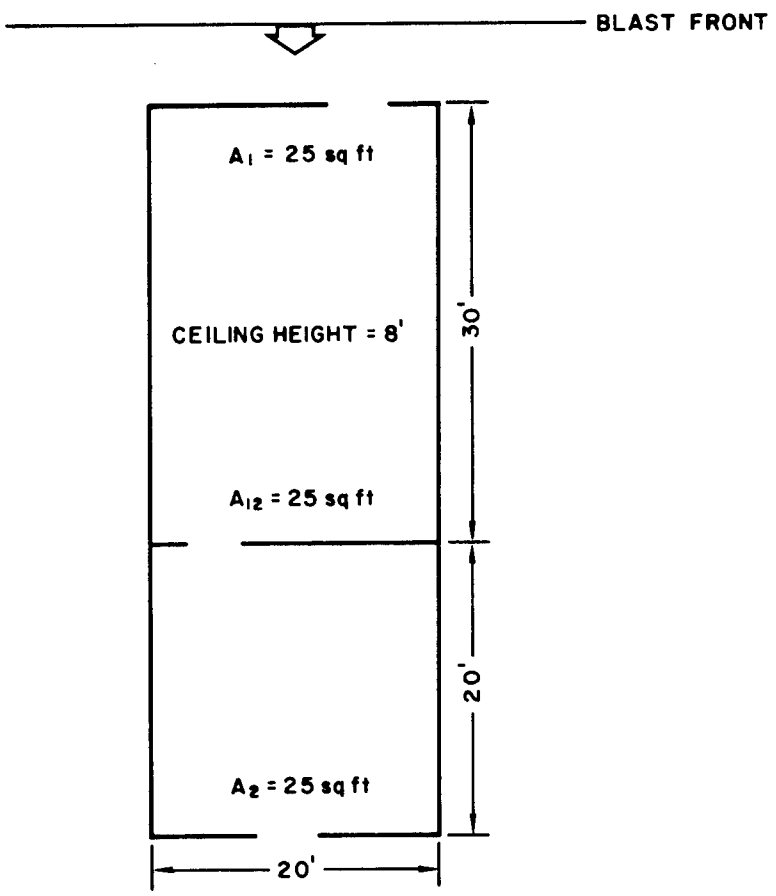

FIGURE E-14 SKETCH ILLUSTRATING NUMERICAL EXAMPLE

head-on incidence upon the opening to the larger room, and positive phase duration of 1 sec. Standard ambient conditions will be assumed, i.e., P_o = 14.7 psia and ρ_o = 0.0761 lb/ft^3. In the front wall the opening area is 25 ft^2 and there is a like opening in the rear wall. Because the door between the rooms has an area comparable to the area of each of the outside doors, the presence of the partition will be ignored and the volume to be filled taken as

$$V_3 = 50 \times 20 \times 8 = 8000 \text{ ft}^3$$

As a first step the pressure histories outside the two doors will be calculated, according to the procedures recommended by Ref. 1. Since the first window is struck head-on, there will be no time delay there and the peak pressure will be the reflected pressure P_R which is calculated as:

$$P_R = 2 \quad P_{so} \cdot \frac{7\,P_o + 4\,P_{so}}{7\,P_o + P_{so}}$$

Here

$P_{so} = 10$ psi and $P_o = 14.7$ psi, hence

$$P_R = 25.3 \text{ psi}$$

This reflected pressure will be felt in declining strength for the duration of the clearing time, t_c, which is estimated as

$$t_c = \frac{3s}{c}$$

where s is a dimension of the wall undergoing pressure clearing and c is sound speed. In this case

$$c = \left[\gamma\, P_o/\rho_o\right]^{1/2} = \left[1.4 \times 14.7 \times 32 \times 144/0.076096\right]^{1/2} = 1116 \text{ ft/sec}$$

and $s = 20$

so that

$$t_c = 53.7 \text{ ms}$$

As an approximation the decline of reflected pressure during the interval

$$0 \le t \le t_c$$

is treated as linear, that is, at $t = t_c$ the pressure P_c on the first wall is simply the sum of the free field overpressure P_{sc} and the drag P_{dc} arising from the winds behind the shock front. Since during the time t_c free field pressure has fallen exponentially[1] from $P_{so} = 10$ psi

$$P_{sc} = P_{so} \left(1 - \frac{t_c}{t_o}\right) e^{-t_c/t_o}$$

where t_o is the free field duration of positive overpressure; in this case t_o = 1 sec so that

$$P_{sc} = 8.97 \text{ psi}$$

Peak drag pressure P_{do} is computed from the formula

$$P_{do} = \frac{5}{2} \cdot \frac{(P_{so})^2}{7 P_o + P_{so}} = \frac{5}{2} \cdot \frac{100}{7 \times 14.7 + 10} = 2.21 \text{ psi}$$

so that drag pressure at $t = t_c$ is:[1]

$$P_{dc} = P_{do} \left(1 - \frac{t_c}{t_o}\right)^2 e^{(-2\ t_c/t_o)}$$

Numerically this is

$$P_{dc} = 1.78 \text{ psi}$$

Therefore the pressure outside the first opening at $t = t_c$ is:

$$P_c = P_{sc} + P_{dc} = 8.97 + 1.78 = 10.75$$

and, assuming a linear fall from P_{so} to P_c, for $0 \le t \le t_c$, pressure P_1 outside first wall as a function of time becomes:

$$P_1 = P_c + \frac{(t_c - t)}{t_c} \cdot (P_R - P_c) \qquad (68)$$

For the remainder of the positive phase duration outside pressure at the first opening is simply the sum of the decayed side-on pressure

$$P_s = P_{so} \left(1 - \frac{t}{t_o}\right) e^{-t/t_o} \qquad (69)$$

and decayed dynamic pressure

$$P_d = P_{do} \left(1 - \frac{t}{t_o}\right)^2 e^{-2t/t_o} \qquad (70)$$

so that for $t_o > t > t_c$

$$P_1 = P_s + P_d \qquad (71)$$

For the first wall a drag coefficient equal to + 1.0 has been tacitly assumed above but for the second opening this coefficient will be different from 1, and according to Ref. 1, a value of -0.4 may be assumed. At the rear opening there is no reflected pressure and the delay is equal to the time taken by the front to traverse the building (assuming that the opening is already open upon blast arrival or that it is immediately forced open by the blast). Blast front speed can be found from the formula[1]

$$U = c_o \left[1 + \frac{\gamma + 1}{2} \cdot \frac{P_{so} - P_o}{P_o}\right]^{1/2}$$

where c_o = sound speed in ambient air, i.e.,

$$c_o = \left[\gamma P_o \, 32 \times 144/\rho_o\right]^{1/2} = 1116 \text{ ft/sec}$$

Hence

$$U = 1116 \times \left[1 + \frac{2.4}{2.8} \times \frac{10}{14.7}\right]^{1/2} = 1148 \text{ ft/sec}$$

so that delay at the rear entrance is $\frac{50}{1148} = 43.5$ ms.

Beginning at t = 43.5 ms the room starts to fill through the rear opening. (Outflow through openings other than the first can ordinarily be neglected during the delay period: either the other openings are closed to the blast for a certain period or, if not, the blast travel time to them is much shorter than the time required to start outflow through them.) Filling through the rear opening takes place however from a reservoir at lower pressure than that outside the front opening, i.e., outside pressure P_{1r} at the rear is:

$$P_{1r} = P_s - 0.4 P_d \qquad (72)$$

The decline in P_{so} and P_{do} which occurs while the blast front travels from front to rear opening is negligibly small and may be safely neglected for buildings of ordinary size.

For this sample case, the quantities P_1 (pressure outside the front opening) and P_{1r} (pressure outside the rear opening) have been calculated as functions of time and plotted in Figure E-15. The figure shows the discontinuity in the derivative of P_1 with respect to time at the point (t_c, P_c) when the reflected pressure is assumed to disappear and the outside pressure takes on its quasi-steady value.

Also plotted in the figure are inside pressure histories P_3 calculated by two methods: the greatly simplified procedure given in section II-A of this report and the step-by-step method F explained in Section II-B. According to the first of these two procedures the estimated history is given by the line segments ODFG obtained as follows. When the blast arrives at the front opening, filling immediately begins along line OA, where point A is the intersection of the outside pressure history and the abscissa

$$t = \frac{V_3}{2A_1} = \frac{8000}{2 \times 25} = 160 \text{ ms}$$

Line BC is a similar line representing filling through the rear opening, beginning after the delay time of 43.5 ms. Ordinates under the line BC have been added to ordinates of OA to produce the line DE. Since areas of both openings are equal, the point F is placed halfway between current outside pressures outside the front and rear openings and the decline of P_3 represented schematically by the line FG.

The step-by-step calculation results in the curve labelled "Method F" in Figure 15. Because of the high reflected pressure during the interval $0 \leq t \leq t_c$ (which does not influence the results of the simplified method in this example) the more careful calculation shows a faster build-up of room pressure than the line ODF. To demonstrate the method the first step of the stepwise solution will be calculated below.

Since the least sound transit time across the room is approximately 20 ms we will choose a value of $\Delta t = 5$ ms. At $t = 0$ there is only one opening, that in the front wall. Outside pressure there at that time is $P_R = 25.3$ psig. Inside pressure $P_3' = P_o = 14.7$ psia and density is $\rho_3' = \rho_o = 0.076096$ lb/ft^3.

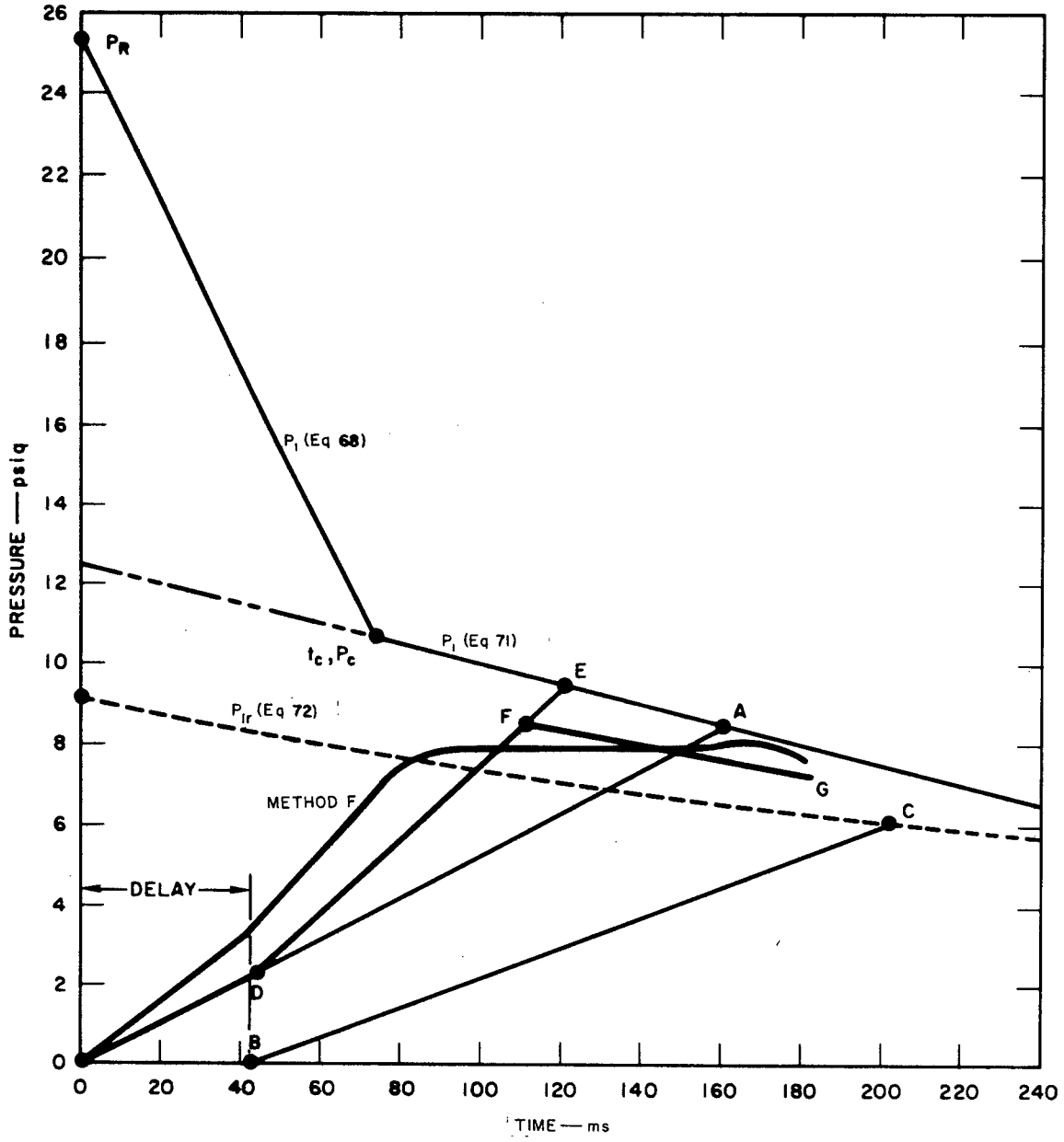

FIGURE E-15 ILLUSTRATIVE EXAMPLE

1. $P_1 = 25.3 + 14.7 = 40.0$ psia

2. $\rho_1 = \left[\frac{P_1}{P_0}\right]^{1/\gamma} \quad \rho_o = \left[\frac{40.0}{14.7}\right]^{1/1.4} (0.076096) = 0.156 \text{ lb/ft}^3$

3. $P_2 = 0.1912 \quad P_1 = (0.1912) \quad (40.0) = 7.65$ psia

4. $\rho_2 = \left[\frac{P_2}{P_1}\right]^{1/\gamma} \quad \rho_1 = (0.307) \cdot (0.156) = 0.04785 \text{ lb/ft}^3$

5. $u_2^2 = \frac{2\gamma}{\gamma - 1}\left[\frac{P_1}{\rho_1} - \frac{P_2}{\rho_2}\right] = \frac{2.8}{0.4}\left[\frac{40.0}{0.156} - \frac{7.65}{0.04785}\right] 32 \times 144 = 3.11 \times 10^6 \frac{\text{ft}^2}{\text{sec}^2}$

6. $q_{21} = \frac{1}{2} \quad u_2^2 \quad \rho_2 = 7.45 \times 10^4 \frac{\text{lb/ft}}{\text{sec}^2}$ (dynamic pressure at front opening)

7. Since $P_1 > P_3'$: $u_2 > 0$, i.e., flow is inward. Were $P_3' > P_1$, u_2 would be negative

8. $\Delta m_{31} = u_2 \quad \rho_2 \quad A_2 \quad \Delta t = 0.0105$ lb

9. $\Delta w_{31} = \frac{P_1 \quad \Delta m_{31}}{\left(\frac{\gamma - 1}{\gamma}\right) \rho_1} = \frac{(40.0)(0.0105)}{\frac{0.4}{1.4} \quad (0.156)} \cdot 144 = 1360$ ft lb

10. Since the rear opening is closed at this time:

$$\Delta m_{32} = \Delta w_{32} = 0$$

Were the second opening available, steps 1 - 9 would be repeated using initial outside pressure at rear opening to calculate Δm_{32} and Δw_{32}

11. $\Delta m_3 = \Delta m_{31} + \Delta m_{32} = 0.0105$ lb

12. $\Delta w_3 = \Delta w_{31} + \Delta w_{32} = 1360$ ft lb

13. $P_3 = P_3' + \frac{(\gamma - 1) \quad \Delta w_3}{V_3} = 14.7 + \frac{(0.4)(1360)}{8000} = 14.768$ psia (room pressure)

14. $\rho_3 = \rho_3' + \frac{\Delta m_3}{V_3} = 0.076096 + \frac{0.0105}{8000} = 0.0760973$ lb/ft^3 (air density in room)

15. Set P_3' equal to P_3 and ρ_3' equal to ρ_3 and return to step 1 with value of P_1 at $t = \Delta t = 5$ ms.

V. Edge Diffraction of an Acoustic Wave

A weak planar shock striking a semi-infinite wall head-on can be treated approximately as a self-similar acoustic wave in the manner demonstrated by Ludloff.[16] Such treatment is two-dimensional and neglects the presence of floor and ceiling.

In the acoustic approximation all disturbances or effects are propagated with sound speed. Thus after the incoming wave front strikes the semi-infinite wall, the influence of the edge will be felt only within a cylinder whose axis is the edge and whose radius is

$$c\,t$$

where c is sound speed and t is elapsed time after initial impact.

If a cartesian coordinate system is placed so that the edge becomes the z-axis and the negative y-axis lies in the wall the location of the circle of disturbance due to the wall is

$$x^2 + y^2 = c^2 t^2$$

and the equation satisfied by the overpressure p is

$$\frac{\partial^2 p}{\partial x^2} + \frac{\partial^2 p}{\partial y^2} = \frac{1}{c^2} \frac{\partial^2 p}{\partial t^2} \tag{73}$$

If a change of variables is made:

$$\eta = \frac{y}{ct}, \quad \sigma = \frac{x}{ct}, \quad \text{and} \quad \tan\theta = \frac{y}{x} = \frac{\eta}{\sigma} \tag{74}$$

then in the new coordinates (η, σ, θ) the disturbance is confined to a circle of unit radius. If, further, radii are changed in scale according to the formula:

$$\rho = \frac{r}{1 + (1 - r^2)^{1/2}} \tag{75}$$

where ρ is the new radius and $r^2 = \eta^2 + \sigma^2$, then the equation satisfied by p in the cylindrical polar coordinates (ρ, θ) can be written

$$\rho \frac{\partial}{\partial \rho}\left(\rho \frac{\partial p}{\partial \rho}\right) + \frac{\partial^2 p}{\partial \theta^2} = 0 \tag{76}$$

This is Laplace's equation and is satisfied by the imaginary component of any analytic function of the complex variable.

$$\zeta = \rho\, e^{i\theta}$$

In the case of edge diffraction of a weak shock the present method yields a solution for $0 \le r \le 1$ (or $0 \le \rho \le 1$). The angle θ lies in the range $-\frac{\pi}{2}$ to $\frac{3\pi}{2}$, as illustrated in Figure E-16. The origin of coordinates is labelled O.

The boundary conditions are determined by physical considerations. Because the acoustic Eq. (73) or (76) is linear in p, the incident overpressure may be taken as unity and the pressure reflected from the wall, as 2. The overpressure in the undisturbed air is of course zero. These conditions imply the following pressure values on the circumference of the circle of disturbance

$$\left.\begin{array}{ll} -\frac{\pi}{2} \le \theta \le 0 & p = 0 \\ 0 \le \theta \le \pi & p = 1 \\ \pi \le \theta \le \frac{3\pi}{2} & p = 2 \end{array}\right\} \tag{77}$$

The areas of uniform pressure are marked in Figure E-16.

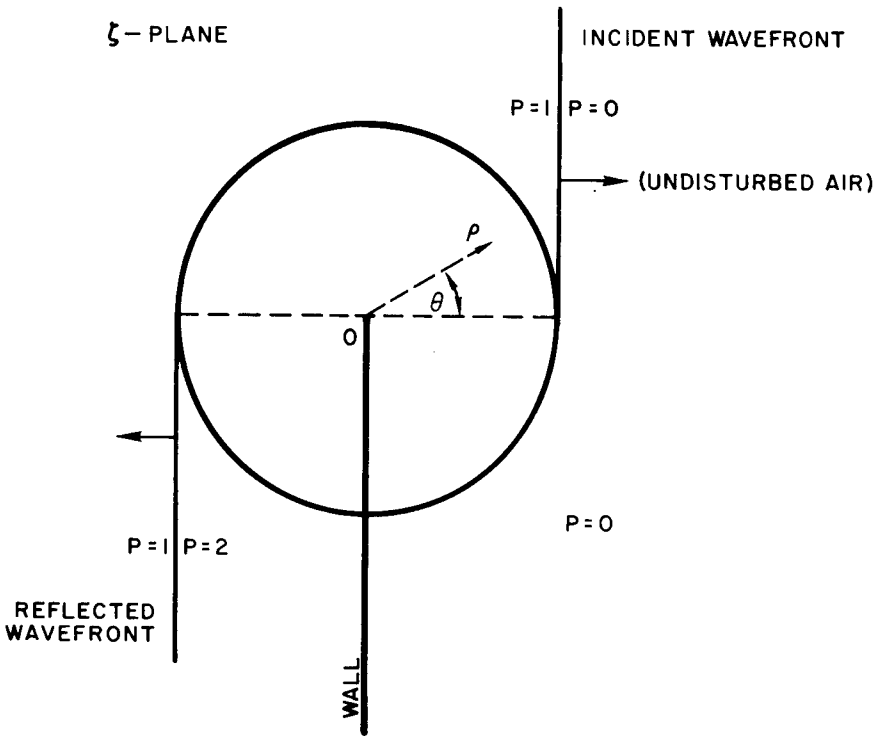

FIGURE E-16 BOUNDARY CONDITIONS ON CIRCLE OF INFLUENCE

Potential theory guarantees that there is only one pressure distribution within the unit circle which satisfies Eq. (76) and meets the foregoing boundary conditions. Solution of Eq. (76) will be guaranteed by the fact that the distribution function is analytic.

A further transformation of variable will make the exposition of the correct distribution function clear. Let

$$w = (i\zeta)^{1/2} = Re^{i\Phi} \tag{78}$$

where $R = \rho^{1/2}$ and $\Phi = \left(\frac{\pi}{2} + \theta\right)\frac{1}{2}$

In the w-plane the unit circle of disturbance becomes a semicircle of radius 1; the back side of the wall lies along the line $\Phi = 0$ while the front side falls along $\Phi = \pi$. The line $\theta = 0$ in the ζ-plane rotates to $\Phi = \frac{\pi}{4}$ and the line $\theta = \pi$ is found along $\Phi = \frac{3\pi}{4}$. Thus in the w-plane the boundary conditions on the semicircle $R = 1$ become

$$\left.\begin{array}{ll} p = 0 & 0 \le \Phi \le \frac{\pi}{4} \\ p = 1 & \frac{\pi}{4} \le \Phi \le \frac{3\pi}{4} \\ p = 2 & \frac{3\pi}{4} \le \Phi \le \pi \end{array}\right\} \qquad (79)$$

Any analytic function of w will also be an analytic function of ζ.

The function $w - e^{i\frac{\pi}{4}}$ is represented by the line BA in Figure E-17 and its argument by the angle α. When A falls on the unit circle, α increases discontinuously from $-\frac{\pi}{4}$ to $\frac{3\pi}{4}$ as A moves counter clockwise through the point B. The function $w - e^{i\frac{5\pi}{4}}$ is continuous within and on the upper semicircle DBE. Furthermore the included angle γ is

$$\gamma = \alpha + \beta$$

where $\text{Arg}\left[w - e^{i\frac{\pi}{4}}\right] = -\alpha$ and $\text{Arg}\left[w - e^{i\frac{5\pi}{4}}\right] = \beta$. But along the arc EB, $\gamma = \frac{\pi}{2}$. Hence the function

$$f_1 = \frac{1}{\pi}\left\{\text{Arg}\left[\frac{w - e^{i\frac{5\pi}{4}}}{w - e^{i\frac{\pi}{4}}}\right] - \frac{\pi}{2}\right\}$$

is zero along EB and 1 along BD.

By a similar argument based on Figure E-18 it is clear that the function

$$f_2 = \frac{1}{\pi}\left\{\text{Arg}\left[\frac{w - e^{i\frac{7\pi}{4}}}{w - e^{i\frac{3\pi}{4}}}\right] - \frac{\pi}{2}\right\}$$

is zero along the arc EB′ and 1 along B′D.

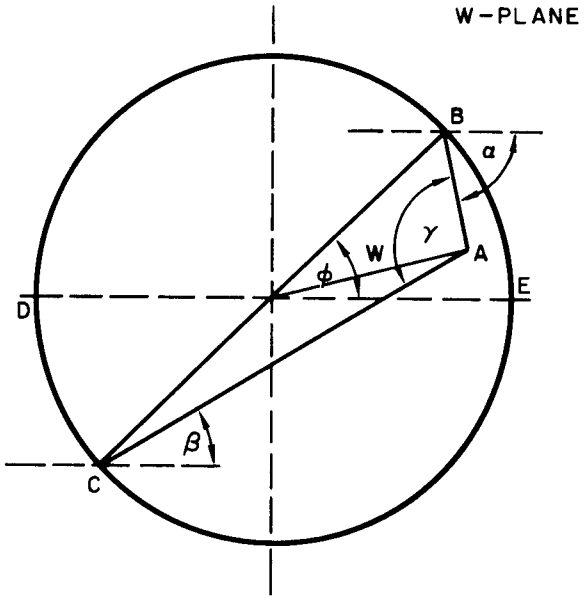

FIGURE E-17 COMPUTATION OF ARGUMENT $\left[\frac{w - e^{5\pi i/4}}{w - e^{\pi i/4}}\right]$

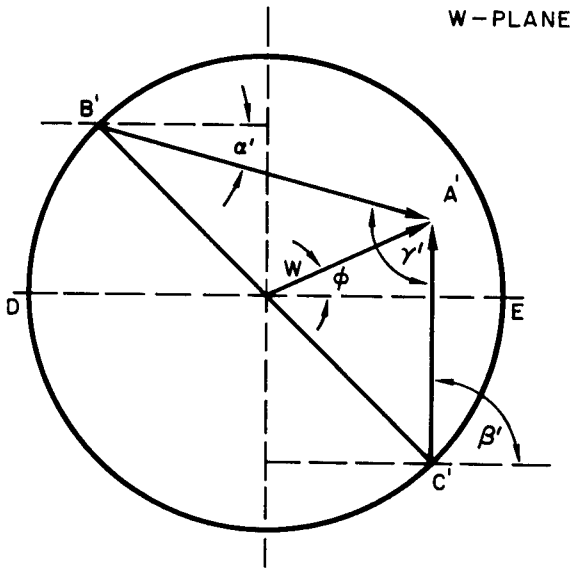

FIGURE E-18 COMPUTATION OF ARGUMENT $\left[\frac{w - e^{7\pi i/4}}{w - e^{3\pi i/4}}\right]$

Thus the sum

$$f_1 + f_2 = \frac{1}{\pi}\left\{ \text{Arg}\left[\frac{w - e^{i\frac{5\pi}{4}}}{w - e^{i\frac{\pi}{4}}} \cdot \frac{w - e^{i\frac{7\pi}{4}}}{w - e^{i\frac{3\pi}{4}}} \right] - \pi \right\} \tag{80}$$

meets the required boundary conditions along the semicircle EBD in the w-plane. But

$$F(w) = \frac{1}{\pi}\left\{ \ln\left[\frac{w - e^{i\frac{5\pi}{4}}}{w - e^{i\frac{\pi}{4}}} \cdot \frac{w - e^{i\frac{7\pi}{4}}}{w - e^{i\frac{3\pi}{4}}} \right] - i\pi \right\}$$

is analytic in w and z and since $f_1 + f_2$ in Eq. (80) is evidently the imaginary part of F(w), Eq. (80) provides the sought-for expression giving the pressure distribution within and on the circle of disturbance $\rho = R = 1$.

Eq. (80) can be written as

$$\pi p = \tan^{-1}\left(\frac{R \sin \Phi + \frac{1}{\sqrt{2}}}{R \cos \Phi - \frac{1}{\sqrt{2}}} \right) + \tan^{-1}\left(\frac{R \sin \Phi + \frac{1}{\sqrt{2}}}{r \cos \Phi - \frac{1}{\sqrt{2}}} \right)$$

$$- \tan^{-1}\left(\frac{R \sin \Phi - \frac{1}{\sqrt{2}}}{R \cos \Phi - \frac{1}{\sqrt{2}}} \right) - \tan^{-1}\left(\frac{R \sin \Phi - \frac{1}{\sqrt{2}}}{R \cos \Phi + \frac{1}{\sqrt{2}}} \right) - \pi \tag{81}$$

where

$$R = \rho^{1/2} = \left[\frac{r}{1 + (1 - r^2)^{1/2}} \right]^{1/2}$$

and

$$\Phi = \frac{\pi}{4} + \frac{\theta}{2}$$

The denominators of the four arctangents in (81) have real roots in the range $0 \le \Phi \le \pi$ when $\rho \ge 1/2$; and care must be taken to evaluate the inverse functions in such a way that p is continuous within the unit circle. There are no zeros in the denominators when $\rho < \frac{1}{2}$.

If $R \cos \Phi_1 + \frac{1}{\sqrt{2}} = 0$ and

$$R \cos \Phi_2 - \frac{1}{\sqrt{2}} = 0$$

then $\frac{3\pi}{4} \leq \Phi_1 \leq \pi$

and $0 \leq \Phi_2 \leq \frac{\pi}{4}$

If the FORTRAN algorithm is used to evaluate the arctangent terms in (81) then for

$$\Phi > \Phi_2 \text{ and } R > \frac{1}{\sqrt{2}}$$

the second term,

$$\tan^{-1}\left(\frac{R \sin \Phi + \frac{1}{\sqrt{2}}}{R \cos \Phi - \frac{1}{\sqrt{2}}}\right)$$

may be increased by π, and the third term

$$\tan^{-1}\left(\frac{R \sin \Phi - \frac{1}{\sqrt{2}}}{R \cos \Phi - \frac{1}{\sqrt{2}}}\right)$$

must be decreased by π, or the sum in (81) increased by 2π. When $\Phi > \Phi_1$ and $R > \frac{1}{\sqrt{2}}$ we must add another 2π to keep the expression for p continuous and insure the existence of its derivatives.

In order to assure continuity with respect to radius the foregoing choices limit the arctangents to certain quadrants where radius R is such that no zeros in the denominators exist, i.e., when $R < \frac{1}{2}$. Thus, since we have chosen to add π to

$$\tan^{-1}\left(\frac{R \sin \Phi + \frac{1}{\sqrt{2}}}{R \cos \Phi - \frac{1}{\sqrt{2}}}\right)$$

for $\Phi > \Phi_2$ and $R > \frac{1}{2}$, we must, when using the FORTRAN algorithm, add π to the same inverse tangent for all Φ when $R < \frac{1}{2}$ in order to place the angle computed in the second quadrant. Similarly, by subtracting π from

$$\tan^{-1}\left(\frac{R \sin \Phi - \frac{1}{\sqrt{2}}}{R \cos \Phi - \frac{1}{\sqrt{2}}}\right)$$

when $\Phi > \Phi_2$ and $R > \frac{1}{2}$ we are placing the arctangent in the range $-\frac{\pi}{2}$ to $-\pi$; hence the same function, when $R < \frac{1}{2}$, must be computed in the same range by subtracting π from the angle as computed by FORTAN. When $R < \frac{1}{2}$ the denominator

$$R \cos \Phi + \frac{1}{\sqrt{2}}$$

is always positive and when $R < \frac{1}{2}$ the FORTRAN choices of quadrant for the two arctangents containing it are consistent with those for $R > \frac{1}{2}$.

Pressure contours, located as outlined above, are shown in Figure E-19.

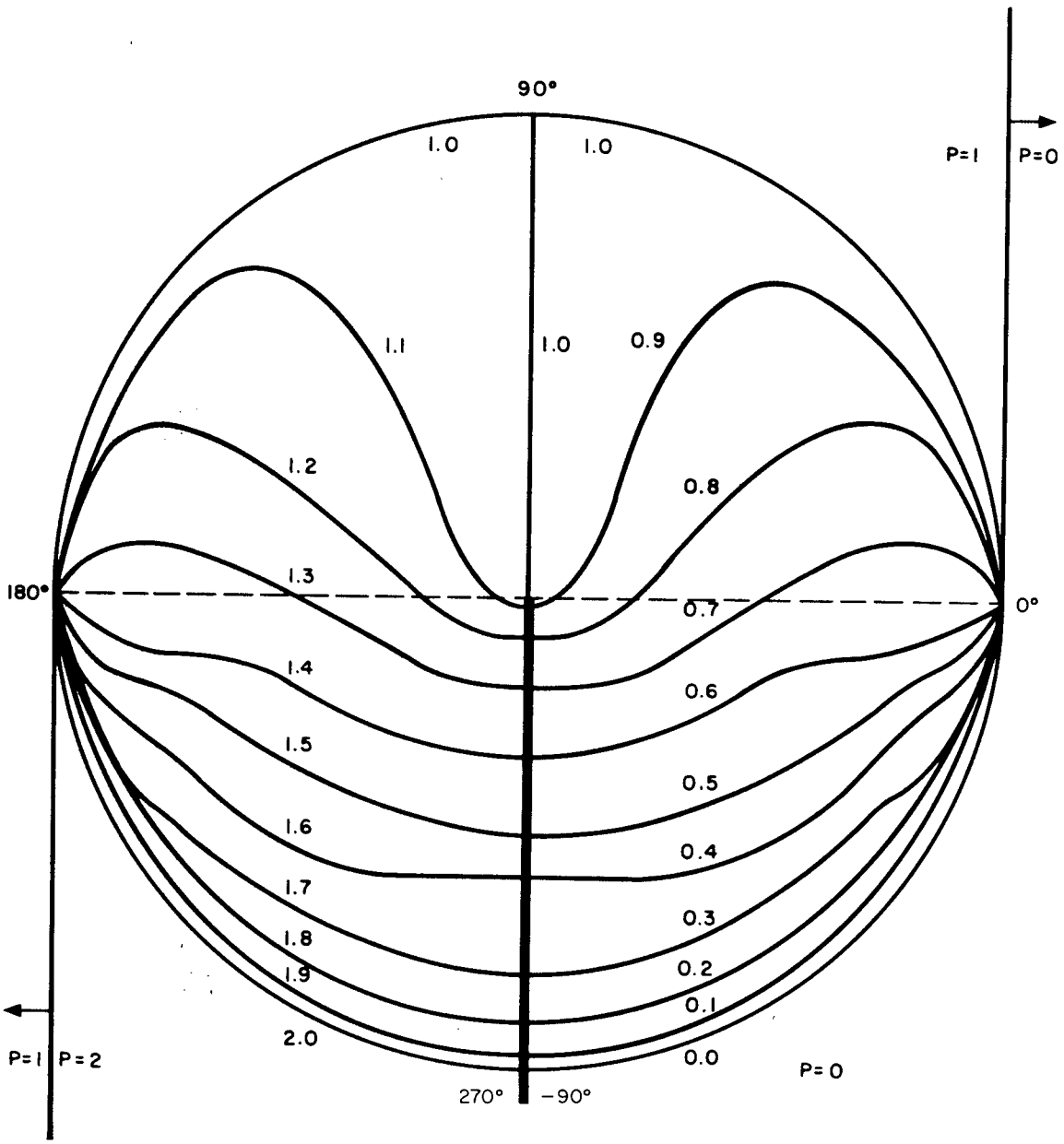

FIGURE E-19 PRESSURE CONTOURS WITHIN CIRCLE OF DISTURBANCE

NOTATION*

A	area of opening or openings through which room fills
A	constant equal to various functions of γ, appearing in Equation (5)
B	constant equal to various functions of γ and/or of interior and exterior conditions, appearing in Equation (5)
c	speed of sound in air
c_v	specific heat at constant volume for air
F	numerical factor for consistency of units
I	integral
K	discharge coefficient
ℓ	distance along jet axis measured from opening
m	mass of air
Δm	increment of air mass corresponding to time increment Δt
P	air pressure
P'	air pressure during immediately preceding time step
P_{lo}	peak overpressure outside front or first wall
P_{lr}	total overpressure outside rear wall
P_c	sum of dynamic and side-on air pressure at time $t = t_c$
P_d	free-field dynamic pressure

* Numerical subscripts may be used with variables to refer to a particular space or volume; see Preface.

P_{dc} dynamic pressure in blast wave at time $t = t_c$

P_{do} peak dynamic pressure in blast wave

P_o ambient air pressure

P_R reflected pressure at a wall struck by blast wave

P_s free-field side-on overpressure

P_{sc} free-field side-on blast overpressure at time $t = t_c$

P_{so} free-field peak side-on overpressure

p acoustic (over)pressure

q dynamic pressure of air

$\overline{q}$ (spatial) average dynamic pressure in jet at one cross section

R gas constant for air (See Ref. 5.)

R radius of jet of streaming air

r radial coordinate, i.e., $r = \eta^2 + \sigma^2$

r radial coordinate measured from axis of jet

S specific entropy of air

ΔS increment of entropy

s wall dimension used to compute clearing time

T absolute temperature

ΔT filling time or interval between first arrival of blast and achievement of pressure equilibrium

t time measured from first arrival of blast at structure

t_c clearing time of structure in blast wave

t_o duration of positive side-on overpressure

Δt increment of time

U blast front speed

u particle speed of air

u^* air particle speed along jet axis

V volume of room or other space to be filled

ΔV increment of air volume

v speed of object in air stream

x Cartesian coordinate

y Cartesian coordinate

y unknown variable in Equation (5)

y_o a specific solution of Equation (5), i.e., $y_o = 0.1912$

w complex variable $Re^{i\Phi}$

Δw energy increment

α angle in complex w-plane

α a certain function of y

α acceleration coefficient of object in air stream

β angle in complex w-plane

γ ratio of specific heat at constant pressure to specific heat at constant volume

γ angle in complex w-plane

Δ correction term applied to momentum balance associated with one control surface

ζ complex variable $\rho\, e^{i\theta}$

η time independent coordinate, i.e., $\eta = y/ct$

θ angle between inward normal to surface and the positive direction of the x-axis

θ angular coordinate, i.e., $\tan \theta = y/x$

ρ density of air

ρ reduced radial coordinate

ρ' air density during immediately preceding time step

ρ_o ambient air density

σ time independent coordinate, i.e., $\sigma = x/ct$

τ time required to transmit a sound signal over the longest room dimension

φ angle in complex w-plane

REFERENCES

1. Glasstone, S., editor, The Effects of Nuclear Weapons, U.S. Dept. of Defense and Atomic Energy Commission, Feb. 1964 reprint (with changes) of 1962 edition

2. Moulton, J., editor, Nuclear Weapons Blast Phenomena, Defense Atomic Support Agency, Washington D.C., DASA 1200 Vol. I, March 1960

3. The Design of Structures to Resist the Effects of Atomic Weapons, EM 1110-345-413, Massachussetts Institute of Technology for the Office of the Chief of Engineers, United States Army, Washington D.C., 1957

4. Iverson, J., Existing Structures Evaluation,Part II: Window Glass and Applications, Stanford Research Institute for the Office of Civil Defense, Menlo Park, Calif., December 1968

5. Eshbach, O. W., editor, Handbook of Engineering Fundamentals, 2nd edition, John Wiley & Sons, 1952, (See chapter 8 for discussion of entropy and internal energy.)

6. Oswatitsch, K., Gas Dynamics, Academic Press, 1956 (for a discussion of the concept and use of control surfaces in the study of flowing compressible fluids)

7. Eshbach, O. W., op. cit., pg 8-23

8. Eshbach, O. W., op. cit., pg 8-21

9. Coulter, G. A., Air Shock Filling of Model Rooms, Ballistic Research Laboratories Memorandum Report No. 1916, Aberdeen Proving Ground, Md., March 1968, Figure 28, pg 54

10. Open Shelter Feasibility Study (DRAFT), The Vertex Corporation, Kensington, Md., June 1968

11. Melichar, J. F., Air-Blast-Induced Aerodynamic Effects in Blast-Slanted Basement Shelters, URS Corporation for Office of Civil Defense, URS 692-3, OCD Work Unit 1126E, Burlingame, Calif., Jan. 1969

12. Melichar, J. F., The Propagation of Blast Waves into Chambers: Aerodynamic Mechanisms, Terminal Ballistics Laboratory, Ballistic Research Laboratories, Aberdeen Proving Ground, Md., November 1967

13. Shapiro, A., The Dynamics and Thermodynamics of Compressible Fluid Flow, Volume I, The Ronald Press Co., 1953 (art. 4.7 for treating flow into a large reservoir which is steadily being evacuated)

14. Bowen, I. G., et al., A Model Designed to Predict the Motion of Objects Translated By Classical Blast Waves, Lovelace Foundation for Medical Education and Research, Albuquerque, N.M., U.S. Atomic Energy Commission CEX-58.9, June 29, 1961

15. Brode, H. L., Point Source Explosion in Air, RM-1824-AEC, The RAND Corporation, December 3, 1956

16. Ludloff, A. F., "On Aerodynamics of Blasts," Advances in Applied Mechanics, Vol. III, R. V. Mises, T. V. Kármán, editors, Academic Press, 1953

17. Kot, C., IIT Research Institute, Chicago, Ill., personal communication

19. Coulter, G. A., op. cit., Fig. 7, pg 27

Appendix F

SLAB AND WALL DESIGN EXAMPLES

By C. K. Wiehle

Appendix F

SLAB AND WALL DESIGN EXAMPLES

By C. K. Wiehle

U.S. POST OFFICE AND COURTHOUSE
NEWNAN, GEORGIA

I. FIRST FLOOR SLAB

A. Loading *

$p_{so} = 15$ psi ; Assume zero rise-time

For $W = 1$ Mt , $t_d = t_i = 1.0$ sec Ref 1, p.3-45

B. Preliminary Slab Design #1

Slab over basement Reserve Room

Design as one-way simply supported slab, $\mu = 3.0$

1. Percent Reinforcing Steel, Assume $\phi_c = 2.0$ (max.) Ref 1, p.8-4

2. Dynamic Material Properties

$f_{dy} = 42{,}000$ psi, structural grade Ref 1, p.6-5

$f'_{dc} = 3{,}750$ psi, for concrete with $f'_c = 3000$ psi " , p6-10

3. Slab Dead Load, Assume $t = 12"$

Equivalent dynamic load $= \frac{145}{172B} t \left(1 - \frac{1}{2\mu}\right)$ Ref 1, p. 9-4 & Ref 2, p.145

$= \frac{145 \times 12}{172B}\left(\frac{5}{6}\right) = 0.84$ psi

4. Required Resistance

$p_m = p_{so} + 0.84 = \left(1 - \frac{1}{2\mu}\right) q$ Ref 2, p.145

$q = \frac{6}{5}(15 + .84) = 19.0$ psi

$\frac{d}{L} = \left(\frac{q_f}{0.072\, \phi_c\, f_{dy}}\right)^{1/2}$ Ref 1, p.8-5

where $q_f = q$

---

* Blast is assumed excluded from entering the shelter area.

$$\frac{d}{L} = \left(\frac{19.0}{(.072)(2.0)(42,000)}\right)^{1/2} = 0.05605$$

$L = 32'-2" - (7'-7" + 1'-0" + 8") = 22'-11"$ (clear span)

(Assume outer wall $t = 12"$, inner wall $t = 8"$)

Therefore, $d = (.05605)(22.92)(12) = 15.42"$

Use $d = 15\frac{1}{2}"$

5. Shear Check

For $\frac{d}{L} = 0.05605$, $f_c' = 3000$ psi — Ref. 1, Fig. 9-3

$\phi_m' \simeq 50$ psi > 15.84 psi — Ref. 1, Fig. 9-3

Therefore, section adequate for shear

6. Diagonal Tension Check

$$q_y = 100\left(\frac{1}{2+\phi'/\phi_c}\right)\left(1 + \frac{2\phi_v f_{dy}}{10^5}\right)\left(\phi_c f_c'\right)^{1/2}\left(\frac{d}{L}\right)^2$$ — Ref. 1, Fig. 8-26

$$q_y = 100\left(\frac{1}{2+.25}\right)(1+0)(2\times 3000)^{1/2}(.05605)^2$$

where $\phi' = 0.25\,\phi_c$ (assumed)

$q_y = 10.8$ psi < 19.0 psi $\therefore$ Section inadequate

However, minimum $q_y = 3.5(f_c')^{1/2}\frac{d}{L}$ — Ref. 1, Fig. 8-26

Therefore,

$q_y = (3.5)(3000)^{1/2}(.05605) = 10.7$ psi < 19.0 psi

and section is inadequate for diagonal tension.

Required ϕ_v for $q_y = 19.0$ psi is

$$19.0 = (100)\left(\frac{1}{2.25}\right)\left(1 + \frac{2\phi_v\, 42,000}{10^5}\right)(6000)^{1/2}(.05605)^2$$

or

$\phi_v = 0.90$

Since $\phi_c = 2.0$, provide required web reinforcement by bending up longitudinal rebar and stirrups if required.

7. Dynamic Analysis of Preliminary Slab Design #1

Determine slab thickness

$A_s = \rho b d = (.020)(12)(15.5) = 3.72$ sq"/ft

Therefore use #11 @ 5", $A_s = 3.740$ sq"/ft, $D = 1.410$"

For a 0.75" cover on the reinforcement — Ref. 3

$t = 15.5 + 0.75 + \frac{1.410}{2} = 16.96$" Use 17"

$W = \frac{(17)(1)(12)}{1728}(145)(22.92) = 392.3$ #/in. width

$m_t = \frac{W}{g} = \frac{392.3}{32.2} = 12.183$ #-sec^2/ft/in. width

$I = \frac{b(k'd)^3}{3} + \frac{n b \phi d^3}{100}(1-k')^2$ — Ref. 1, Fig. 8-1

$n = \frac{E_s}{E_c} = \frac{30}{3} = 10$

For $f_c' = 3000$ psi, $\phi_c = 2.0$

$k' \simeq 0.46$ (By extrapolation) — Ref. 1, Fig. 8-1

$I = \frac{(1)(.46 \times 15.5)^3}{3} + \frac{(10)(1)(2.0)(15.5)^3}{100}(1-.46)^2$

$I = 120.8 + 217.2 = 338$ in.^{4}/in. width

$k = \frac{384 E_c I}{5L^3} = \frac{(384)(3 \times 10^6)(338)}{(5)(22.92)^3(144)}$ — Ref. 1, Fig. 8-1

$k = 4.4915 \times 10^4$ #/ft

Equivalent Single-Degree-of-Freedom System — Ref. 4 (-416)

Mass factor, $K_M = 0.5$ *
Load factor, $K_L = 0.64$ *
Resistance factor, $K_R = K_L = 0.64$ *

$m_e = m_t K_M = (12.183)(.5) = 6.0915$ #-sec^2/ft/in. width

$k_e = k K_L = (4.4915 \times 10^4)(.64) = 2.87456 \times 10^4$ #/ft

---

*See also Table 6.3 herein.

$$T_e = 2\pi\sqrt{\frac{m_e}{k_e}} = 2\pi\sqrt{\frac{6.0915}{2.87456\times10^4}}$$

$T_e = 0.091$ sec

$t_d = 1.0$

$$\frac{t_d}{T_e} = \frac{1.0}{.091} = 10.99$$

For $\mu = 3.0$, $\frac{p_{me}}{q_e} = 0.87$ Ref. 1, Fig. 9-1

$p_{me} = (15.84)\,K_L$

$$q_e = \frac{(15.84)\,K_L}{0.87}$$

$$q = \frac{q_e}{K_R} = \frac{15.84}{0.87} = 18.2 \text{ psi}$$

Therefore, preliminary design is adequate since the resistance required for dynamic load is less than the resistance required for design (see step 4). Section will not be redesigned for purposes of cost estimating.

8. Rebound

$$T = \frac{L^2}{(42,500)\sqrt{\phi_c}\,d}$$ Ref. 1, p. B-11

$$T = \frac{(22.92\times12)^2}{(42,500)(2.0)^{1/2}(15.5)} = 0.081 \text{ sec}$$

$$\frac{t_d}{T} = \frac{1.0}{0.081} = 12.3$$

For $\mu = 3.0$ Ref. 1, Fig. B-10

$\phi' \simeq 0.25 \phi_c$ *

$\phi' = (.25)(2.0) = 0.50$

$A_s' = p'bd = (.005)(12)(15.5)$

$A_s' = 0.93$ □"/ft

Use #8 @ 10", $A_s' = 0.95$ □"/ft

9. Slab Summary

$f_c' = 3000$ psi

$d = 15.5"$

$t = 17.0"$

$L = 22'\text{-}11"$ (clear span)

A_s = #11 @ 5" with every other rebar bent up for diagonal tension.

A_s' = #8 @ 10", bent and anchored in both support walls.

Transverse $A_s = 0.0020\, t\, b$ Ref. 3

$= 0.41$ □"/ft

Use #4 @ 11½" each face

Wt. rebars $= (5.313)\left(\frac{12}{5}\right) + (2.670)\left(\frac{12}{10}\right) + (.668)\left(\frac{12}{11.5}\right)(2)$

$= 17.35$ psf

---

* For simple supports, $\frac{r}{3y} = \frac{\phi'}{\phi_c}$

II. EXTERIOR WALL

A. Loading — Wall Design #1

Assume that the exterior dynamic soil pressure acts as a uniformly distributed load on the walls, without attenuation with depth. Since there is no interior pressure build-up in the basement, the horizontal dynamic pressure on the wall is taken as

$$p_h = K_o\, p_v$$ Ref. 1, p. 5-54

If it is assumed that $K_o = 0.5$, for an unsaturated cohesive soil of medium to stiff consistency, Ref. 1, p. 4-67 and that $p_v = p_{so}$, then the peak horizontal soil pressure due to the blast loading is

$$p_h = (.5)(15) = 7.5 \text{ psi}$$

The static soil pressure at the top of the wall, with the top of the first floor slab at grade, is

$$p_h = \frac{(30)(1)}{144} = 0.21 \text{ psi}$$ Ref. 5 Sec. 2310

The static soil pressure at the bottom of the wall, for a depth to the top of the footing of 14'-11", is

$$p_h = \frac{(30)(14.917)}{144} = 3.11 \text{ psi}$$

If it is assumed that the static soil pressure is equivalent to a uniformly distributed dynamic soil pressure of

$$p_h = \frac{(.21 + 3.11)}{2}\,\frac{5}{6} = 1.38 \text{ psi},$$ Ref. 1, p. 9-4

then the peak dynamic pressure for design of the wall is

$$p_m = 7.5 + 1.4 = 8.9 \text{ psi.}$$

B. Preliminary Wall Design # 1

All exterior walls with soil backfill are of similar construction. Design as one-way, simply supported wall, with $\mu = 3.0$.

1. Percent Reinforcing Steel. Assume existing wall thickness is adequate and calculate required steel area. See step 3, below.

2. Dynamic Material Properties

See p. 1.

3. Required Resistance

$$p_m = \frac{5}{6} q = 8.9 \text{ psi}$$

$$q = \frac{6}{5}(8.9) = 10.7 \text{ psi}$$

$$t = 12"$$

For #5 rebar with 1" cover on interior surface

$$d = 12 - \left(1 + \frac{.625}{2}\right) = 10.69"$$

Use $d = 10.5"$

$$q_f = 0.072 \phi_c f_{dy} \left(\frac{d}{L}\right)^2$$ Ref. 1, p. 8-5

The clear span of the wall, between the first floor slab and the top of the footing, varies from 13'-6" to 13'-11" (see p. F-10). Therefore assume a span

length of 13'-9" for design purposes. The required percent tensile steel is

$$\phi_c = \frac{(10.7)}{(.072)(42,000)}\left(\frac{13.75 \times 12}{10.5}\right)^2$$

$$\phi_c = 0.87$$

$$A_s = \rho bd = (.0087)(12)(10.5) = 1.10 \quad \square"/ft$$

Use #8 @8½", $A_s = 1.12$ □"/ft, $\phi_c = 0.89$

4. Shear Check

$$\frac{d}{L} = \frac{10.5}{(13.75)(12)} = 0.06364$$

For $f_c' = 3000$ psi

$\rho_m' \simeq 55$ psi $\gg$ 8.9 psi Ref. 1, Fig. 9-3

Therefore, section adequate for shear.

5. Diagonal Tension Check

For the existing wall with #4@18"

$A_s' = \rho' bd = 0.13$

where $d = 12 - (2 + \frac{0.5}{2}) = 9.75"$

Therefore,

$$\rho' = \frac{0.13}{(9.75)(12)} = 0.0011, \text{ or } \phi' = 0.11$$

For ductility $\phi_v = 0.25$ min., and Ref. 1, p. B-6

$$g_y = 100\left(\frac{1}{2+\frac{.11}{.89}}\right)\left(1+\frac{(2)(.25)(42{,}000)}{10^5}\right)(.89\times 3000)^{1/2}(.06364)^2 \quad \text{p. F-2}$$

$g_y = 11.9$ psi > 10.7 psi

Therefore, section adequate for diagonal tension.

6. Dynamic Analysis of Preliminary Wall Design #1

$$T = \frac{(13.75\times 12)^2}{(42{,}500)(.89)^{1/2}(10.5)} = 0.065 \text{ sec} \quad \text{p. F-4}$$

With $t_d = 1.0$ sec for dynamic portion of loading, a dynamic analysis is not warranted for cost estimating purposes. See p. F-4.

7. Rebound

$$\frac{t_d}{T} = \frac{1.0}{.065} = 15.4$$

For $\mu = 3.0$

$\phi' \simeq 0.25\,\phi_c$ Ref. 1, Fig. B-10

Existing reinforcement in wall provides

$$\phi' = \frac{.11}{.89}\,\phi_c = 0.12\,\phi_c$$

Therefore, since soil backfill would provide considerable rebound resistance, the existing reinforcing steel is assumed adequate.

8. Exterior Wall Summary

f'_c = 3000 psi

d = 10.5"

t = 12"

A_s = #8 @ 8½" Since ϕ_c = 0.89 (p. F-8), provide minimum web reinforcement by bending up every third long. rebar.

A'_s = #4 @ 18" (existing)

Horizontal A_s = #4 @ 12" each face (existing)

$$\text{Wt. rebars} = (2.670)\left(\frac{12}{8.5}\right) + (1.668)\left(\frac{12}{18}\right) + (1.668)(2)$$

$$= 5.55 \text{ psf of wall.}$$

The height, or clear span, of the exterior wall varies due to differences in slab thickness as follows:

(a) Reserve Room

$L = (14'\text{-}11") - (1'\text{-}5") = 13'\text{-}6"$

(b) Shop Storage Room *

$L = (14'\text{-}11") - (1'\text{-}0") = 13'\text{-}11"$

(c) Shop Room *

$L = (14'\text{-}11") - (1'\text{-}3\frac{1}{4}") = 13'\text{-}7\frac{3}{4}"$

(d) Rooms Off Main Corridor *

$L = (14'\text{-}11") - (1'\text{-}2\frac{1}{2})" = 13'\text{-}8\frac{1}{2}"$

* Calculations for the slabs over these rooms not included in this example.

9. Check Wall Design #1 for Vertical Load

Maximum vertical load occurs in wall supporting Slab Design #1 in Reserve Room and is equal to

$V = 0.39Q + 0.11F$ Ref. 4

$L = (32'-2") - (7'-7") = 24'-7"$ p. F-2

$q = 19.0$ psi

$Q = qL = (19.0)(24.583 \times 12) = 5605$ #/in. width

$F = p_m L = (15.8)(24.583 \times 12) = 4661$ #/in. width

If it is assumed that the peak reaction occurs prior to any significant decay in the blast wave then,

$V = (.39)(5605) + (.11)(4661) = 2699$ #/in. width

From other wall analyses, it can be concluded that a vertical load of this magnitude would probably increase the wall resistance above that for lateral load only. Therefore, it is assumed for this example that the Wall Design #1 is adequate to resist the vertical load only, and the combined lateral and vertical load without modification.

10. Footing Design

(a) Allowable Soil Bearing Pressure

Assume a medium stiff clay or sandy clay

Static

$p_v = 2000 + 200H$ psf (max. = 6000 psf) Ref. 5 Sec. 2805

where H = depth below minimum depth

$\simeq 15 - 1 \simeq 14'$

$p_v = 2000 + (200)(14) = 4800$ psf

Dynamic

Allowable dynamic soil bearing is taken as twice the static value plus the peak free-field soil pressure. Ref. 1, p. 9-14

$$p_v = \frac{(2)(4800)}{144} + 15 = 82 \text{ psi}$$

(b) Total Force on Wall Footing

Slab

$t = 17''$, $L = 24'\text{-}7''$

$$D.L. = \frac{(17)(1)(12)}{1728}(145)\left(\frac{24.583}{2}\right) = 210 \text{ \#/in. wall width.}$$

$L.L. = 0$ (Assumed removed by blast)

Wall

$t = 12''$, $L = 13'\text{-}6''$

$$D.L. = \frac{(12)(1)(12)}{1728}(145)(13.5) = 163 \text{ \#/in. width}$$

Dynamic Equivalent for D.L. Ref. 1, p. 9-4

$P_1 = (210 + 163)\left(\frac{5}{6}\right) = 311$ #/in. width

Total Vertical Load on Wall Footing

$P_T = P_1 + V$ (neglecting footing weight)

$P_T = 311 + 2699 = 3010$ #/in. width.

(c) Wall Footing Width

Use continuous wall spread footing.

Required width

$L = \frac{P_T}{p_v} = \frac{3010}{82} = 36.7''$

Use $L = 38''$

Design pressure $p_m = \frac{3010}{38} = 79$ psi

(d) Wall Footing Thickness

Span from wall face

$\ell = \frac{38-12}{2} = 13''$

$q_f = 0.018\,\phi_e\, f_{dy} \left(\frac{d}{\ell}\right)^2$ Ref. 1, p. 8-47

For $q_f = p_m$, $d = 8.5''$, $t = 12''$

and

$\phi_e = \frac{79}{(.018)(42{,}000)}\left(\frac{13}{8.5}\right)^2 = 0.244$

$A_s = \rho bd = (.00244)(12)(8.5) = 0.25 \square''/ft$

Use #4 @ 9½", $A_s = 0.25 \square''/ft$

(e) Diagonal Tension Check

$$q_y \simeq 25\sqrt{f_c'}\,\phi \left(\frac{d}{L}\right)^2$$ Ref. 1, p. B-48

For $f_c' = 2000$ psi

$$q_y \simeq (25)(.244 \times 2000)^{1/2}\left(\frac{8.5}{13}\right)^2$$

$q_y \simeq 236$ psi > 79 psi

Therefore, section is adequate for diagonal tension.

(f) Wall Footing Summary

$f_c' = 2000$ psi

$d = 8.5''$

$t = 12''$

$L = 38''$

$A_s =$ #4 @ 9½"

Transverse $A_s = 0.0020\,t\,b$

$= 0.91 \square''$

Use 3-#5, $A_s = 0.930''$

Dowels, 3'-0" long to match wall rebars

Use #8 @ 8½" and #4 @ 18"

Wt. rebars $= (.668)\left(\frac{12}{9.5}\right)\left(\frac{38}{12}\right) + (1.043)(3) + (2.670)\left(\frac{12}{8.5}\right)(3)$
$+ (.668)\left(\frac{12}{18}\right)(3)$

$= 18.45$ plf

$= 5.82$ psf

III. INTERIOR SHELTER WALL

A. Loading - Wall Design #2

Assume that the blast loading on the interior shelter wall, due to the blast pressure build-up in the non-slanted area of the basement, is equal to the incident blast overpressure. The critical wall loading is for the lateral blast loading acting on the wall alone without considering vertical forces on the wall due to slab reactions.

B. Preliminary Interior Shelter Wall Design #2

Assume for design purposes that all interior walls enclosing the shelter area are similar. Design as one-way wall spanning between first and basement floor slabs, with $\mu = 3.0$.

1. Percent Reinforcing Steel, Assume $\phi_c = 2.0$ (max.) Ref. 1, p. B-4

2. Dynamic Material Properties

   $f_{dy} = 42{,}000$ psi, structural grade

   $f'_{dc} = 3{,}750$ psi, for concrete with $f'_c = 3000$ psi

3. Required Resistance

   $q = 19.0$ psi. p. F-1

   $$\frac{d}{L} = \left(\frac{qf}{0.072 \phi_c f_{dy}} \right)^{1/2}$$ Ref. 1, p. B-5

   $L = (14'-0") - (1'-2\frac{1}{2}") = 12'-9\frac{1}{2}"$

   (Maximum clear span for corridor wall).

$$d = (12.792 \times 12)\left(\frac{19.0}{(0.072)(2.0)(42{,}000}\right)^{1/2}$$

$d = 8.6''$

Use $d = 8\frac{3}{4}''$, $\phi_c = 1.93$

$A_s = \rho bd = (.0193)(12)(8.75) = 2.03$ □"/ft

Use #11 @ 9", $A_s = 2.08$ □"/ft

$t = 8.75 + 0.75 + \frac{1.410}{2} = 10.2''$

Use 10"

4. Shear Check

$$\frac{d}{L} = \frac{8.75}{(12.792 \times 12)} = 0.0570$$

$\phi_m' \simeq 5{,}0$ psi > 15.8 psi Ref. 1, Fig. 9-3

Therefore, section adequate for shear.

5. Diagonal Tension Check

For $\phi' = 0.25\,\phi_c$, $\phi_v = 0.25$ (min.) Ref. 1, p. B-6

$$\beta_y = 100\left(\frac{1}{27.25}\right)\left(1 + \frac{(2)(.25)(42{,}000)}{10^5}\right)(1.93 \times 3000)^{1/2}(.0570)^2$$ p. F-2

$\beta_y = 13.3$ psi < 19.0 psi

However, minimum p. F-2

$\beta_y = (3.5)(3000)^{1/2}(.0570) = 10.9 < 19.0$ psi

Therefore, section insufficient for diagonal tension.

For $q_y = 19.0$ psi

$$19.0 = (100)\left(\frac{1}{2.25}\right)\left(1 + \frac{2\phi_v\, 42{,}000}{10^5}\right)(1.93 \times 3000)^{1/2}(.0570)^2$$

$\phi_v = 0.87$

Since $\phi_c = 1.93$, provide required web reinforcement by bending up every other longitudinal rebar.

6. Dynamic Analysis of Preliminary Wall Design #2

$$T = \frac{(12.792 \times 12)^2}{(42{,}500)(1.93)^{1/2}(8.75)} = 0.046 \text{ sec}$$ p. F-4

With $t_d = 1.0$ sec for dynamic portion of loading, a dynamic analysis is not warranted for cost estimating purposes. See p. F-4.

7. Rebound

$$\frac{t_d}{T} = \frac{1.0}{.046} = 21.7$$

For $\mu = 3.0$

$\phi' \simeq 0.25\,\phi_c \simeq 0.48$ Ref. 1, Fig. B-10

$A_s' = \phi' b d = (.0048)(12)(8.75) = 0.50$ in²/ft

Use #6 @ 10½", $A_s' = 0.50$ in²/ft

B. Interior Wall Summary

f'_c = 3000 psi

d = 8 3/4"

t = 10"

A_s = #11 @ 9" with every other rebar bent up for diagonal tension.

A'_s = #6 @ 10½"

Horizontal $A_s = 0.0020\,t\,b$

$= 0.24$ □"/ft

Use #4 @ 18", each face

Wt. rebars $= (5.313)\left(\frac{12}{9}\right) + (1.502)\left(\frac{12}{10.5}\right) + (.668)\left(\frac{12}{18}\right)(2)$

$= 9.69$ psf

The height of the interior wall (for cost estimating) varies due to the difference in slab thickness as follows:

(a) Reserve Room

L = 13'-6" p.F-10

(b) Elevator Corridor-South

$L = (14'-11") - (1'-0") = 13'-11"$

(c) Elevator Corridor - North

$L = (14'-11") - (7\,3/4") = 14'-3\,1/4"$

(d) Main Corridor

L = 13'-8½" p.F-10

9. Check Wall Design #2 for Vertical Load.

Maximum vertical load occurs on interior wall supporting Slab Design #1 in Reserve Room, and is equal to

$V = 2699$ #/in. width p. F-11

This load is not critical, and the wall is assumed adequate to resist the vertical load without modification.

10. Footing Design

(a) Allowable Soil Bearing Pressure

$p_v = 82$ psi p. F-12

(b) Total Force on Wall Footing

Slab

D.L. = 210 #/in. p. F-12

Wall

$t = 10''$, $L = 13'\text{-}6''$

$$D.L. = \frac{(10)(1)(12)}{1728}(145)(13.5) = 136 \text{ \#/in.}$$

$$P_T = 2699 + (210+136)\left(\frac{5}{6}\right) = 2987 \text{ \#/in.}$$ p. F-13

(c) Footing Width

Use continuous wall spread footing.

Required width

$$L = \frac{P_T}{p_v} = \frac{2987}{82} = 36.4''$$

Use $L = 38''$; design pressure $p_m = \frac{2987}{38} = 79$ psi.

(d) Footing Thickness

Span from wall face

$$\ell = \frac{38-10}{2} = 14''$$

For $\phi_f = \phi_m$, $d = 8.5$, $t = 12''$

$$\phi_e = \frac{79}{(.018)(42{,}000)}\left(\frac{14}{8.5}\right)^2 = 0.283 \qquad \text{p. F-13}$$

$$A_s = \rho bd = (.00283)(12)(8.5) = 0.29 \text{ in}^2/\text{ft}$$

Use #5 @ 13", $A_s = 0.29$ in²/ft

(e) Diagonal Tension Check

$$\phi_y \simeq (25)(.283 \times 2000)^{1/2}\left(\frac{8.5}{14}\right)^2 \qquad \text{p. F-14}$$

$$\phi_y \simeq 219 \text{ psi} > 81 \text{ psi}$$

Therefore, section is adequate for diagonal tension.

(f) Wall Footing Summary

$f'_c = 2000$ psi

$d = 8.5''$

$t = 12''$

$L = 38''$

$A_s =$ #5 @ 13"

Transverse $A_s = (.002)(12)(38) = 0.91$ in² p. F-14

Use 3-#5, $A_s = 0.93$ in²

Dowels, 3'-0" long to match vertical wall rebars

Use #11 @ 9" and #6 @ 10½"

Wt. rebars $= (1.043)\left(\frac{12}{13}\right)\left(\frac{38}{12}\right) + (1.043)(3) + (5.313)\left(\frac{12}{9}\right)(3) + (1.502)\left(\frac{12}{10.5}\right)(3)$

$= 32.58$ plf

$= 10.29$ psf

REFERENCES

1. Newmark, N. M., and J. D. Haltiwanger, Principles and Practices for Design of Hardened Structures, Air Force Design Manual, published by Air Force Special Weapons Center, Kirtland AFB, N.M., Rpt. No. SWC-TDR 62-138, December 1962. (AD-295 408)

2. Newmark, N. M., Design of Openings for Buried Shelters, Rpt. 2-67 U.S. Army Engineer Waterways Experiment Station, Vicksburg, Miss., July 1963.

3. Building Code Requirements for Reinforced Concrete (ACI 318-63), American Concrete Institute, Detroit, June 1963.

4. Manuals-Corps of Engineers, U.S. Army, Engineering and Design, Design of Structures to Resist the Effects of Atomic Weapons, EM 1110-345-413 (July 1959), -414 to -416 (March 1957), -417 (January 1958), and -418 to -421 (January 1960). Govt. Printing Office, Washington, D.C.

5. Uniform Building Code, 1967 edition, Vol. I, International Conference of Building Officials, Pasadena, California.

Appendix G

TYPICAL DESIGNS - PRELIMINARY DESIGN TECHNIQUES, COMPUTER PROGRAMS AND OTHER DATA

By H. L. Murphy and J. R. Rempel

Appendix G

TYPICAL DESIGNS - PRELIMINARY DESIGN TECHNIQUES, COMPUTER PROGRAMS AND OTHER DATA

By H. L. Murphy and J. R. Rempel

The purpose of this appendix is to present additional information relative to the Typical Designs section of Chapter 6 - information that includes backup and other data to allow the guide user to extrapolate/interpolate for additional values, delve into other situations, and gain further understanding of the approach and techniques used in the Typical Designs section, without further enlarging that section.

Appendix G

TYPICAL DESIGNS - PRELIMINARY DESIGN TECHNIQUES, COMPUTER PROGRAMS AND OTHER DATA

I. One-Way Slabs - Simply Supported

Preliminary Design Procedure

This procedure is briefly described in the Slab Design section of Chapter 6 (and illustrated in Appendix F), and was used for preliminary design of several one-way slabs, based on the following common parameters:

$f'_c = 3$ ksi; $f'_{dc} = 1.25\, f'_c$; $f_{dy} = 42$ ksi; $p_{so} = 15$ psi;

$t_i = 1$ sec; $\mu = 3$.

The design steps were as follows: Using a step loading pulse, required unit resistance q (also termed an equivalent static load) equals $p_{so}/(1 - 1/2\mu)$. Flexural requirements were met by assuming d and using Equation 8-4* to obtain the slab clear span L. T was calculated from Equation 6-4, then Figure B-10* was entered with μ and t_d/T ($t_d = t_i = 1$ sec) to determine the required elastic rebound steel ratio p'. Diagonal tension requirements then dictated the required web steel ratio p_v by use of Equations 6-9a and 6-9b (first two equations of Figure 8-2b*; Equations 8-6 and 8-7* are also applicable but in a less convenient form). Pure shear capacity proved to be much larger than required, in all cases.

One-way slabs were similarly designed with p and p' adjusted so that the required web steel ratio p_v equaled zero.

Arithmetic plots of L versus d, L versus A_s, and L versus A'_s all yielded straight lines for each of the two families of slabs. One small and one large value of d for each slab family were, therefore, selected for further work (steel was detailed sufficiently to determine slab thickness); descriptive values for the four one-way slabs are:

---

* Reference 2 of Volume 1.

		Slab 1	Slab 2	Slab 3	Slab 4
Slab depth d*		7"	20.6"	10"	27.5"
Slab span L		130"	360"	135"	360"
Tens. steel p	At mid-	0.02	0.02	0.014	0.014
Compr. steel p′	span	.0052	.0052	.0029	.0029
Web steel p_v (required)		.0091	.0091	--	--
Slab thickness t*		8-5/8"	23-5/8"	11-9/6"	29-1/2"
Ratio t/d		1.233	1.148	1.156	1.072

Based on the steel detailing of these few slabs, approximate values of slab thickness versus depth were developed from slabs 1 and 2 into an upper limit equation for rough cost estimating and from slabs 3 and 4 into a lower limit equation that can be considered in estimating mass that is used later in equations of motion.† The resulting equations may be useful until a more complete study is made; they are as follows:

$t = 1.27d - 0.006d^2$, but t not less than 1.1d (for rough cost estimating) (6-7)

$t = 1.20d - 0.005d^2$, but t not less than 1.1d (for least mass estimate) (G-1)

Modified Preliminary Design Procedure

The preliminary design procedure described just above may well provide designs adequate for final design use - a few design comparisons are included below - but there were three changes in the procedure that were recognized and may be used to improve the resulting designs (that is, as a part of "Step 7"of Reference 2, art. 9.2), to make them give results closer to those from a final design technique that includes all refinements reasonably available at this time (Chapter 6).

The blast load pulse assumed to apply to one-way slabs over basements has a zero rise-time and an exponential decay from its peak value

---

* Such odd dimensions would certainly not be used in practice; however, it was the t/d ratios that were sought for rough cost and mass estimating purposes.

† Equation 6-7 was used for both purposes in the typical designs in Chapter 6.

(Eq. 3.51.1 of Ref. 1). The convenient chart solutions for single-degree-of-freedom dynamic systems, Figure 6-1 (p. 11-3), are exact only for triangular load pulses; however, techniques are available for using the chart solutions for decay pulses consisting of two or three straight lines (Figures 3-8 and -9*), thereby more closely approximating the exponential decay pulse. Some comparisons were made between the results from triangular and exponential decay pulses, using the positive phase duration times from Figures 3-7 and 3-5, respectively, of Reference 2. Solutions were obtained using dynamic load factors, Table 6.3, and the Newmark β Method[21] with a one msec time interval and $\beta = 1/6$. Using a single problem example about in the middle of a range of one-way slab designs and a peak blast overpressure $p_{so} = 15$ psi, the maximum resistance q and ductility μ values varied as follows:

q_{max}(psi)	23.6	17.0	16.0	15.8	14.5	13.8
$\mu_{triangular}$	1.24	2.69	3.43	3.71	6.27	8.83
$\mu_{exponential}$	1.25	2.75	3.57	3.88	6.86	10.03
μ_t/μ_e †	.995	.977	.961	.956	.914	.880

These tabulated values vary over a range of μ values, but are related to one midrange beam design situation. The following tabulated values compare μ_t with μ_e for a range of preliminary one-way slab designs, but with μ varied only over a narrow range (again, $p_{so} = 15$ psi):

d;L	7";138"	20";398"	7";151"	20";440"
f'_c; f_{dy}(ksi)	3;44	3;44	5;52	5;52
q_{max}(psi)	16.2	16.0	16.1	15.5
$\mu_{triangular}$	4.31	3.42	4.41	3.71
$\mu_{exponential}$	4.40	3.57	4.53	3.92
μ_t/μ_e †	.979	.960	.974	.945

Using the 10 pairs of values tabulated, a curve-fitting equation for "adjusting" μ_t (calculated using a triangular decay pulse approximation, t_{00} of Figure 3-7*) to an estimated μ_e for an exponential decay pulse was developed; it is reiterated that the equation is for estimating only, and then only in the particular realm of applications from which it was derived:

---

* Reference 2 of Volume 1.

† Using more precise values of μ_t and μ_e than those tabulated.

$$\mu_e = \mu_t/(-.012747\ \mu_t + 1.00822)$$

where significant figures shown are simply those resulting from a library computer program run, not an implication of accuracy. The equation is most useful with computer programs; a simple figure is generally more useful (Figure G-1). This change in μ is the first of the three changes mentioned above.

The second change that may be readily applied as a part of "Step 7" is to use a "weighted" dynamic load factor, Table 6.3, tailored to the μ desired. In review, it should be recalled that only one (combined) dynamic load factor K_M/K_L need be used, applied to the mass as follows:

If the fundamental equation of motion

$$p(t) - kx = ma$$

includes dynamic load factors, it becomes

$$K_L\ p(t) - K_R\ kx = K_M\ ma$$

Recognizing that $K_R = K_L$* and dividing through by K_L leads to

$$p(t) - kx = (K_M/K_L)\ ma$$

The combined factor K_M/K_L is given directly in Table 6.3. The unanswered question is how K_M/K_L elastic and plastic values are to be "weighted" (a procedure suggested without explanation by at least two sources[22,33]). Two methods of weighting the factors were tested by use, first in a chart solution, discussed earlier in this section, then with the results compared to those from a full β-method solution (triangular decay load pulses used in both solutions). The two "weighting" methods were:

1. Apply elastic and plastic factors in accordance with relative areas under the elasto-plastic resistance plot (center figure, page 11-4) - for example, using K_e (=K_M/K_L elastic) and K_p (= K_M/K_L plastic) and $\mu = 7$, the weighted factor $K = (0.5/6.5)K_e + (6/6.5)\ K_p$.

2. Apply elastic and plastic factors in accordance with the relative displacements for elastic and plastic phases - for example, using K_e and K_p with $\mu = 7$, the weighted factor $K = (1/7)\ K_e + 6/7)\ K_p$.

The latter is recommended for use, because it is easier to apply and no discernible difference was found in the test applications of the two weighting methods.

---

* Reference 34 (Equation 7.17, p. 148) of Volume 1.

FIG. G-1 PEAK/YIELD DEFLECTION (μ): EXPONENTIAL VERSUS TRIANGULAR DECAY OF LOAD PULSE

The third change that may be readily applied as a part of "Step 7" is to use an ultimate moment capacity formula that takes into account rebound steel acting as compressive reinforcement. The change may be seen by comparing Equations 6-1 and 6-6; the effect is to allow a slighter smaller section depth d for a given clear span L.

The first two changes described for consideration involve changing a preliminary design procedure that already has certain elements incorporated in it that at least partially correct for the discrepancies discussed; for example, refer to the discussion of the calculation of the natural period of vibration T that follows Equation 6-5. On the other hand, incorporating a final "refinement" such as the third change discussed does not necessarily upset the assumptions made in the preliminary design procedure. For these reasons, the usefulness of the third change was tested first in developing the modified preliminary design procedure that follows.

A preliminary design (first cut) might then be improved ("Step 7") by using instead the following modified procedure:	Numerical Example:
1. Given values for the following parameters: f'_c (ksi); f'_{dc} (ksi); f_{dy} (ksi); p_{so} (psi); t_o (sec); L (in.); p; b (in.)	3; 3.75; 44; 15; 1.55; 255; .02; 1
2. Obtain t_{00} (sec) from Figure 3-7.*	0.71
3. Assume values for μ and T (sec); calculate t_{00}/T.	6; .08; 8.9
4. Using Figure 6-1, page 11-5, read p_m/q; calculate q, using $p_m = p_{so}$.	.985; 15.23
5. Calculate L/d, using the following modification of Equation 6.1: $(L/d)^2 = [8\ pbf_{dy}/aq]\ [1 - 0.554\ pf_{dy}/(0.85\ f'_{dc})]$ (G-2) obtaining L/d, then calculating d (in.).	19.788; 12.89†
6. Using Equation 6-4, calculate T (sec), then t_{00}/T.	.0839; 8.46

* Reference 2 of Volume 1.

† Carrying more decimal places than justified, for demonstration purposes.

	Numerical Example:
7. Using Figure B-10* with μ and t_{00}/T, read r/q (equals p′/p); calculate p' (=p(r/q), but not less than .0025), then μ (= 0.1/(p-p′)); iterate this sequence until compatible values are found for p' and μ.	6; 8.46 .0046; 6.5
8. Using Equations 6-7 and -8, calculate "corrected" p_{so} to include effect of slab weight.	15+1.23 = 16.23†
9. Using corrected values for μ and t_{00}/T, repeat item 4 for new p_m/q and, with new p_m, calculate new q (psi); repeat item 5 for a new d(in.). Repeating items 6-8 should be unnecessary.	6.5; 8.46 1.00; 16.23; 16.23 13.31
10. Web steel to meet diagonal tension requirements should be calculated, and a check for pure shear strength should be made, using Equations 6-9 and -10, respectively.	

Another example with the same parameters except for changing f'_c (5 ksi), f'_{dc} (6.25 ksi), f_{dy} (78 ksi), and L (22'2") led to a design d = 10.21".†

A comparison with results from calculations using the final design procedure (Chapter 6) was then made at this point:

	d†	L	p'	μ	q
Trial 1, modified design	13.31"	21'3"	.0046	6.5	16.1
Final design	12.82"	21'3"	.0048	6.6	15.9
Trial 2, modified design	10.21"	22'2"	.0054	6.9	15.4
Final design	9.86"	22'2"	.0054	6.9	15.2

* Reference 2 of Volume 1.

† Carrying more decimal places than justified, for demonstration purposes.

Of the changes discussed earlier, the third one can be an inserted item in the modified procedure:

9.1 Adjust d slightly to take into account the rebound steel acting as compressive reinforcement, by using the following form of Equation 6-6 (with d appearing on both sides of the equation, a cut-and-try solution is indicated; however, for most designs it should be sufficiently accurate to simply use the d from item 9, in the right-end term below):

$$(L/d)^2 = [8\ (p-p')\ bf_{dy}/aq]\ [1 - 0.554\ (p-p')f_{dy}/(0.85\ f'_{dc})]$$
$$+ [8\ p'bf_{dy}/aq]\ [1 - d'/d]^* \qquad \text{(G-3)}$$

A new comparison of results was made, adding those where step 9.1 had been applied:

	d†	L	p′	μ	q
Trial 1, modified design	13.31"	21'3"	.0046	6.5	16.1
Modified design with step 9.1	12.92"	21'3"	.0046	6.5	16.1
Final design procedure	12.82"	21'3"	.0048	6.6	15.9
Trial 2, modified design	10.21"	22'2"	.0054	6.9	15.4
Modified design with step 9.1	9.91"	22'2"	.0054	6.9	15.4
Final design procedure	9.86"	22'2"	.0054	6.9	15.2

The close agreement of results from the modified preliminary design procedure with step 9.1 inserted and the final design procedure results made it appear that further work on the modified form of the preliminary design procedure was unwarranted. If further design refinement is thought to be warranted, the final design procedure (Chapter 6) may be used.

---

* As in final design procedure (Chapter 6), d′ assumed as one in.

† Carrying more decimal places than justified, for demonstration purposes.

Tabular Data on Typical Designs

Table G.1 contains tabular data on the typical designs, made using the final design procedure of Chapter 6, for preparation of Figures 6-3 and 6-6.

Computer Program Used for Typical Designs

Table G-2 shows a listing of the computer program used in calculating the typical designs for which data are shown in Table G.1. The programming language is Dartmouth BASIC as used by one of the largest commercial time-sharing organizations. For ease of handling data and plotting results, d was assumed and L calculated (rounded-off to a whole number, in inches). In retrospect, the beta method* time interval of one msec was smaller than necessary; one might calculate a time interval based on the estimated T in the program, using 0.05 T or 0.1 T (accuracy has been estimated to be within about 1% or 3.6%, respectively, of results obtained from a very small time interval, 0.001 T).† Also, the time interval could be increased considerably once the plastic phase is reached.

---

* Reference 21 of Volume 1.

† Reference 20 (p. 33) of Volume 1.

Table G.1

DATA FOR TYPICAL DESIGNS - ONE-WAY SLABS, SIMPLY SUPPORTED

p = .02

f'_c/f_{dy} (ksi)	d (in.)	L (in.)	p′ (%)	p_v (%)	M_{max} (ft-kip)	q (psi)	x_e (in.)	x_m (in.)	μ	t_m (msec)	p_m (psi)
3/52	6	126	.38	.97	31.8	16.0	.896	5.6	6.25	89	15.59
	10	214	.45	1.04	90.4	15.8	1.58	10.3	6.54	148	15.96
	14	304	.52	1.10	179.9	15.6	2.31	15.6	6.76	204	16.32
	18	397	.61	1.18	301.8	15.3	3.125	22.5	7.20	265	16.66
	21	471	.71	1.25	416.4	15.0	3.82	29.2	7.65	315	16.91
4/52	6	128	.38	.77	32.9	16.0	.869	5.5	6.28	88	15.59
	10	217	.45	.83	93.2	15.8	1.52	10.1	6.60	147	15.96
	14	308	.53	.88	185.1	15.6	2.22	15.2	6.86	202	16.32
	18	402	.62	.94	309.4	15.3	2.97	21.8	7.35	262	16.66
	21	476	.73	1.01	425.6	15.0	3.615	28.4	7.85	313	16.91
5/52	6	130	.38	.62	33.6	16.0	.845	5.3	6.33	88	15.59
	10	218	.45	.67	94.9	15.9	1.465	9.3	6.36	140	15.96
	14	311	.53	.72	188.0	15.6	2.137	14.9	6.95	201	16.32
	18	405	.63	.77	313.9	15.3	2.858	21.3	7.47	261	16.66
	21	479	.74	.82	430.8	15.0	3.457	27.7	8.02	311	16.91
3/72	6	146	.41	1.15	41.9	15.7	1.58	10.3	6.48	118	15.59
	9	223	.48	1.23	96.7	15.5	2.53	16.3	6.45	173	15.87
	12	305	.56	1.30	175.6	15.1	3.62	25.2	6.95	237	16.14
	15	395	.71	1.43	282.6	14.5	4.995	39.3	7.86	319	16.41
	18	501	.99	1.65	424.0	13.5	6.99	68.0	9.74	440	16.66
4/72	6	150	.42	.99	44.0	15.7	1.58	10.2	6.48	118	15.59
	9	229	.49	1.05	101.0	15.4	2.52	17.0	6.77	178	15.87
	12	311	.58	1.12	182.7	15.1	3.55	24.8	7.00	237	16.14
	15	401	.73	1.21	291.6	14.5	4.82	38.5	8.00	317	16.41
	18	499	.95	1.35	430.1	13.8	6.37	58.4	9.16	410	16.66
5/72	6	152	.42	.85	45.2	15.7	1.56	10.1	6.50	118	15.59
	9	231	.49	.90	103.5	15.5	2.45	16.0	6.51	172	15.87
	12	314	.58	.96	186.7	15.1	3.455	24.4	7.07	235	16.14
	15	405	.74	1.05	296.7	14.5	4.655	37.8	8.13	315	16.41
	18	502	.97	1.17	435.4	13.8	6.095	57.2	9.39	408	16.66

Table G.1 (continued)

p = .015

f'_c/f_{dy} (ksi)	d (in.)	L (in.)	p′ (%)	p_v (%)	M_{max} (ft-kip)	q (psi)	x_e (in.)	x_m (in.)	μ	t_m (msec)	p_m (psi)
3/52	6	112	.27	.76	24.7	15.7	.664	5.3	8.05	93	15.59
	11	210	.34	.83	84.8	15.4	1.296	11.4	8.79	170	16.05
	16	311	.42	.90	182.2	15.1	1.98	18.6	9.37	244	16.495
	20	395	.53	.99	288.8	14.8	2.60	25.9	9.95	306	16.83
	24	480	.63	1.07	420.9	14.6	3.245	32.6	10.05	358	17.15
4/52	6	114	.27	.57	25.3	15.7	.64	5.2	8.12	92	15.59
	11	212	.34	.63	86.7	15.4	1.24	11.1	8.93	169	16.05
	16	314	.43	.69	185.8	15.1	1.89	18.1	9.58	242	16.495
	20	397	.53	.76	293.2	14.9	2.44	24.0	9.82	296	16.83
	24	482	.63	.82	426.1	14.7	3.025	30.3	10.02	347	17.15
5/52	6	114	.27	.50	25.7	15.7	.62	5.1	8.19	92	15.59
	11	213	.34	.50	87.8	15.5	1.19	10.2	8.55	162	16.05
	16	314	.43	.53	187.8	15.2	1.81	16.8	9.29	234	16.495
	20	399	.54	.59	296.0	14.9	2.34	23.5	10.03	294	16.83
	24	482	.63	.64	429.1	14.8	2.87	28.3	9.88	337	17.15
3/72	6	131	.30	.98	32.9	15.4	1.20	10.0	8.33	124	15.59
	10	224	.38	1.06	94.0	15.0	2.176	19.2	8.82	205	15.96
	13	298	.47	1.15	162.0	14.6	3.023	28.7	9.51	272	16.23
	16	376	.59	1.25	250.6	14.2	3.99	40.1	10.04	340	16.495
	20	482	.74	1.38	400.5	13.8	5.37	54.5	10.14	418	16.83
4/72	6	133	.30	.80	34.1	15.4	1.18	9.9	8.37	124	15.59
	10	227	.38	.87	96.8	15.0	2.15	18.9	8.92	204	15.96
	13	302	.49	.95	166.3	14.6	2.92	28.2	9.67	271	16.23
	16	378	.59	1.02	255.4	14.3	3.77	37.3	9.90	329	16.495
	20	483	.74	1.12	405.7	13.9	5.013	50.9	10.15	406	16.83
5/72	6	134	.30	.67	34.8	15.4	1.159	9.8	8.42	123	15.59
	10	229	.39	.74	98.5	15.0	2.063	18.6	9.01	203	15.96
	13	304	.49	.80	168.8	14.6	2.825	27.7	9.82	270	16.23
	16	380	.60	.86	258.4	14.3	3.632	36.7	10.10	328	16.495
	20	483	.74	.95	408.9	14.0	4.756	47.8	10.05	395	16.83

Table G.1 (continued)

p = .01

f'_c/f_{dy} (ksi)	d (in.)	L (in.)	p′ (%)	p_v (%)	M_{max} (ft-kip)	q (psi)	x_e (in.)	x_m (in.)	μ	t_m (msec)	p_m (psi)
3/52	6	93	.25	.53	17.0	15.6	.421	4.10	9.79	87	15.59
	12	189	.25	.57	69.5	15.5	.887	8.70	9.77	160	16.14
	18	286	.27	.60	157.8	15.4	1.363	13.5	9.88	224	16.66
	24	385	.34	.66	283.5	15.3	1.87	18.5	9.92	282	17.15
	30	485	.42	.73	447.2	15.2	2.396	23.9	9.96	337	17.626
4/52	6	94	.25	.50	17.2	15.6	.402	4.0	9.91	86	15.59
	12	191	.25	.50	70.5	15.5	.847	8.4	9.94	158	16.14
	18	288	.28	.50	159.5	15.4	1.301	13.1	10.08	222	16.664
	24	387	.35	.50	286.6	15.3	1.774	18.0	10.17	280	17.15
	30	485	.42	.52	450.8	15.3	2.247	22.2	9.89	327	17.626
5/52	6	94	.25	.26	17.4	15.6	.389	3.9	10.00	85	15.59
	12	191	.25	.26	71.0	15.5	.818	8.2	10.06	157	16.144
	18	289	.28	.50	161.1	15.4	1.255	12.9	10.24	221	16.664
	24	387	.34	.50	288.2	15.4	1.694	16.8	9.94	271	17.15
	30	487	.42	.50	452.9	15.3	2.157	21.8	10.10	326	17.626
3/72	6	110	.25	.77	23.0	15.3	.788	8.0	10.21	117	15.59
	11	205	.25	.80	79.0	15.1	1.527	15.0	9.79	195	16.054
	15	283	.30	.85	148.8	14.9	2.165	21.2	9.81	254	16.408
	20	384	.40	.95	269.3	14.6	3.051	30.6	10.01	327	16.830
	25	488	.49	1.03	426.5	14.3	4.00	40.7	10.16	398	17.228
4/72	6	111	.25	.60	23.5	15.3	.762	7.9	10.34	117	15.59
	11	207	.25	.63	80.5	15.1	1.474	14.6	9.93	194	16.054
	15	285	.31	.68	151.4	14.9	2.083	20.8	9.99	252	16.408
	20	385	.40	.75	272.5	14.7	2.885	28.5	9.87	317	16.83
	25	489	.49	.82	430.2	14.4	3.758	38.1	10.13	387	17.228
5/72	6	111	.25	.50	23.7	15.4	.736	7.1	9.71	110	15.59
	11	208	.25	.50	81.5	15.1	1.434	14.4	10.04	193	16.054
	15	286	.31	.54	152.9	14.9	2.018	20.5	10.14	251	16.408
	20	386	.40	.60	274.5	14.7	2.782	28.0	10.06	316	16.83
	25	488	.49	.66	432.4	14.5	3.584	35.8	10.0	377	17.228
	26	508	.50	.67	468.2	14.5	3.736	36.8	9.85	385	17.305
5/52	12.2	195	.25	.26	73.4	15.5	.832	8.4	10.0	159	16.16
	12.4	198	.25	.26	75.9	15.5	.847	8.5	10.0	161	16.18
	12.6	201	.25	.26	78.4	15.5	.861	8.6	10.0	163	16.20
	12.8	204	.25	.50	80.9	15.5	.875	8.8	10.01	165	16.215
	12.9	206	.25	.50	82.2	15.5	.882	8.8	10.0	166	16.22
	13.0	208	.25	.50	83.5	15.5	.889	8.9	10.0	167	16.23
	14.0	224	.25	.50	97.0	15.5	.961	9.5	9.93	177	16.32

Table G.1 (concluded)

$p = .005$

f'_c/f_{dy} (ksi)	d (in.)	L (in.)	p′ (%)	p_v (%)	M_{max} (ft-kip)	q (psi)	x_e (in.)	x_m (in.)	μ	t_m (msec)	p_m (psi)
3/52	6	66	.25	.26	8.5	15.8	.176	1.8	10.29	60	15.59
	16	179	.25	.28	63.7	16.0	.518	5.1	9.82	142	16.495
	25	280	.25	.29	157.4	16.1	.824	8.3	10.02	204	17.228
	36	402	.25	.30	328.5	16.3	1.187	12.0	10.08	270	18.15
	43	477	.25	.30	469.7	16.5	1.407	14.0	9.94	306	18.764
	47	520	.25	.31	561.7	16.6	1.532	15.2	9.93	326	19.114
4/52	6	66	.25	.26	8.5	15.8	.168	1.7	10.38	59	15.59
	16	179	.25	.26	63.9	16.0	.494	4.9	9.97	140	16.495
	26	291	.25	.26	170.9	16.2	.813	8.0	9.80	203	17.305
	36	401	.25	.26	329.4	16.4	1.125	11.1	9.89	261	18.151
	43	478	.25	.26	471.1	16.5	1.342	13.7	10.18	304	18.764
	47	519	.25	.26	563.4	16.7	1.452	14.3	9.83	317	19.114
5/52	6	66	.25	.26	8.5	15.8	.162	1.7	10.43	58	15.59
	16	179	.25	.26	64.0	16.0	.478	4.8	10.09	139	16.495
	26	291	.25	.26	171.2	16.2	.787	7.8	9.93	202	17.305
	36	401	.25	.26	330.0	16.4	1.088	10.9	10.05	260	18.151
	43	477	.25	.26	471.9	16.6	1.290	12.9	9.97	296	18.764
	47	520	.25	.26	564.3	16.7	1.404	14.0	10.00	316	19.114
3/72	6	77	.25	.50	11.7	15.7	.336	3.2	9.62	77	15.59
	14	185	.25	.54	66.9	15.6	.876	8.5	9.74	168	16.321
	22	294	.25	.55	167.6	15.5	1.423	14.2	9.97	245	16.992
	31	417	.25	.56	335.0	15.4	2.046	20.8	10.16	323	17.713
	36	485	.25	.56	452.8	15.4	2.387	24.2	10.15	362	18.15
	40	539	.26	.58	560.2	15.4	2.664	27.0	10.15	393	18.501
4/72	6	77	.25	.32	11.7	15.7	.322	3.1	9.73	76	15.59
	14	186	.25	.38	67.2	15.6	.837	8.3	9.92	166	16.321
	23	308	.25	.39	184.1	15.5	1.425	14.5	10.15	251	17.072
	32	430	.25	.40	358.6	15.5	2.008	20.1	10.01	321	17.801
	36	484	.25	.40	454.6	15.5	2.267	22.8	10.04	353	18.15
	40	539	.26	.41	562.3	15.5	2.528	25.5	10.07	383	18.501
5/72	6	77	.25	.26	11.8	15.7	.312	3.1	9.80	75	15.59
	14	186	.25	.27	67.4	15.6	.811	8.1	10.04	165	16.321
	22	294	.25	.28	168.6	15.6	1.309	12.9	9.85	235	16.992
	31	417	.25	.29	337.1	15.5	1.882	19.1	10.17	312	17.713
	36	483	.25	.29	455.7	15.6	2.181	21.5	9.86	344	18.151
	40	538	.26	.30	563.5	15.6	2.432	24.1	9.92	374	18.501

```
100 PRINT "LEVEL 1:"
110 PRINT "ENTER VALUES OF ELASTIC FACTOR, PLASTIC FACTOR"
120 PRINT "AND TIME INTERVAL (SEC)"
130 INPUT K8,K9,H
140 PRINT USING 150 ,K8,K9,H
150:DATA ARE  0.##  0.##  0.###
160 PRINT
170 PRINT "LEVEL 2:"
180 PRINT "ENTER VALUES OF PEAK OVERPRESSURE (PSI), RISE-TIME (SEC)"
190 PRINT "AND POSITIVE PHASE DURATION (SEC)"
200 INPUT PO,T1,TO
210:DATA ARE  ##.#  #.###  #.###  #
220 PRINT "ENTER 1 IF BLAST DECAY LINEAR, 2 IF EXPONENTIAL"
230 INPUT Z
240 PRINT USING 210 ,PO,T1,TO,Z
250 PRINT
260 PRINT "LEVEL 3:"
270 PRINT "ENTER VALUES OF STEEL DYNAMIC YIELD STRESS (PSI),"
280 PRINT "CONCRETE COMPRESSIVE STRESS (STATIC) (PSI) AND TENSION"
290 PRINT "STEEL RATIO"
300 INPUT F2,F1,P9
310 PRINT USING 330 , F2,F1,P9
320 PRINT
330:DATA ARE #####  ####  0.###
340 PRINT "LEVEL 4:"
350 PRINT "ENTER SLAB DEPTH (INCHES)"
360 INPUT D
370 PRINT USING 380 , D
380:DEPTH IS  ##.#
390 PRINT
400 PRINT
410 PRINT
420 LET A=30000/F1
430 LET A1=P9*A
440 LET K0=SQR(2.*A1+A1*A1)-A1
460 PRINT
470 PRINT
480 LET Q0=15.5
490 LET Q0 = INT(Q0*10+0.5)/10.+0.05
500 LET C,W=1
510 LET Q2,Q3,Q4,K2,N1=0
520 LET G1=7
530 LET K2 = 0
540 REM                                        FLEXURE (INCL. REBOUND)
550 LET M1 = P9*D↑2*F2*(1 - .554*P9*F2/(1.0625*F1))
560 LET D1 = 1.27*D - .006*D↑2
570 IF D1 >= 1.1*D THEN 590
580 LET D1 = 1.1*D
590 LET P1 = PO
600 LET PO = PO + (150/1728)*D1*(1 - 1/2/6)
610 LET T2 = .87*SQR(10/P1)*W↑(1/3)
620 LET I1 = (K0*D)↑3/3 + (30000/F1)*P9*D↑3*(1-K0)↑2
630 LET L = SQR(8*M1/Q0)
640 PRINT "M1= ";M1;" L= ";L
650 LET M9 = D1*(L-12.)*150./1728./386./L
660 LET K1= 76800*F1*I1/L↑4
680 LET T9 = T0*.425000*D*SQR(P9)/L↑2
690 LET N1=N1+1
700 IF N1>100 THEN 720
710 GOTO 740
720 PRINT "LOOPING: Q0= ";Q0
730 GOTO 3180
740 REM                                        REBOUND STEEL RATIO
750 LET X=T2*T9/TO
760 LET G3=X
770 IF X>50 THEN 990
780 LET Y=LOG(G1)*3.6916
790 LET G2=LOG(X)*3.6916
800 IF Y > 2.419*G2 THEN 820
810 GOTO 890
820 IF Y < 2.419*G2+11.3 THEN 850
830 PRINT "OUT OF RANGE OF CURVE-FITTING: MU=";G1;"  X=";X
840 GOTO 2280
850 LET Z6=Y/2.419-G2
860 LET Z7=Z6*Z6
870 LET P8=.499+.06143*Z6+.3206*Z7-.12775*Z7*Z6
880 GOTO 1010
890 LET X=-4.67475475+.855*G2+.52*Y
900 LET Y=-.806-.52*G2+.855*Y
910 IF Y>0 THEN 940
920 LET B=X-.15175*Y*Y-.1008
930 GOTO 950
940 LET B=X-.2811*Y*Y-.2380
950 LET B2=B*B
960 LET B4=B2*B2
970 LET P8=.40082-.046716*B+.001678*B2+.00037242*B*B2-.000035524*B4
980 GOTO 1010
990 PRINT "DURATION/NAT. PERIOD IS TOO LARGE",X
1000 GOTO 2250
1010 LET P8 = INT(10000*P8*P9+.5)/10000
1020 IF P8 < 0.0025 THEN 1040
1030 GOTO 1100
1040 LET P8 = 0.0025
1060 GOTO 1100
1090:REBOUND STEEL RATIO =  0.####
1100 LET M2 = (P9-P8)*D↑2*F2*(1-.554*(P9-P8)*F2/1.0625/F1)
1110 LET M2 = M2 + P8*D*F2*(D - 1)
1120 LET L = SQR(8*M2/Q0)
1130 LET K1=76800*F1*I1/L↑4
1140 LET M9 = D1*(L-12.)*150./1728./386./L
1150 IF C < 3 THEN 1290
1160 PRINT USING 1090 , P8
```

```
1170 PRINT "M2= ";M2;"  L= ";L
1180 LET R=D/L
1190 IF R > .2 THEN 1210
1200 GØTØ 1240
1210 PRINT "PRØGRAM STØPPED BECAUSE DIAGØNAL TENSIØN PØRTIØN"
1220 PRINT "HANDLES THE CASE D/L < 0.2 ØNLY"
1230 GØTØ 3180
1240 LET Z9=.74*PO*(1.-R)/(R*F1)
1250 PRINT "BEAM THICKNESS, D1 ØR T= ";D1;" MASS, M9= ";M9
1260 PRINT "EQUIV. DURATIØN / NAT. PERIØD = ";G3
1270 PRINT "PURE SHEAR FACTØR= ";Z9
1280 PRINT
1290 GØSUB 2380
1300 GØ TØ 1310,1330,1650,ØN C
1310 LET S0 = 1.0
1320 LET J0 = 0
1330 LET J=.1/(P9-P8)
1340 IF J<=10 THEN 1360
1350 LET J=10
1360 LET J=X9/X8-J
1370 IF(J0*J)>=0 THEN 1580
1380 IF S0 > 0.1 THEN 1520
1390 IF X9/X8>10 THEN 1410
1400 GØTØ 1440
1410 IF Q3=0 THEN 1460
1420 IF (X9/X8-10)<Q3 THEN 1440
1430 LET Q0=Q4
1440 LET C=3
1450 GØTØ 1500
1460 LET Q4=Q0
1470 LET Q0=Q2
1480 LET Q3=(X9/X8-10)
1490 GØTØ 1600
1500 LET Q0=Q0+.05*J/ABS(J)
1510 GØTØ 1620
1520 LET S1=.5*S0
1530 IF S1 <= 0.1 THEN 1550
1540 GØTØ 1570
1550 LET S0 = 0.1
1560 GØ TØ 1580
1570 LET S0 = INT(10.*S1+0.5)/10.
1580 LET Q2=Q0
1590 LET Q0=Q0+S0*J/ABS(J)
1600 LET C = 2
1610 LET J0=J
1620 LET L=SQR(8*M2/Q0)
1630 GØTØ 680
1640 REM                                    DIAGØNAL TENSIØN
1650 GØ SUB 2980
1660 LET Q1=3.5*R*SQR(F1)
1670 LET P7=0
1680 IF Q1 >= Q0 THEN 1790
1690 LET P7=.0049
1700 FØR I = 1 TØ 200
1710     LET P7 = P7 + .0001
1720     LET Q1 = 1000*(1/(2+P8/P9))*(1+2*P7*F2/1000)*(R)↑2
1730     LET Q1 = Q1*SQR(P9*F1)
1740     IF Q1>=Q0 THEN 1840
1750 NEXT I
1760 PRINT
1770 PRINT "***NØT ENØUGH DIAGØNAL TENSIØN STEEL***"
1780 PRINT
1790 IF P7>=.0026 THEN 1840
1800 IF X9/X8<=1.5 THEN 1840
1810 LET P7=.0026
1830 GØTØ 1720
1840 PRINT USING 1850 ,P7,Q1,Q0
1850:FØR PV (P7)= 0.####    Q1=###.###    LAST Q0= ##.#
1860 PRINT
1870 PRINT USING 1880
1880:DEPTH   SPAN    T.STL    C.STL   WEB ST  Q-YLD    K1       X9       X9/X8=MU

1890 PRINT
1900 LET $1=INT(L+1/2)
1910 LET $2=INT(1E4*X9+1/2)/1E4
1920 LET $3=INT(1000*X9/X8+1/2)/1000
1930 PRINT USING 1940 ,D,$1,P9,P8,P7,Q0,INT(10*K1+.5)/10,$2,$3
1940: ###    ####   #.####   #.####   #.####   ###.#   ##.#   ###.####   ##.###

1950 PRINT
1960 PRINT
1970 LET N1,N2,N3,N4,N5,N6,N7,N8=0
1980 LET N1 = INT(100*12*P9*D + 1/2)/100
1990 LET N2 = INT(100*12*P8*D + 1/2)/100
2000 LET N3 = INT(100*12*.002*D1 + 1/2)/100
2010 LET N4 = INT(100*144*P7 + 1/2)/100
2020 LET L9 = (360 - L)/230
2030 IF L9 < 0 THEN 2050
2040 GØ TØ 2070
2050 LET L9 = 0
2060 GØ TØ 2100
2070 IF L9 > 1 THEN 2090
2080 GØ TØ 2100
2090 LET L9 = 1
2100 LET L9 = .23*L9 + 1.12
2110 LET N5 = INT(1000*L9 + 1/2)/1000
2120 LET N6=INT(12*D*(1.03*P9+1.15*P8)*(L+2*(D+11))*490/1728+.5)
2130 LET N7 = INT(12*.002*D1*(L-12)*490/1728 + 1/2)
2140 LET N8 = INT(144*P7*1.68*D*(L-12)/12*490/1728 + 1/2)
2150 PRINT USING 2170
2160 PRINT USING 2180
2170:    STEEL/FT WIDTH    STL/SF   LENGTH   TØTAL   STEEL/FT    WIDTH (LBS)
```

Table G.2 (continued)

```
2180: AS-     AS+  A-TEMP    A-WEB  CØRR.    AS-&+   TEMP   WEB     TØTAL
2190 PRINT
2200 PRINT USING 2210 ,N1,N2,N3,N4,N5,N6,N7,N8,N6+N7+N8
2210:##.##  ##.##  ##.##   ##.##  ##.##   #####  ###  ####     #####
2220 LET P0=P1
2230 LET N1,N2,N3,N4,N5,N6,N7,N8=0
2250 PRINT
2260 PRINT
2270 PRINT
2280 PRINT "IS THERE ANØTHER CASE (ENTER 0 FØR NØ, 1 FØR YES)"
2290 INPUT N1
2300 IF N1 = 0 THEN 3180
2310 PRINT "ENTER INPUT LEVEL AT WHICH NEXT CASE BEGINS"
2320 INPUT N1
2330 PRINT
2340 PRINT
2350 PRINT
2360 GØTØ 100,170,260,340, ØN N1
2380 REM
2390 IF Q0 = 0 THEN 3170
2400 LET V0,X0,T=0
2410 LET X8 = Q0/K1
2420 GØSUB 2750
2430 LET A0 = P/K8/M9
2440 REM                              BETA EQUATIØNS
2450 REM                       ASSIGN NEW BETA TØ NEXT LINE IF DESIRED
2460 LET B = 1/6
2470 LET A2,A1=A0
2480 LET T = T + H
2490 GØSUB 2750
2500 FØR I = 1 TØ 10
2510     LET A1 = A2
2520     LET V1 = V0 + (A0 + A1)*H/2
2530     LET X1 = X0 + H*V0 + (1/2 - B)*A0*H↑2 + B*A1*H↑2
2540     GØSUB 2900
2550     IF X1 <= X8 THEN 2580
2560     LET A2 = (P - Q)/K9/M9
2570     GØ TØ 2590
2580     LET A2 = (P - Q)/K8/M9
2590     IF ABS(A2-A1)/A1 <= .01 THEN 2630
2600 NEXT I
2610 IF ABS(A2-A1)/A1 <= .01 THEN 2630
2620 PRINT "AT T=";T;"ABS(A2-A1)/A2=";ABS(A2-A1)/A2
2630 LET V1 = V0 + (A0+A2)*H/2
2640 LET X1 = X0 + H*V0 + (1/2 - B)*A0*H↑2 + B*A2*H↑2
2650 LET X9 = (X0 + X1)/2
2660 LET G1=X9/X8
2670 IF G1 < 50 THEN 2690
2680 GØ TØ 3160
2690 IF V1 < 0 THEN 2970
2700  LET A0 = A2
2710  LET V0 = V1
2720  LET X0 = X1
2730 GØ TØ 2480
2740 REM                              FØRCE FUNCTIØN SUBRØUTINE
2750 IF T < T0 THEN 2790
2760 LET P = 0
2770 RETURN
2780 REM                                   TRIANGULAR RISE PULSE
2790 IF T >= T1 THEN 2820
2800 LET P = P0 * T/T1
2810 RETURN
2820 IF Z = 2 THEN 2870
2830 REM                                   TRIANGULAR DECAY PULSE
2840 LET P = P0 * (T0-T)/(T0-T1)
2850 RETURN
2860 REM                                   EXPØNENTIAL DECAY PULSE
2870 LET P=P0*(1-((T-T1)/(T0-T1)))*EXP(-((T-T1)/(T0-T1)))
2880 RETURN
2890 REM                            RESISTANCE FUNCTIØN SUBRØUTINE
2900 IF Q0 - K1*X1 < 0 THEN 2950
2910 REM                                   ELASTIC PHASE
2920 LET Q = K1*X1
2930 RETURN
2940 REM                                   PLASTIC PHASE
2950 LET Q = Q0 + K2*(X1 - X8)
2970 RETURN
2980 REM                           BETA RØUTINE PRINTØUT
3000 PRINT "TIME     ACCELERATIØN    VELØCITY     DISPLACEMENT"
3010 PRINT
3020 LET $5=INT(1E4*A0+1/2)/1E4
3030 LET $6=INT(1E4*V0+1/2)/1E4
3040 LET $7=INT(1E4*X0+1/2)/1E4
3050 LET $8=INT(1E4*A2+1/2)/1E4
3060 LET $9=INT(1E4*V1+1/2)/1E4
3070 LET $0=INT(1E4*X1+1/2)/1E4
3080 PRINT USING 3100 ,T-H,$5,$6,$7
3090 PRINT USING 3100 ,T,$8,$9,$0
3100       :#.###      ######.##     ###.####         ###.####
3110 PRINT
3120 PRINT "P=";P;"    Q=";Q;"    YIELD DEFL.=";X8
3130 PRINT
3140 PRINT "MAX/YIELD DEFL = MU =";X9/X8
3150 PRINT
3170 RETURN
3180 END
```

Table G.2 (concluded)

NOTATION

See Notation section at end of Chapter 6.

Refer to Volume 1 of this report for:

- Distribution List
- DD 1473 Form, and
- Abstract Cards